STUDIES ON THE LOCALIZATION OF TAMM-HORSFALL GLYCOPROTEIN IN THE KIDNEY OF THE SYRIAN HAMSTER BY IMMUNOFLUORESCENCE AND BY LIGHT AND ELECTRON MICROSCOPICAL IMMUNOPEROXIDASE TECHNIQUES, TOGETHER WITH A DISCUSSION OF ITS POSSIBLE ROLE.

A Thesis submitted by

Krishan Lal Sikri

for the degree of

Doctor of Philosophy

of the

University of London

October, 1979

Dept. of Cellular Biology & Histology,
St. Mary's Hospital Medical School,
London W.2.

VOLUME

— TWO —

FIGURES

LIST OF FIGURES

Figure		Page
1.	Gel filtration of hamster T-H glycoprotein on Sepharose 4B column.	24
2.	Disc gel electrophoresis of (A) hamster (B) human and (C) rat T-H glycoprotein by the method of Marshall and Zamecnik (1969).	24
3.	Gel filtration of rabbit anti hamster T-H antiserum on DEAE-cellulose column.	25
4.	Gel filtration of sheep anti rabbit immunoglobulin antiserum on DEAE-cellulose column.	25
5.	Gel filtration of peroxidase labelled sheep anti rabbit antibody (prepared by the two step procedure of Avrameas and Ternynck,1971) on Sephadex G-200 column.	26
6.	Gel filtration of peroxidase labelled sheep anti rabbit antibody (prepared by the method of Nakane and Kawaoi, 1974) on Sephadex G-200 column.	26
7.	Diagram of the apparatus used for the perfusion fixation of kidneys.	27
8.	Fluorescein staining for T-H glycoprotein in the ascending limbs of loops of Henle of the outer medulla of the adult hamster kidney. Fixation by perfusion with formal calcium chloride.	27

Figure		Page
9.	Fluorescein staining for T-H glycoprotein in the distal convoluted tubules of the outer cortex of the adult hamster kidney. Fixation by perfusion with formal calcium chloride.	27
10.	Light microscopic photograph to show the absence of T-H glycoprotein in the macula densa of the adult hamster kidney by immunofluorescence microscopy. Fixation by immersion with formal calcium chloride.	28
11.	Light microscopic photograph from the inner medulla to show the absence of T-H glycoprotein in the thin ascending and descending limbs of loops of Henle and collecting ducts by immuno-fluorescence microscopy. Fixation by perfusion with formal calcium chloride.	28
12.	Localization of T-H glycoprotein by immunofluorescence microscopy in the distal convoluted tubules of the adult hamster kidney. Fixation by immersion with 80% ethanol.	28
13.	Localization of T-H glycoprotein by immunofluorescence microscopy in the ascending limbs of loops of Henle of the adult hamster kidney. Fixation by immersion with 80% ethanol.	28

Figure		Page
14.	Localization of T-H glycoprotein by immunofluorescence microscopy in the distal convoluted tubules and ascending limbs of loops of Henle of the adult hamster kidney. Fixation by perfusion with periodate-lysine-paraformaldehyde.	29
15.	Localization of T-H glycoprotein by immunofluorescence microscopy in the distal convoluted tubules and ascending limbs of loops of Henle of the adult hamster kidney. Fixation by perfusion with paraformaldehyde-glutaraldehyde.	29
16.	Light microscopic photograph of the adult hamster kidney to show the presence of T-H glycoprotein in the distal convoluted tubules (and its absence in the macula densa) of the adult hamster kidney by immunoperoxidase technique. Fixation by perfusion in formal calcium chloride.	29
17.	Light microscopic photograph of the adult hamster kidney at higher magnification. By immunoperoxidase technique, T-H is shown to be present on the luminal border as well as in the basal part of the cells. Fixation by perfusion with PLP reagent.	29

Figure		Page
18.	Light microscopic photograph of a 1 µm thick araldite embedded section obtained from a 40 µm thick cryostat section. Staining by immunoperoxidase method. T-H is shown to be present on the luminal border of the distal convoluted tubules but is absent on that of the macula densa. Fixation by perfusion with paraformaldehyde-glutaraldehyde.	30
19.	Immunoelectron microscopic photograph of the adult hamster kidney to show the presence of T-H glycoprotein on the luminal surface of the distal convoluted tubule and the ascending limb of loop of Henle. The glycoprotein is absent in the proximal convoluted tubule. Fixation by perfusion with paraformaldehyde-glutaraldehyde.	30
20.	Immunoelectron photomicrograph of the adult hamster kidney to show the absence of T-H glycoprotein in the macula densa cells. Fixation by perfusion with paraformaldehyde-glutaraldehyde.	31
21.	Immunoelectron photomicrograph of the adult hamster kidney to show the absence of T-H glycoprotein in the cells of the	31

Figure		Page
	thin ascending (descending?) limb of loop of Henle. Fixation by perfusion with paraformaldehyde-glutaraldehyde.	
22.	Immunoelectron photomicrograph of the adult hamster kidney to show the absence of T-H glycoprotein in the cells of the collecting duct. Fixation by perfusion with paraformaldehyde-glutaraldehyde.	32
23.	Immunoelectron photomicrograph from a ultrathin section cut very close to the surface of 20 µm thick cryostat section of the adult hamster kidney. T-H glycoprotein is shown to be present not only on the luminal surface of the distal convoluted tubule, but also in the lateral membranes and the invaginations of the basal plasma membrane. Fixation by perfusion with paraformaldehyde-glutaraldehyde.	32
24.	A section of the renal cortex from hamster showing the junctions of the collecting duct cells with those of the distal convoluted tubule. T-H is present on the luminal surface of the cells of the latter but is absent on those of the former. Fixation by perfusion with paraformaldehyde-glutaraldehyde.	33

Figure		Page
25.	High power electron photomicrograph of a portion of the distal convoluted tubule of the hamster kidney to show the presence of T-H glycoprotein on the luminal border, lateral membrane and the invaginations of the basal plasma membrane. Fixation by perfusion with periodate-lysine-paraformaldehyde.	33
26.	High power electron photomicrograph of a portion of the ascending limb of loop of Henle of the hamster kidney to show the presence of T-H on the luminal border, lateral membrane, infoldings of the basal plasma membrane and also perhaps in the cisternae of the endoplasmic reticulum.	34
27.	High power immunoelectron photomicrograph of a cell of the distal convoluted tubule of the hamster kidney to show the presence of T-H in the Golgi body and also perhaps in the cisternae of the endoplasmic reticulum.	34
28.	High power immunoelectron photomicrograph of the adult hamster kidney to show the absence of T-H in the cells of the macula densa. Fixation by perfusion with periodate-lysine-periodate.	35

Figure		Page
29.	Diagram of a single nephron of the adult hamster kidney to show the presence of T-H glycoprotein in the membrane system of the cells of the ascending limb of Henle and the distal tubule and its absence in those of the glomerulus, proximal convoluted tubule, macula densa and collecting duct.	35
30.	Light microscopic photograph of adult human kidney to show that by immuno-fluorescence microscopy, T-H can be seen to be present in the ascending limbs of loops of Henle and distal convoluted tubules of the inner cortex. Fixation by immersion with formal calcium chloride.	36
31.	Light microscopic photograph of adult human kidney to show by immunofluorescence microscopy, the presence of T-H glyco-protein in the ascending limbs of loops of Henle of the outer medullary zone and its absence in the collecting ducts. Fixation by immersion with formal calcium chloride.	36

Figure		Page
32.	Light microscopic photograph from the outer cortex of the adult human kidney showing the uniform distribution of T-H glycoprotein in the cells of distal convoluted tubules and its absence in those of the proximal convoluted tubules.	36
33.	Light microscopic photograph of the adult human kidney showing the absence of T-H in the macula densa cells by immunofluorescence microscopy. Fixation by immersion in formal calcium chloride.	36
34.	Immunoelectron photomicrograph of adult human kidney to show the presence of T-H glycoprotein in the membrane system of the ascending limb of Henle's loop and its absence in that of the proximal tubule. Fixation by immersion with periodate-lysine-paraformaldehyde.	37
35.	Immunoelectron micrograph of a portion of the distal convoluted tubule of the human kidney to show the presence of T-H glycoprotein in the membrane system.	37
36 A & B	Immunoelectron micrograph to show the absence of T-H glycoprotein in the cells of the macula densa of the human kidney.	38

Figure		Page
37.	Light microscopic photograph to show the presence of T-H specific fluorescence on the luminal border of the medullary distal tubule (undifferentiated ALH) of the 12 days foetal hamster kidney.	39
38.	Light microscopic photograph to show by immunofluorescence microscopy the presence of T-H glycoprotein in the medullary distal tubules of the kidneys foetal hamster kidney.	39
39.	T-H positive immunofluorescence staining in the distal tubules of the inner cortical region of the 14 days foetal hamster kidney.	39
40.	15 days foetal hamster kidney showing rays of positively stained tubules which extend from deep in the medulla towards the presumed cortical region.	39
41.	1 day old hamster kidney demonstrating T-H positive fluorescence in the undiffentiated distal tubules of both cortex as well as medulla.	40
42.	3 days old hamster kidney demonstrating T-H positive fluorescent staining in the ascending limbs of loops of Henle.	40

Figure		Page
43.	3 days old hamster kidney demonstrating the absence of T-H specific fluorescence in the cells of the macula densa.	40
44.	23 days old hamster kidney demonstrating the presence of T-H specific fluorescence in the cells of ascending limbs of Henle's and distal convoluted tubules.	40
45.	Immunoelectron micrograph showing the presence of T-H glycoprotein on the luminal border of the medullary distal tubule of the 12 days foetal hamster kidney.	41
46.	In the 13 days foetal hamster kidney, T-H is shown to be present on the luminal surface of the medullary distal tubule and its absent in the collecting duct and mesenchymal tissue.	41
47.	Immunoperoxidase staining for T-H in the 14 days foetal hamster kidney. Photomicrograph shows the presence of staining on the luminal surface as well as some scattered staining in the invaginations of the basal plasma membrane of a distal tubular cell.	42
48.	Immunoperoxidase staining for T-H in the 4 days old hamster kidney. Photomicrograph shows the presence of	42

Figure		Page
	T-H positive staining not only on the luminal surface but also in the lateral membranes and the invaginations of basal plasma membrane.	
49.	4 days adrenalectomized hamster kidney showing a masked reduction in the amount of T-H specific fluorescence in some of the distal convoluted tubular cells of the outer cortex.	43
50.	4 days adrenalectomized hamster kidney showing the presence of brilliantly fluorescing casts in the affected distal tubules of the outer cortex.	43
51.	6 days adrenalectomized hamster kidney to show by immunofluorescence microscopy that almost all the distal tubules of the outer cortex have been affected.	43
52.	Section from the outer medulla of a 6 days adrenalectomized hamster kidney showing reduction of T-H specific fluorescence in the ascending limbs of loops of Henle and the presence of brilliantly fluorescing casts in their lumina.	43
53.	By immunofluorescence microscopy it is shown that in the 8 days adrenalectomized hamster kidney, the loss of T-H is even	44

Figure		Page
	more apparent in the ascending limbs of Henle's loops.	
54.	As in fig. 53, the loss of T-H specific fluorescence in the 8 days adrenalectomized animal is also clearly visible in the distal convoluted tubules and their lumina are completely blocked with the brilliantly fluorescing casts.	44
55.	In the sham operated hamster kidney no loss of T-H glycoprotein is seen by the immunofluorescence microscopy.	44
56.	Electron micrograph of a portion of the proximal convoluted tubule of the 8 days adrenalectomized hamster kidney to show that no significant alterations in the ultrastructure of the important cell organelles is observed.	45
57.	Electron micrograph of a position of the proximal convoluted tubule of the normal hamster kidney.	45
58.	Electron micrograph to show that the cells organelles of the ascending limb of Henle's loop are in no way different from that of the normal animals.	46
59.	Electron micrograph of a cell of the ascending limb of loop of Henle of the normal hamster kidney.	46

Figure		Page
60.	Electron micrograph of a portion of the distal convoluted tubule of the normal hamster kidney.	47
61.	By electron microscopy it is shown that the cell organelles of the distal convoluted tubule of the 8 days adrenalectomized hamster appears to be normal.	47
62.	High power electron micrograph of a cell of the collecting duct of the 8 days adrenalectomized hamster showing normal looking cell organelles.	48
63.	High power electron micrograph of a portion of the collecting duct of the normal hamster kidney.	48
64.	Light microscopic photograph of a 1 μm resin embedded section of the normal hamster kidney showing a macula densa.	49
65.	Low power electron micrograph of the normal hamster kidney showing a macula densa, mesangial cells, glomerulus and the distal tubule.	49
66.	Electron micrograph of a portion of the normal hamster kidney macula densa to show that in certain regions its epithelium appears to be more than one layer in thickness.	50

Figure		Page
67.	Electron micrograph of a cell of the normal hamster kidney macula densa showing microvilli, a cilium and a supra nuclear Golgi body.	50
68.	Electron micrograph of a cell of the normal hamster kidney macula densa showing folds of luminal membrane, profiles of Golgi body in para as well as infranuclear positions and infoldings of the basal plasma membrane etc.	51
69.	Macula densa cell at a higher magnification showing one vesicle which appears to be derived by the invagination of the luminal plasma membrane. Also shown are numerous subsurface vesicles and the so called tight functions.	51
70.	A macula densa cell at higher magnification showing the basal region with dark membrane bounded granules, large vesicles and rough endoplasmic reticulum.	52
71.	High power electron micrograph of the base of a macula densa cell of normal hamster kidney showing infra nuclear Golgi body, microtubules and the basal lamina which appears to be continuous.	52
72.	Electron micrograph of a macula densa cell showing a lysosome, mitochondria	53

Figure		Page
	with circular and oval profiles and single membrane bounded vacuoles.	
73.	Electron micrograph of a cell of the normal hamster kidney ascending limb of loop of Henle showing two profiles of Golgi body in paranuclear positions.	53
74.	Electron micrograph of a cell of the normal hamster kidney macula densa showing two profiles of the Golgi body in para nuclear positions.	54
75.	Electron micrograph of the macula densa showing two cells with profiles of infra nuclear Golgi bodies.	54
76.	A part of the hamster kidney macula densa showing cristae mitochondriales which appears to be lamellate in form.	55
77.	Electron micrograph of a part of the normal hamster kidney collecting duct showing large and numerous acid phosphatase containing lysosomes.	55
78.	Electron micrograph of a part of the normal hamster kidney proximal tubule showing numerous acid phosphatase containing lysosomes.	56
79.	Electron micrograph of a part of the normal hamster kidney distal tubule showing large acid phosphatase	56

Figure		Page
	containing lysosomes.	
80.	Electron micrograph of a part of normal hamster kidney macula densa showing sporadic distribution of lysosomes.	57
81.	Light microscopic photograph of the hamster kidney cortex showing catalase containing peroxisomes or microbodies in the proximal convoluted tubules and their absence in the macula densa, distal convoluted tubule, glomerulus, and the collecting duct.	57
82.	Adult Wistar rat kidney showing uniform distribution of T-H specific fluorescence in the ascending limbs of loops of Henle.	58
83.	Adult Wistar rat kidney showing uniform distribution of T-H specific fluorescence in the distal convoluted tubules.	58
84.	Adult Wistar rat kidney showing the complete absence of T-H glycoprotein specific fluorescence in the macula densa cells.	58
85.	Adult Wistar rat kidney showing fluorescent staining on the luminal side of the cells of the macula densa.	58
86.	Immunoelectron micrograph of a portion of the ascending limb of Henle's loop	59

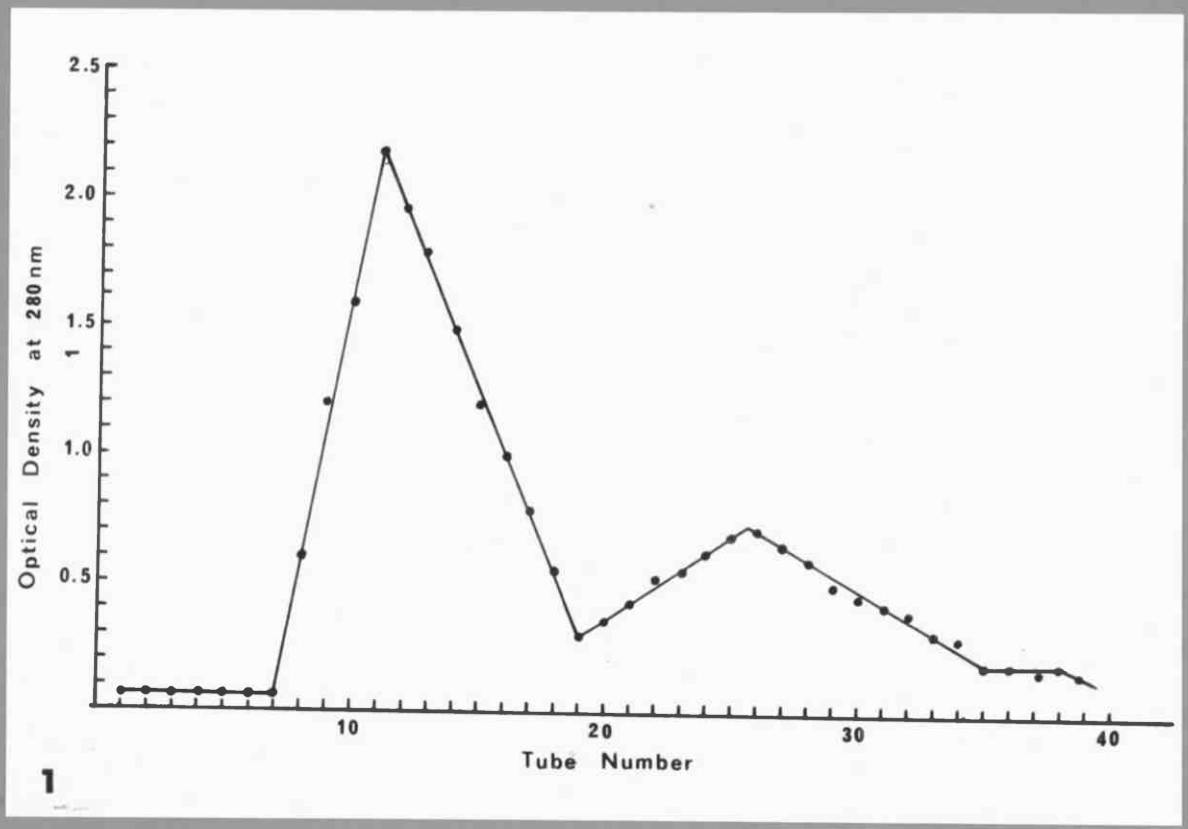
Figure		Page
	of the adult Wistar rat kidney showing localization of T-H glycoprotein on the luminal border, lateral cell membrane and the infoldings of the basal plasma membrane.	
87.	Immunoelectron micrograph of a portion of the distal convoluted tubule of the adult Wistar rat kidney showing the localization of T-H glycoprotein in the complete membrane system.	59
88.	Immunoelectron micrograph of a macula densa of the adult Wistar rat kidney showing localization of T-H glycoprotein on the luminal border.	60
89.	High power immunoelectron micrograph of a portion of the macula densa of the adult Wistar rat kidney showing its junction with the distal convoluted tubular cell.	60
90.	Immunoelectron micrograph of a macula densa of the adult Wistar rat kidney showing complete absence of the glycoprotein.	61
91.	Kidney of adult Wistar rat kidney killed 3 days post-adrenalectomy showing a substantial reduction of T-H specific fluorescence in some of	62

Figure		Page
	the distal convoluted tubules of the outer cortex.	
92.	Kidney of 3 days adrenalectomized Wistar rat showing the presence of brilliantly fluorescing casts in the lumina of some of the affected distal convoluted tubules.	62
93.	15 days adrenalectomized Wistar rat kidney showing that in the cells of the affected distal convoluted tubules, T-H has started to come back.	62
94.	7 days adrenalectomized Wistar rat kidney showing that there is no effect of adrenalectomy on the cells of the macula densa.	62
95.	Immunoelectron micrograph of a cell of the 3 days adrenalectomized rat kidney showing the disappearance of T-H glycoprotein from the invaginations of the basal plasma membrane.	63
96.	Immunoelectron micrograph of a cell of the 20 days adrenalectomized Wistar rat kidney to show that the glycoprotein has come back in the invaginations of the basal plasma membrane.	63
97.	Light microscopic photograph of a part of accessory adrenal cortical tissue	64

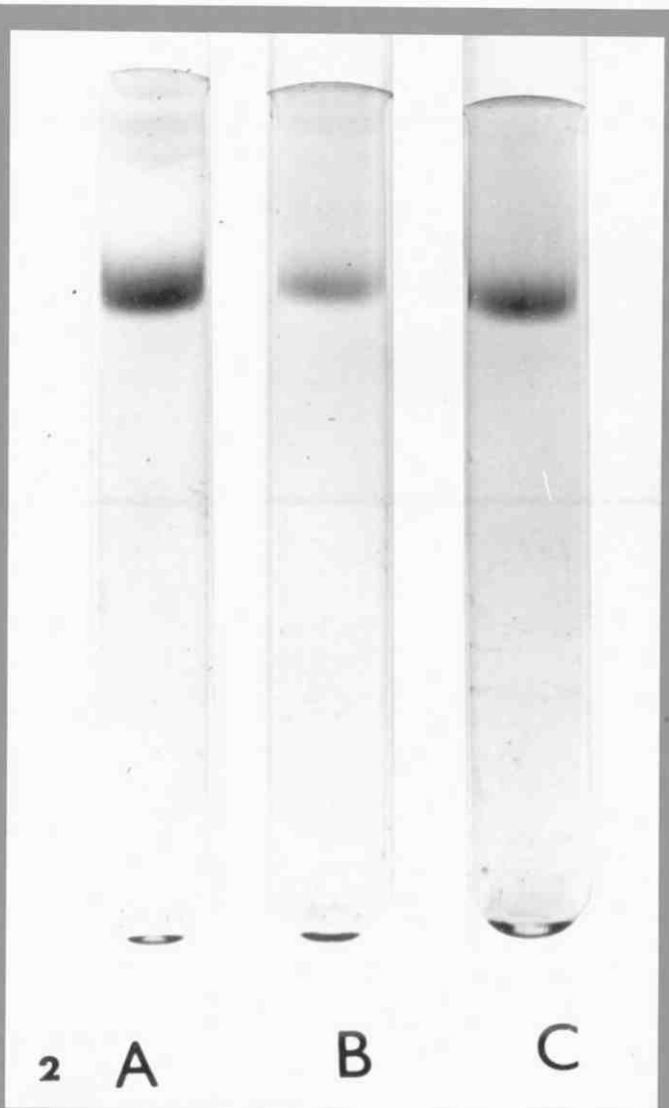
Figure		Page
	obtained from a 15 days adrenalectomized Sprague-Dawley rat.	
98.	Light microscopic photograph of a part of the adrenal gland obtained from a normal Sprague-Dawley rat.	64

Fig 1. Gel filtration at 4°c on Sepharose 4B (60 cm x 1.6 cm) of crude hamster T-H glycoprotein in sodium phosphate buffer, pH 7.0 containing urea. Elution was affected by upward flow rate of 4 ml/hour. Fractions (tubes 8-18) obtained in the first peak which contained pure T-H were combined.

Fig 2. Polyacrylamide-gel electrophoresis in the presence of sodium dodecyl sulphate (Marshall and Zamecnik, 1969) of (A) hamster T-H glycoprotein (B) human T-H glycoprotein and (C) Rat T-H glycoprotein. The purity of the glycoprotein is demonstrated by the single band obtained in each case.


Optical Density at 280 nm
2.5
2.0
1.5
1.0
0.5
10
20
30
40
Tube Number

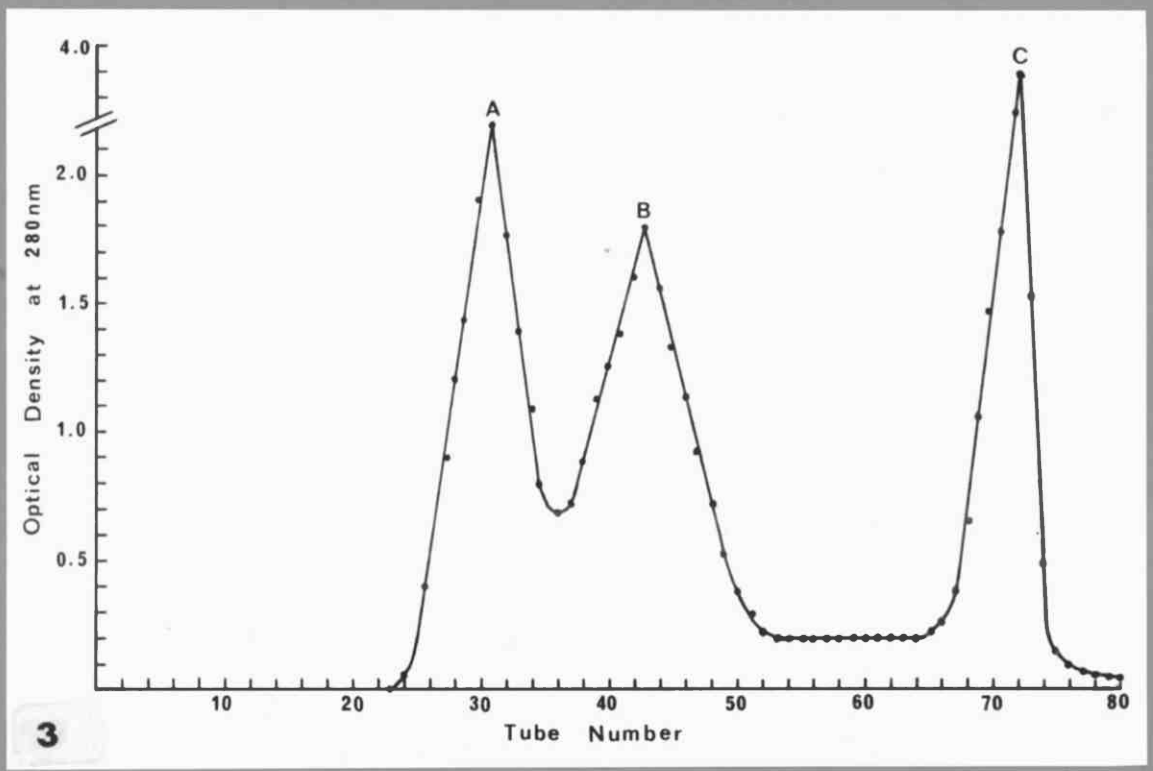
1


A
B
C

2

Fig 3. Gel filtration at 4°c on a column (60 cm x 1.6 cm) of DEAE-cellulose of antiserum raised in rabbits against hamster T-H glycoprotein. The eluting buffer was 0.04M Tris-phosphate, pH 8.6. The first peak (A) contained IgM, the second (B) IgG and the third (C) albumin. Fractions obtained in tubes 39-48 containing IgG were combined.

Fig 4. Gel filtration at 4°c on a column (60 cm x 1.6 cm) of DEAE-cellulose of sheep anti-rabbit immunoglobulin antiserum. Fractions (Tubes 30-36) obtained in the second peak (B) containing IgG were combined.


4.0
2.0
1.5
1.0
0.5
Optical Density at 280nm
A
B
C
10
20
30
40
50
60
70
80
Tube Number
3

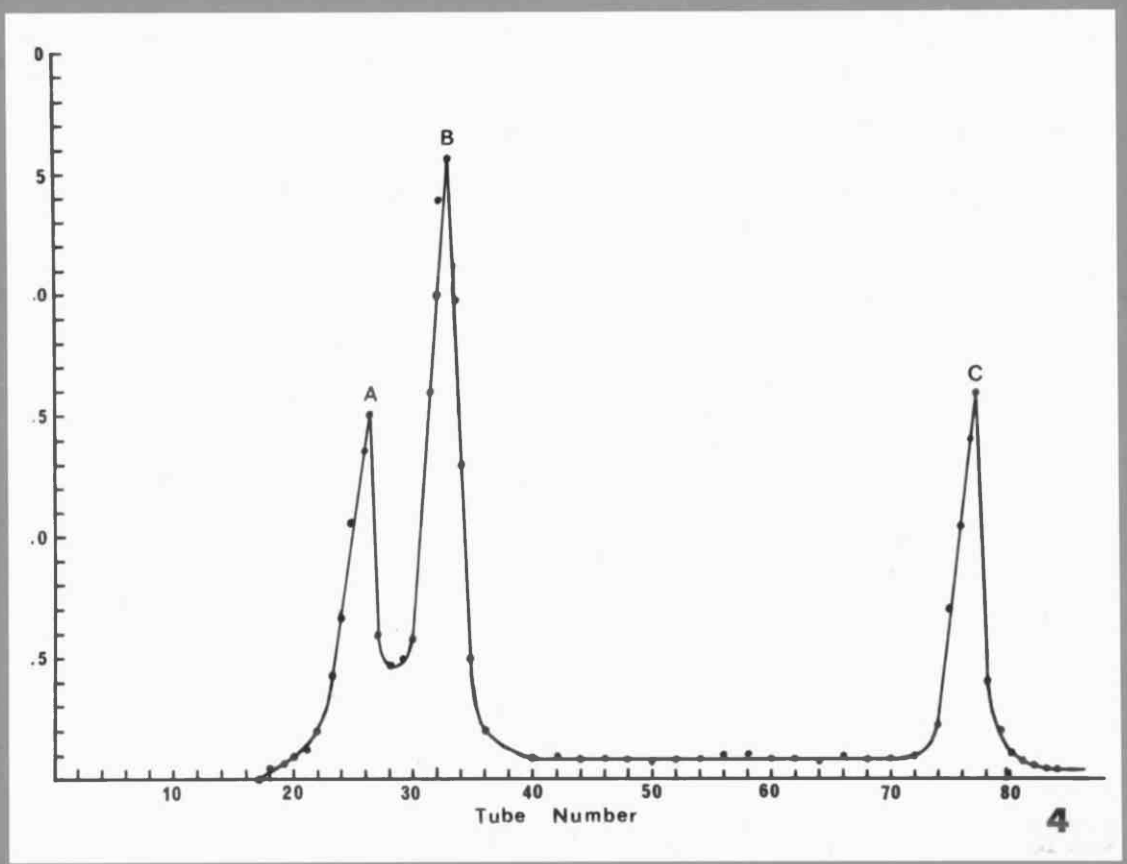
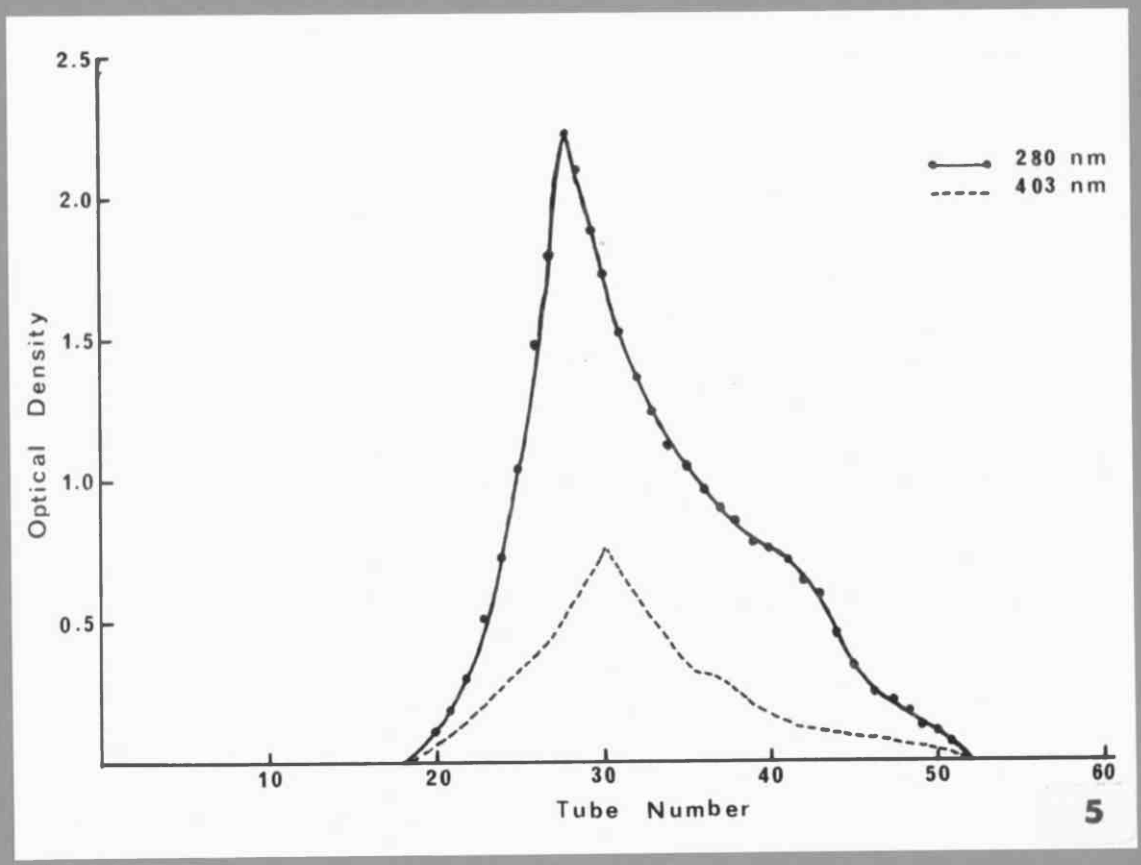
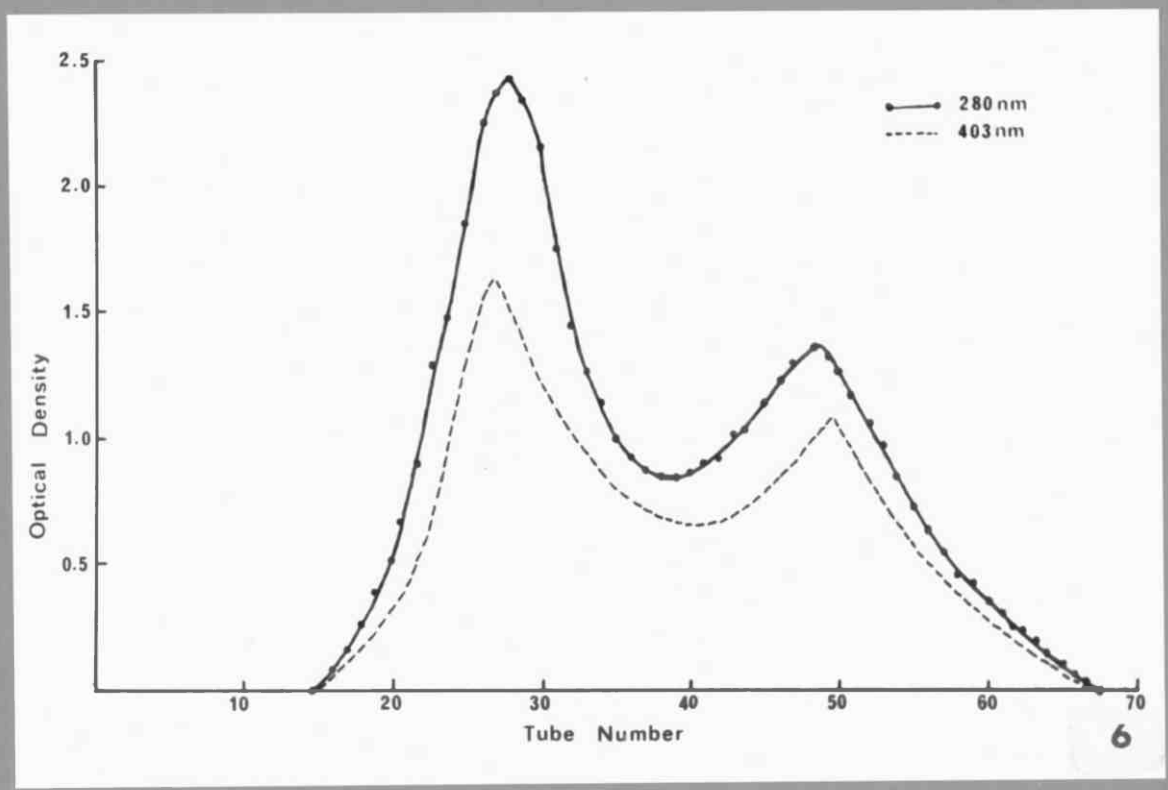

0
5
.0
.5
.0
.5
A
B
C
10
20
30
40
50
60
70
80
Tube Number
4

Fig 5. Chromatography on Sephadex G-200 column (60 cm x 1.6 cm) equilibrated with 0.1M phosphate buffer, pH 6.8 of peroxidase labelled sheep anti-rabbit antibody prepared by the two step procedure of Avrameas and Ternynck (1971). Only one asymmetric peak was obtained. Samples containing pure antibodies (fractions 24-38) were combined.

Fig 6. Elution pattern of sodium periodate activated sheep antirabbit IgG labelled with HRPO by the method of Nakane and Kawaoi (1974). The conjugate was chromatographed on a column of Sephadex G-200, equilibrated with PBSA. Optical densities at 280 nm (——) and 403 nm (----) were measured and fractions (22-34) containing pure antibodies, obtained in the first peak were combined.


2.5
2.0
1.5
1.0
0.5
Optical Density
280 nm
403 nm
10
20
30
40
50
60
Tube Number

5

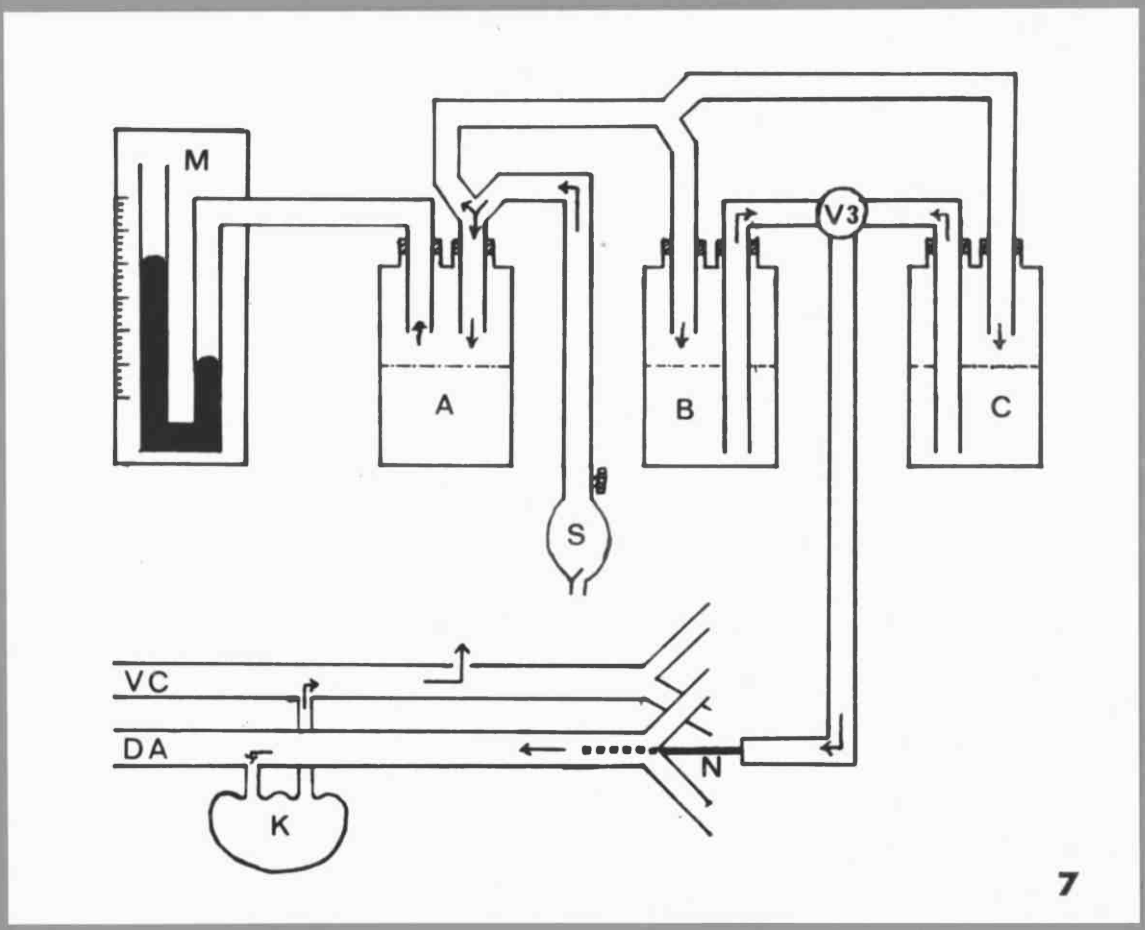

2.5
2.0
1.5
1.0
0.5
Optical Density
280nm
403nm
10
20
30
40
50
60
70
Tube Number

6

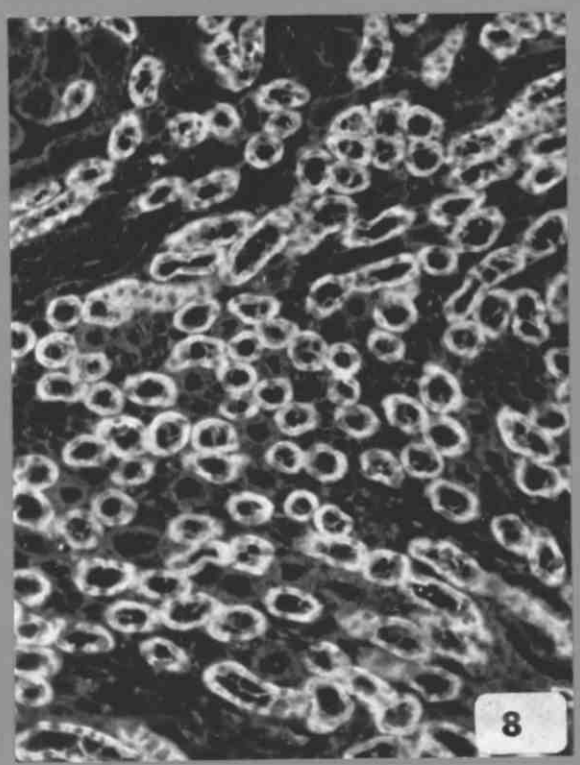
Fig 7. Diagram of the apparatus used for the perfusion fixation of kidneys. The apparatus consisted of 3 bottled - bottle A contained water and was used for creating pressure, bottle B contained the fixative and bottle C, the buffer.
(M), Manometer; (S), rubber ball syringe; (N), syringe needle; (V3), 3-way valve; (VC), vena cava; (DA) dorsal aorta; (K), kidney.

Fig 8. Fluorescein staining for T-H glycoprotein in ALH of the outer medulla. 5 μm thick paraffin section from the adult hamster kidney fixed by perfusion with formal calcium chloride. An almost uniform distribution of T-H is seen in the cells of ALH, except their nuclei. Magnification x 400.
N.B. Figures 8-13 were taken with an epifluorescence microscope.

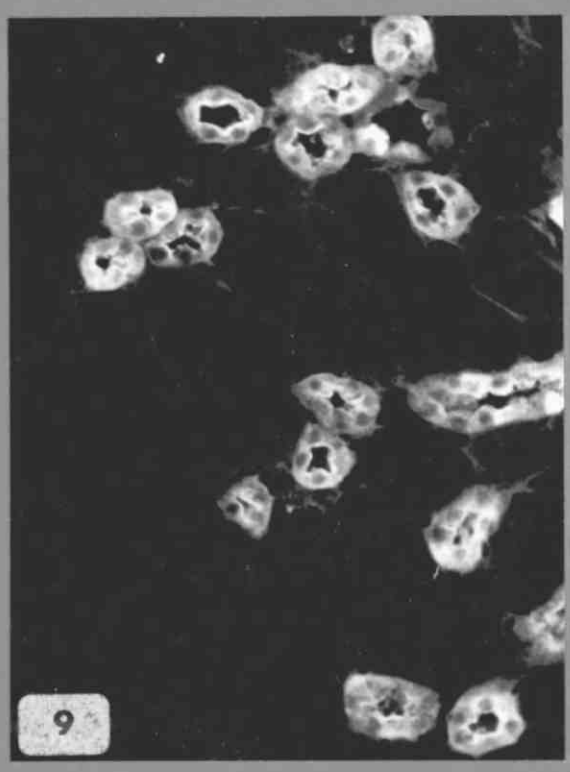
Fig 9. Fluorescein staining for T-H glycoprotein in DCT of the outer cortex. 5 μm thick paraffin section from the adult hamster kidney fixed by perfusion with formal calcium chloride. As in Fig. 8, a similar distribution of T-H is seen in the cells of DCT. Magnification x 800.



7



8



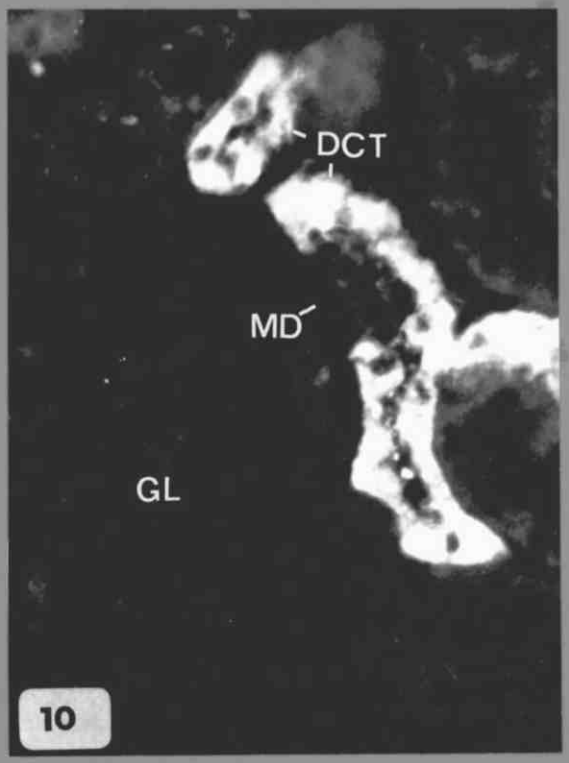
9

Fig 10. Adult hamster kidney. Localization of T-H glycoprotein in the DCT by immunofluorescence microscopy. Note that the cells of the MD lack the glycoprotein. Fixation was by immersion with formal calcium chloride. (GL), Glomerulus. Magnification x 800.

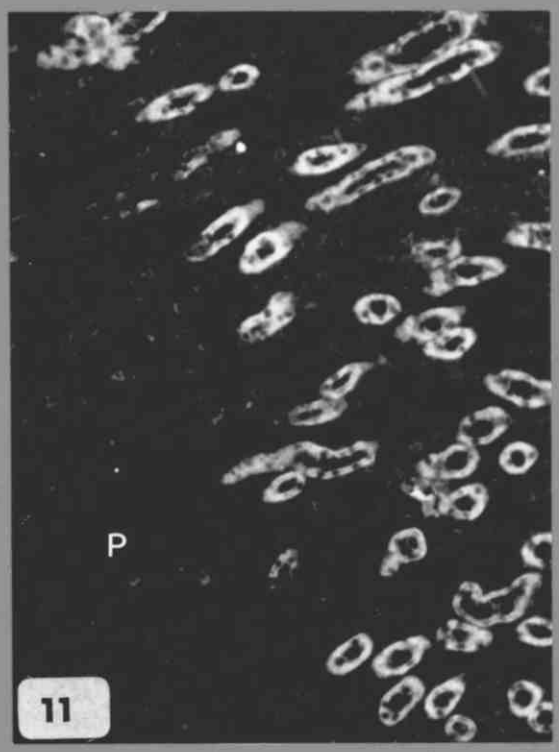
Fig 11. Adult hamster kidney, inner medullary zone. T-H specific fluorescence in the cells of ALH which lie among the nonstained thin descending and ascending limbs of loops of Henle and CD. No staining is observed in the papillary region (P) which predominantly contains CD and thin descending and ascending limbs of loops of Henle. Magnification x 400.

Fig 12. Adult hamster kidney. Outer cortical region showing DCT specifically stained for T-H glycoprotein by immunofluorescence. Fixation was by immersion with 80% ethanol. Note that the tubules are collapsed thus, resulting in closed limina. Magnification x 800.

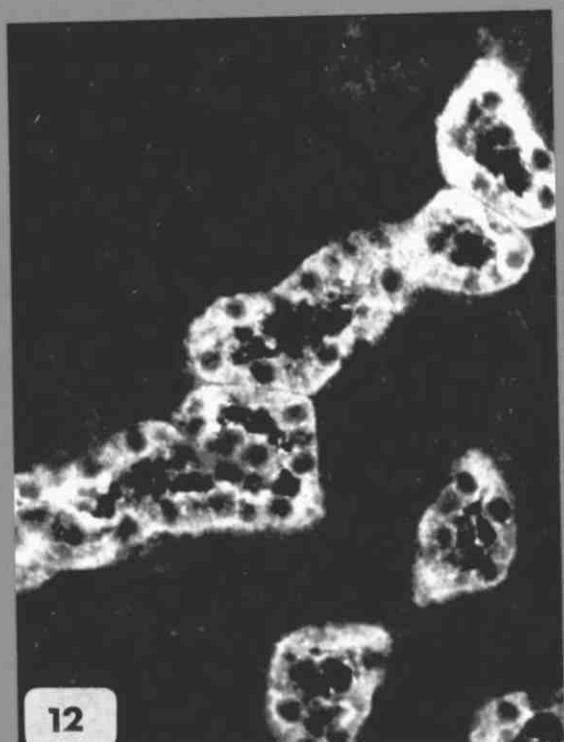
Fig 13. Adult hamster kidney. Outer medullary region showing ALH specifically stained for T-H. As in Fig 12, fixation was by immersion with 80% ethanol. Once again, tubules are collapsed and thus with closed lumina. Magnification x 800.



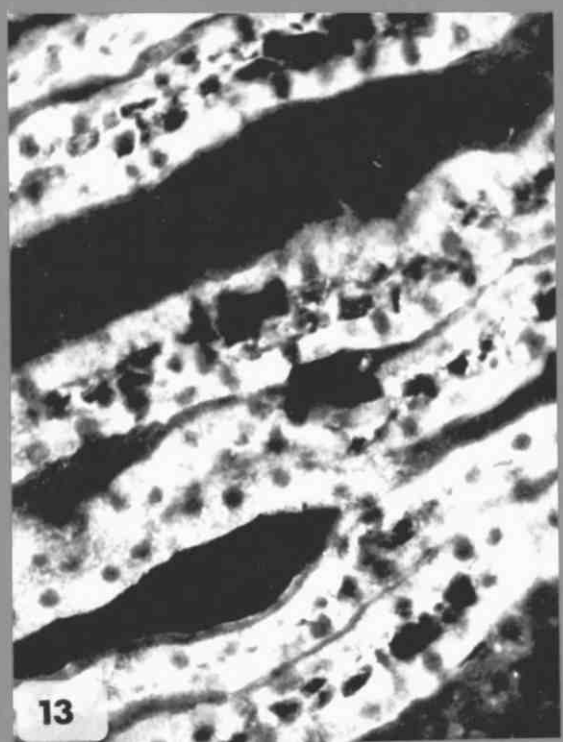
10



11



12



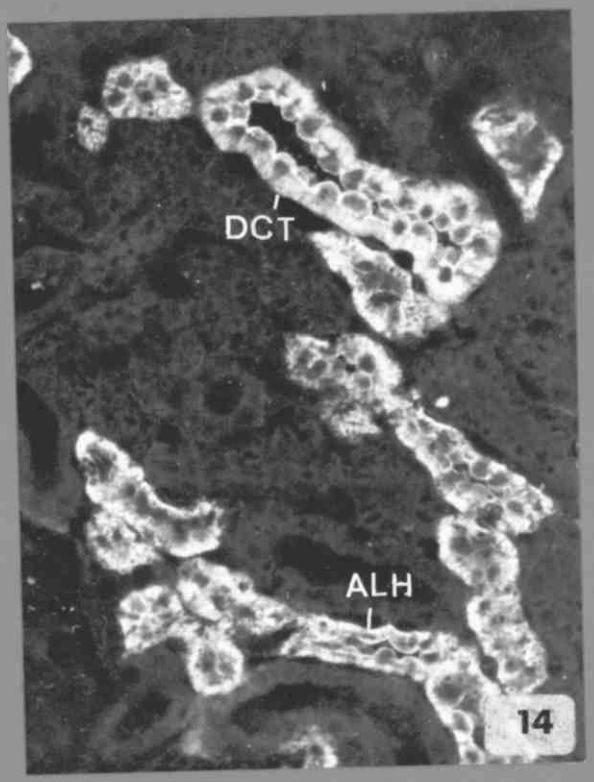
13

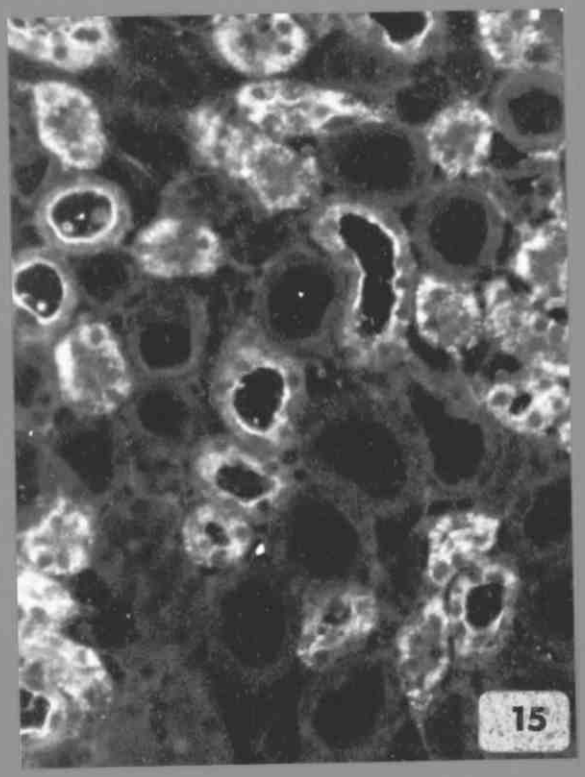
Fig 14. Adult hamster kidney by perfusion with PLP reagent. Note that the luminal border of ALH and DCT is heavily stained for T-H. In the interior of the cells however, the staining is somewhat selective. The basal half of the cells can be seen fluorescing brilliantly, suggesting the presence of T-H glycoprotein in the invaginations of the basal plasma membrane and/or perhaps also in the basally placed mitochondria. (N.B. The subsequent work by immunoelectron microscopy showed that the glycoprotein is infact present in the basal plasma membranes, including its invaginations, see later). Magnification x 600.

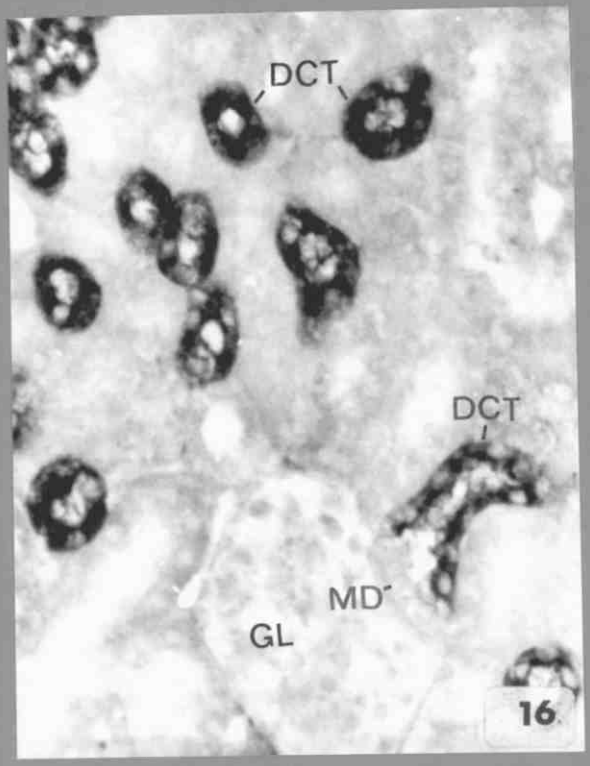
Fig 15. Adult hamster kidney fixed by perfusion with paraformaldehyde-glutaraldehyde. The luminal border of well fixed ALH and DCT stains prominently. On the other hand, fluorescent staining within the cells is somewhat patchy. Magnification x 600.

Fig 16. Localization of T-H glycoprotein in the adult hamster kidney by immunoperoxidase technique at the light microscopical level utilizing PAP reagent. 5 μm thick paraffin section obtained from the kidney fixed by immersion with formal calcium chloride. The glycoprotein can be seen present in DCT but absent in the MD. (GL), Glomerulus. Magnification x 600.

Fig 17. Localization of T-H glycoprotein in the adult hamster kidney by immunoperoxidate technique at the light microscopical level. 5 μm thick section obtained from the PLP perfused fixed material was treated with the PAP reagent. The luminal border of DCT is heavily stained for T-H (arrows). A selective staining in the basal part of cells was seen to be in the form of parallel striae which again, suggests the presence of T-H in the invaginations of the basal plasma membrane. Note that the nuclei (n) of these cells are clearly devoid of staining. Magnification x 1,500.


DCT
ALH
14

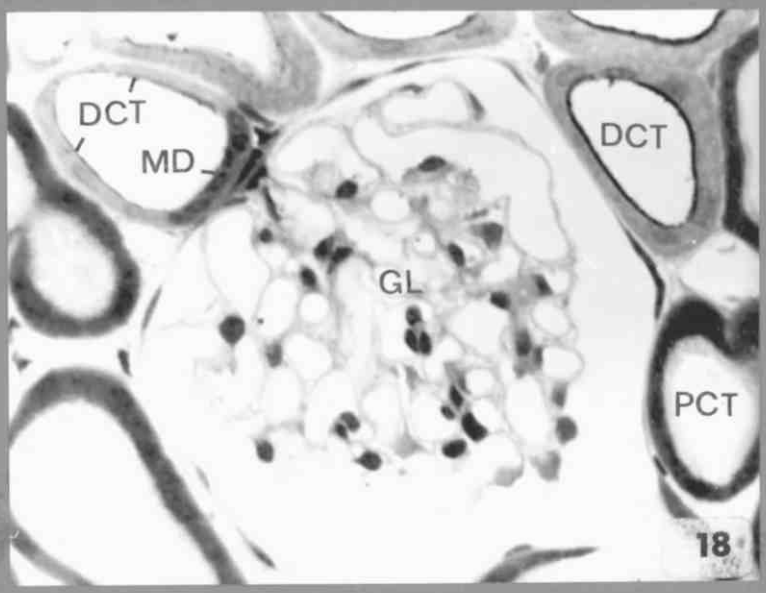

15


DCT
DCT
MD
GL
16


n
n
n
n
17

Fig 18. 1 μm thick araldite embedded section obtained from a 40 μm thick cryostat section of the adult hamster kidney cortex which had been treated with the immunoperoxidase reagents. The thin section after counterstaining with Azure II was examined by light microscopy. T-H glycoprotein may be seen intensely on the luminal border of DCT cells. The glycoprotein is absent from the luminal surface of the MD and PCT cells, but can be seen to be present on the luminal surface of the cells of DCT opposite to the MD. Also, note that the intensity of T-H positive peroxidase staining is considerably less in that part of the DCT near the MD. Fixation by perfusion with paraformaldehyde - glutaraldehyde.(GL), Glomerulus. Magnification x 800.

Fig 19. Identification of T-H glycoprotein, by immunoelectron microscopical method, on the luminal surface of the cells of the DCT and ALH and its absence from the surface of the PCT cells. Fixation was by perfusion with paraformaldehyde -glutaraldehyde and staining was done by the method of Nakane and Kawaoi (1974). Magnification x 10,000.


DCT
MD
DCT
GL
PCT
18

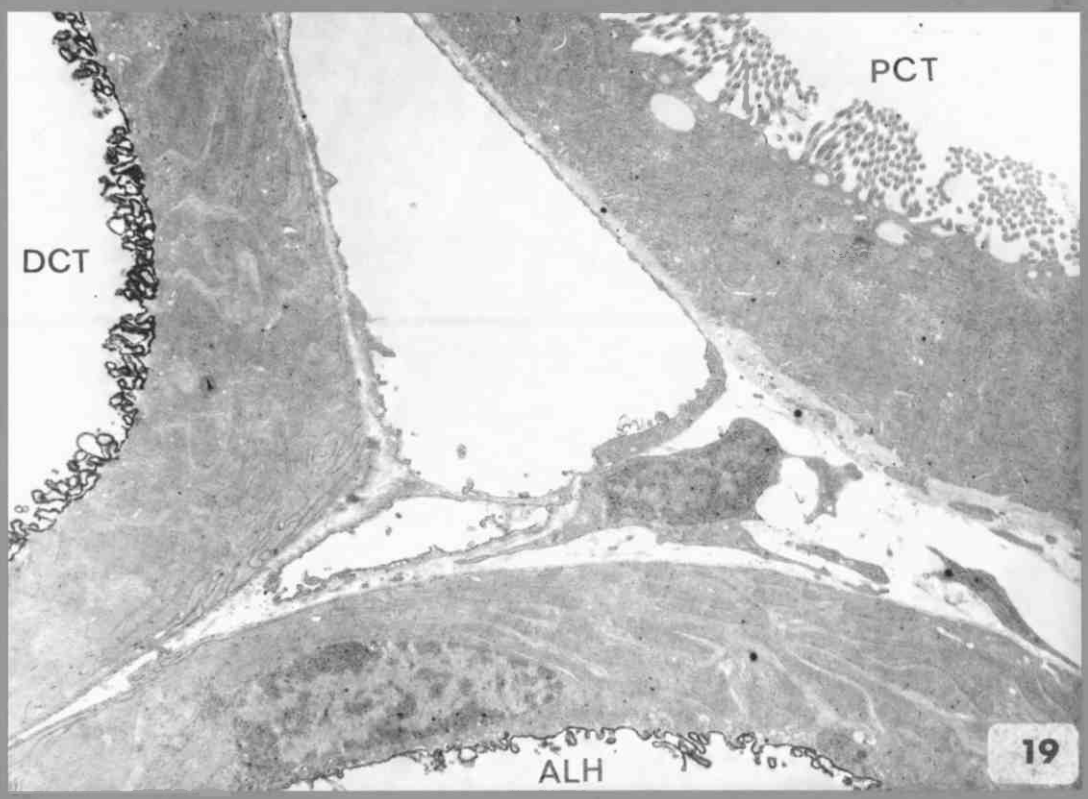
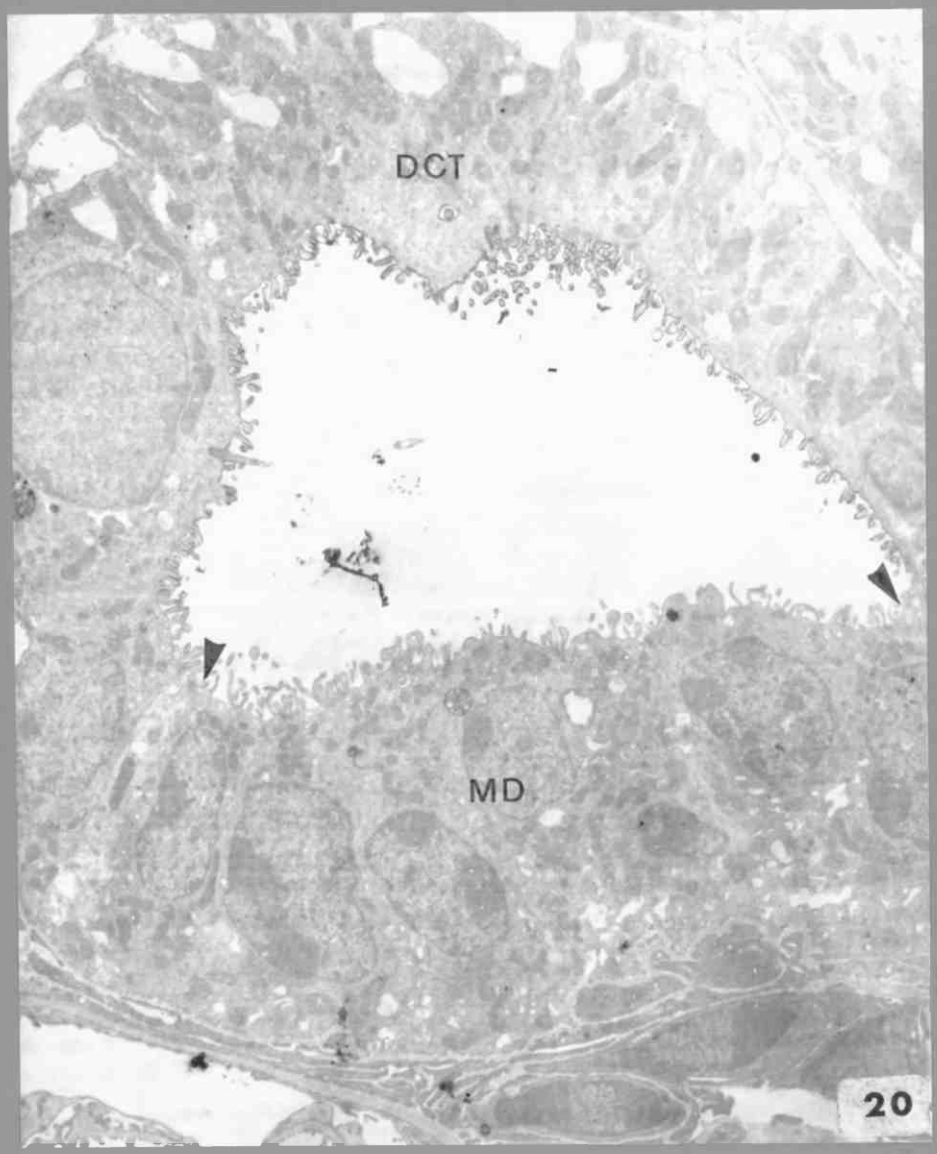

PCT
DCT
ALH
19

Fig 20. A section showing the absence of T-H glycoprotein by immunoelectron microscopy on the luminal surface of the MD cells and its presence on the other cells of the DCT. Fixation and staining procedures were same as in Fig. 19. (GL), glomerulus. Magnification x 10,000.

Fig 21. Identification of T-H glycoprotein by the immunoelectron microscopic method (Nakane and Kawaoi,1974) on the luminal surface of the ALH and its absence on the thin descending (or ascending?) limb of Henle's loop (TLH). Fixation was as in Fig 19. Magnification x 15,000.


DCT
MD
20

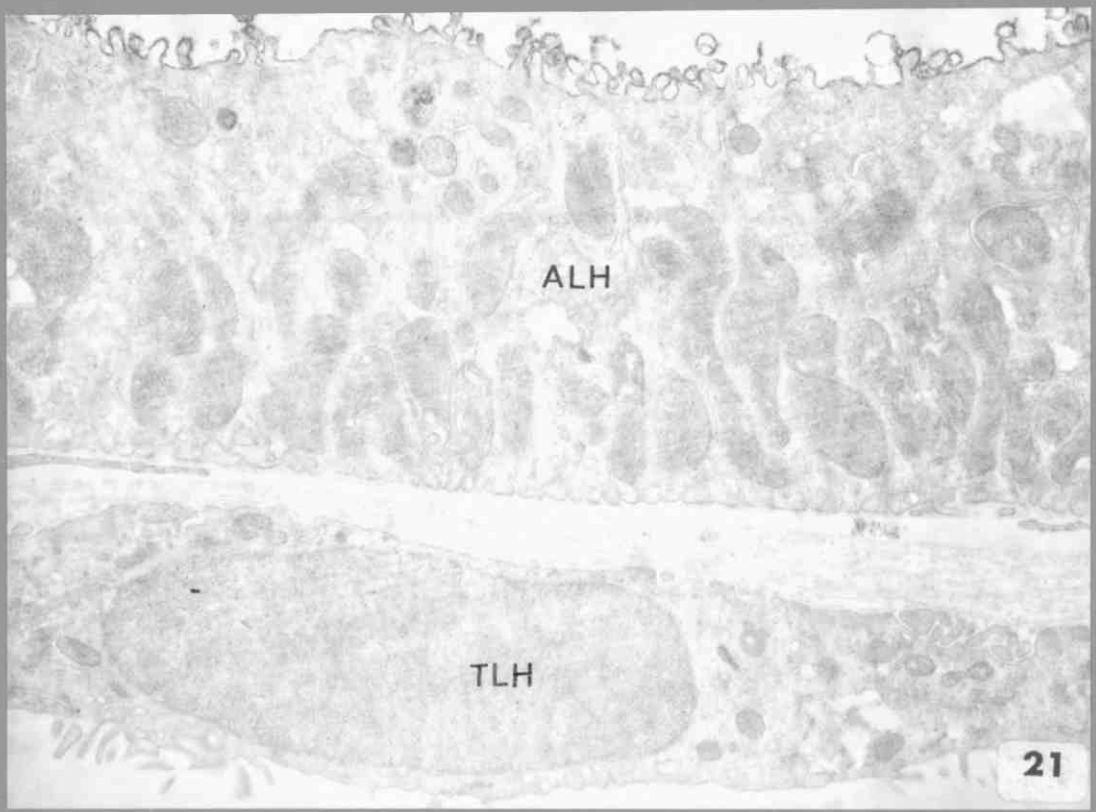
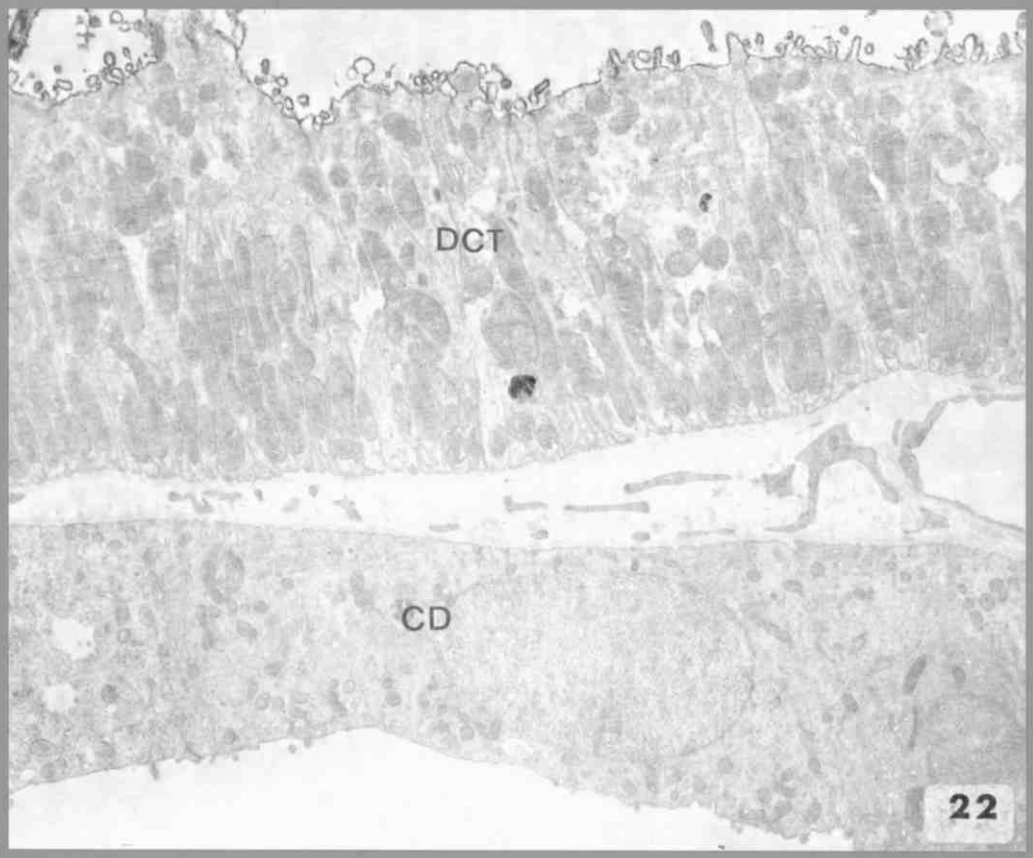

ALH
TLH
21

Fig 22. Identification of T-H glycoprotein by immunoelectron microscopy on the luminal surface of DCT cells and its absence on those of the CD. Fixation and staining procedures were as in Fig 19. Magnification x 10,000.

Fig 23. Photomicrograph from a ultrathin section cut very close to the surface of a 20 μm thick cryostat section, showing the presence of T-H on the luminal border (lb) of a cell of DCT. Traces of the reaction can also be seen in the lateral (lpm) as well as basal plasma membrane (bpm) including its invaginations and also perhaps in the cisternae of endoplasmic reticulum (er). Fixation and staining procedures were similar to those used for Fig 19. Magnification x 12,000.


DCT
CD
22

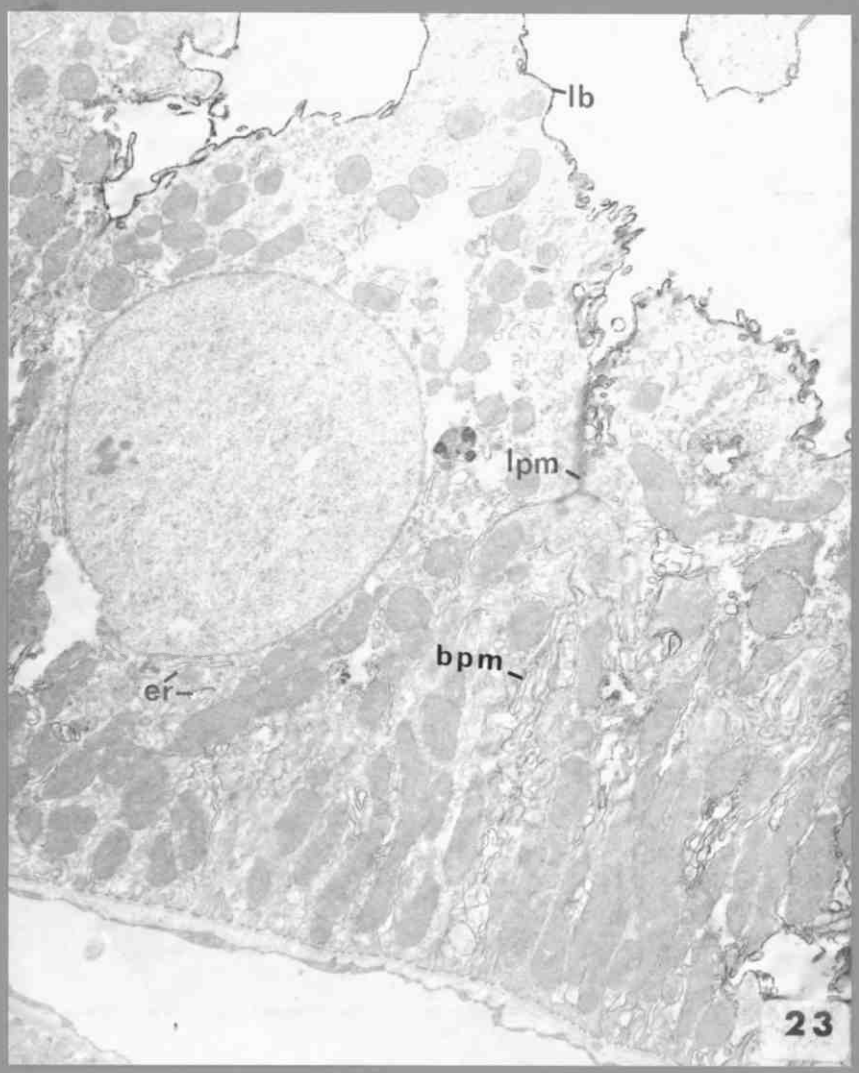
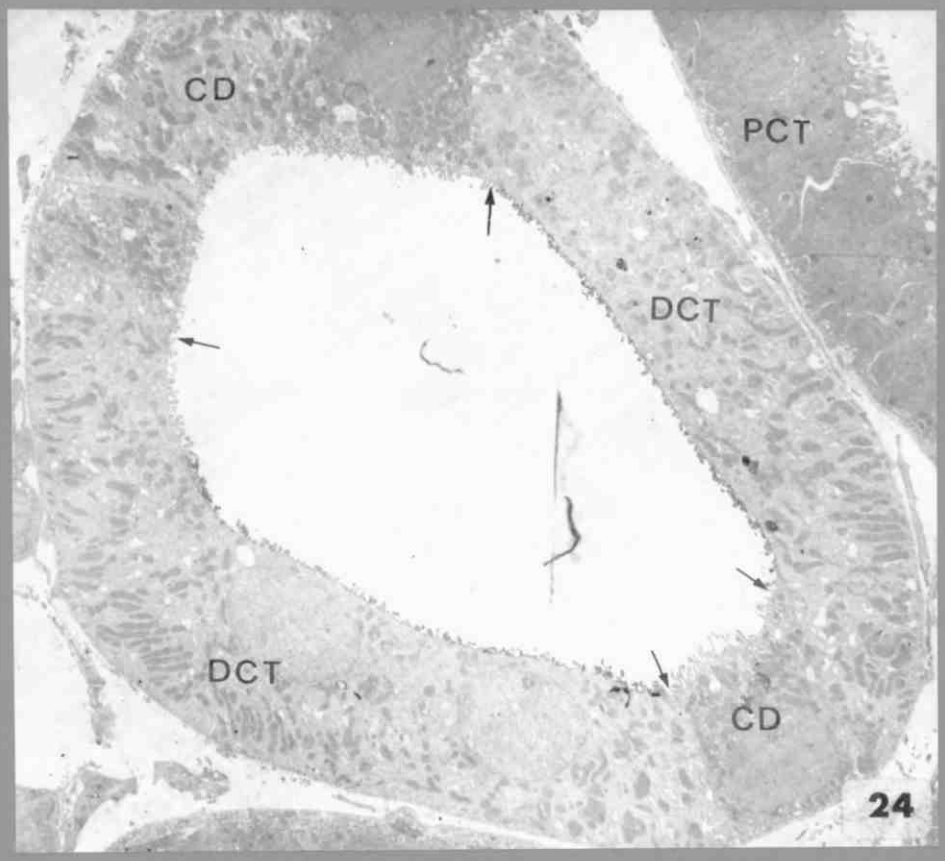

lb
lpm
bpm
er
23

Fig 24. A section of the hamster renal cortex, showing the junctions of the CD with the DCT (arrows). T-H is present on the luminal surface of the cells of the DCT and absent on those of the CD. Fixation and staining procedures were as in Fig 19. Magnification x 7,500.

Fig 25. The presence of T-H glycoprotein on the luminal border (lb), lateral plasma membrane (lpm) and the basal plasma membrane (bpm) including its infolding, of a cell of the DCT. Fixation was by perfusion with PLP (containing 2% paraformaldehyde). Staining was carried out by the method of Nakane and Kawaoi (1974). Note that by the use of PLP as the fixative, T-H is demonstrable in a much greater area of the plasma membrane system as compared with that obtained by paraformaldehyde-glutaraldehyde fixation (Figs. 19-24). Magnification x 15,000.


CD
PCT
DCT
DCT
CD
24

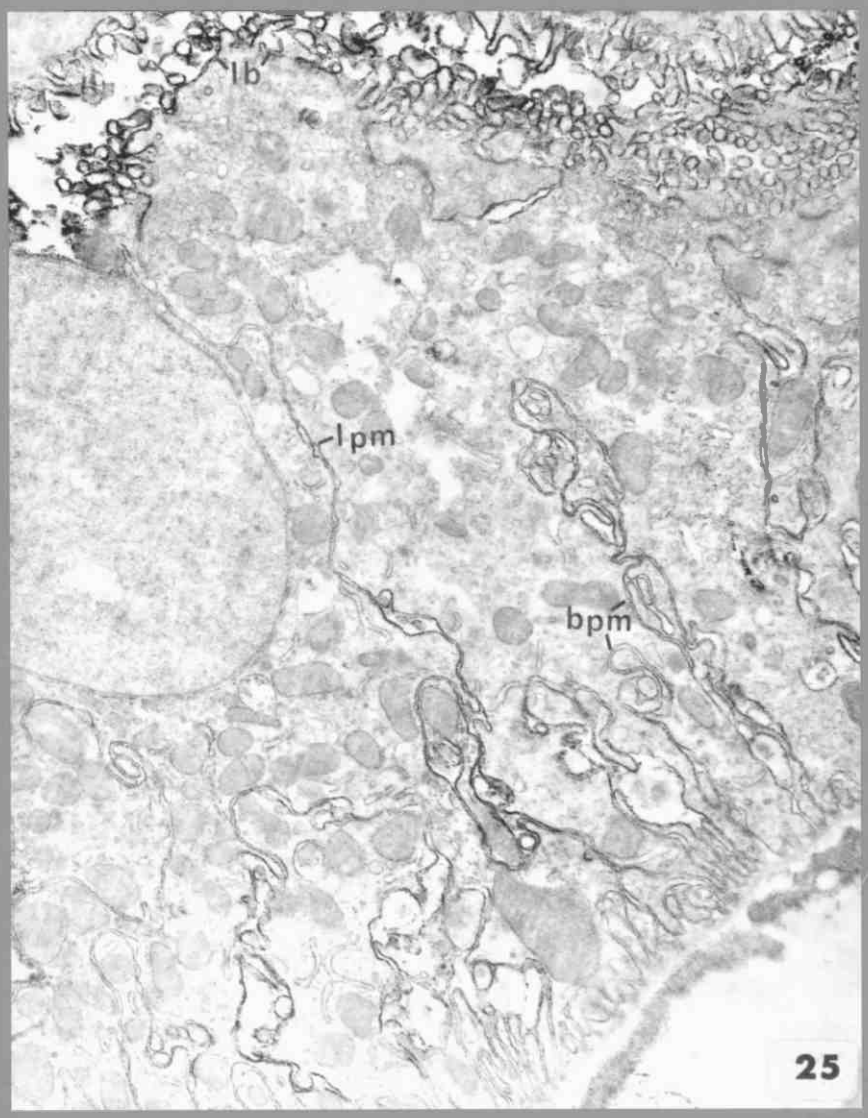
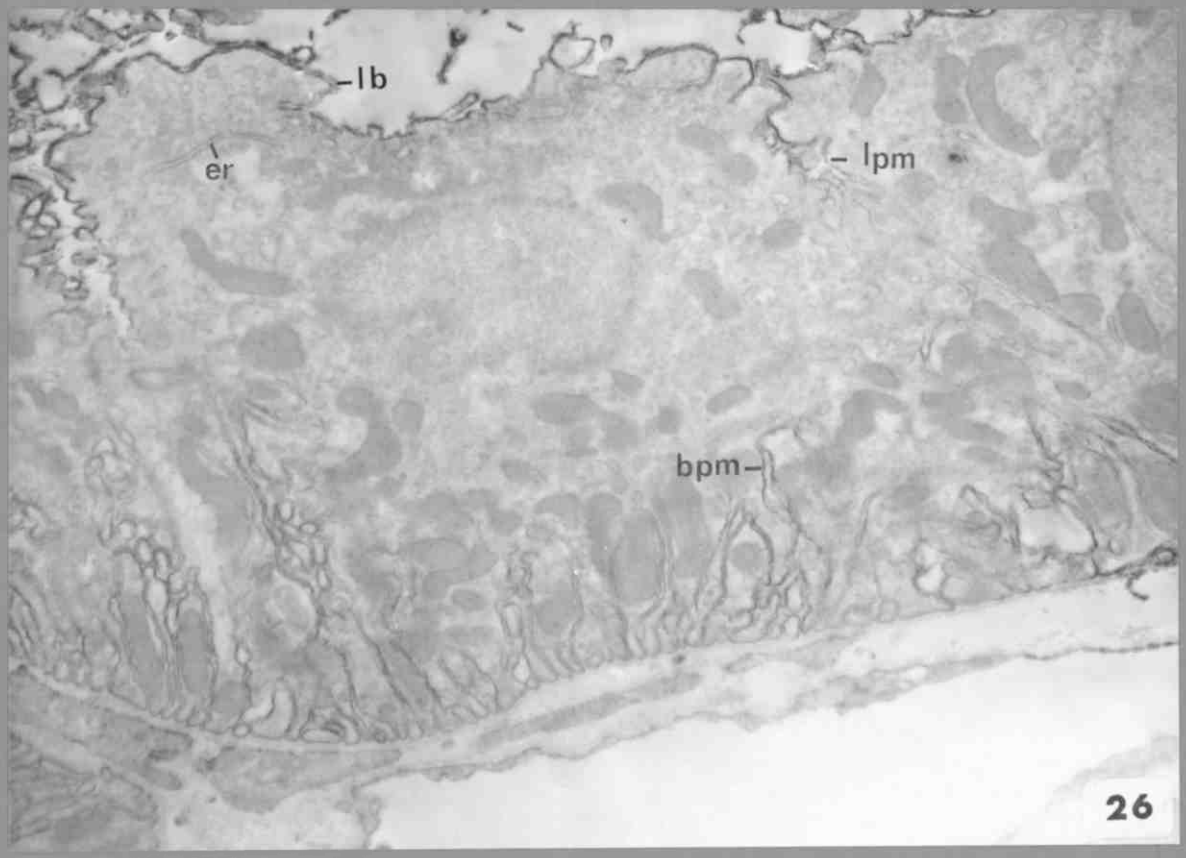

lb
lpm
bpm
25

Fig 26. The presence of T-H glycoprotein in a cell of the ALH of the hamster kidney. Fixation and staining procedures were similar to those used for Fig. 25. Once again, the glycoprotein is seen on the luminal border border (lb), lateral plasma membrane (lpm), basal plasma membrane (bpm) including its infolding and also perhaps in the cisternae of endoplasmic reticulum (er). Fixation and staining as in Fig. 25. Magnification x 12,000.

Fig 27. A high power electron micrograph of a DCT cell of the hamster kidney showing the presence of T-H on the luminal border (lb), lateral plasma membrane (lpm) and Golgi body (g). Fixation and staining procedures were as in Fig. 25. Magnification x 30,000.


lb
er
lpm
bpm
26

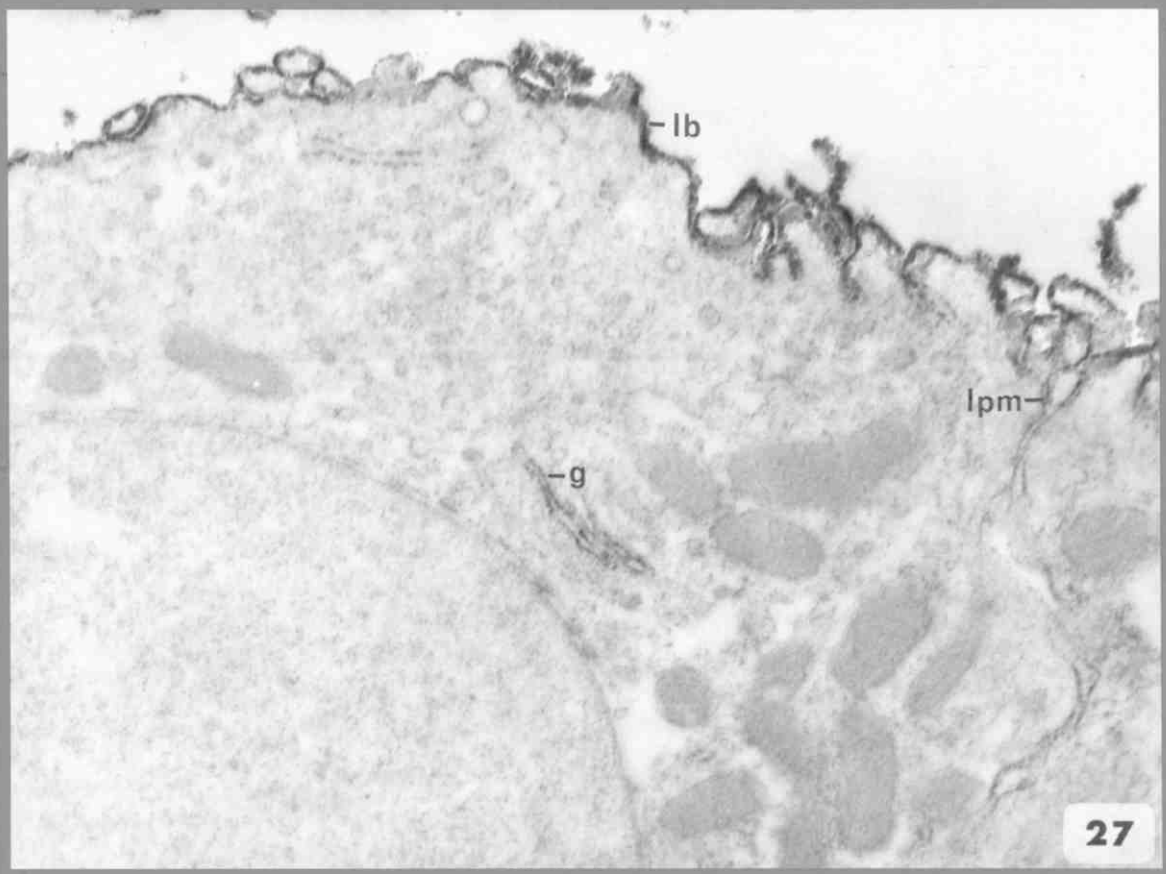
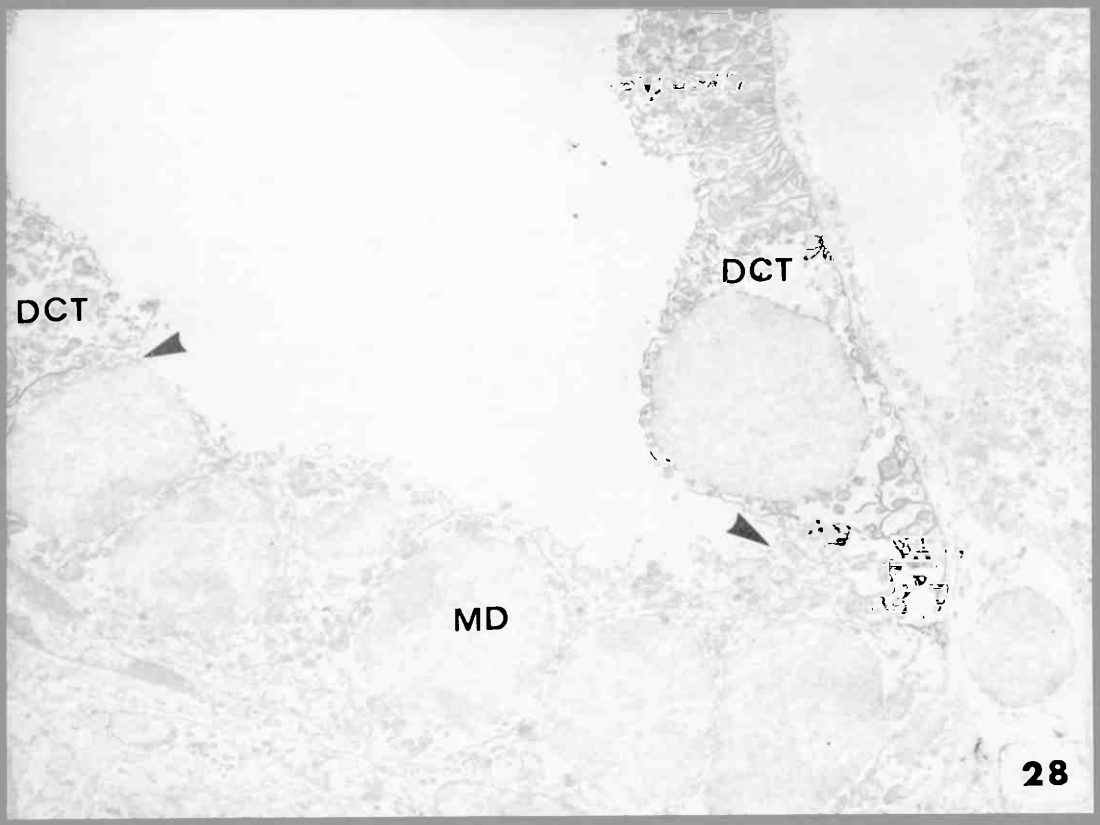
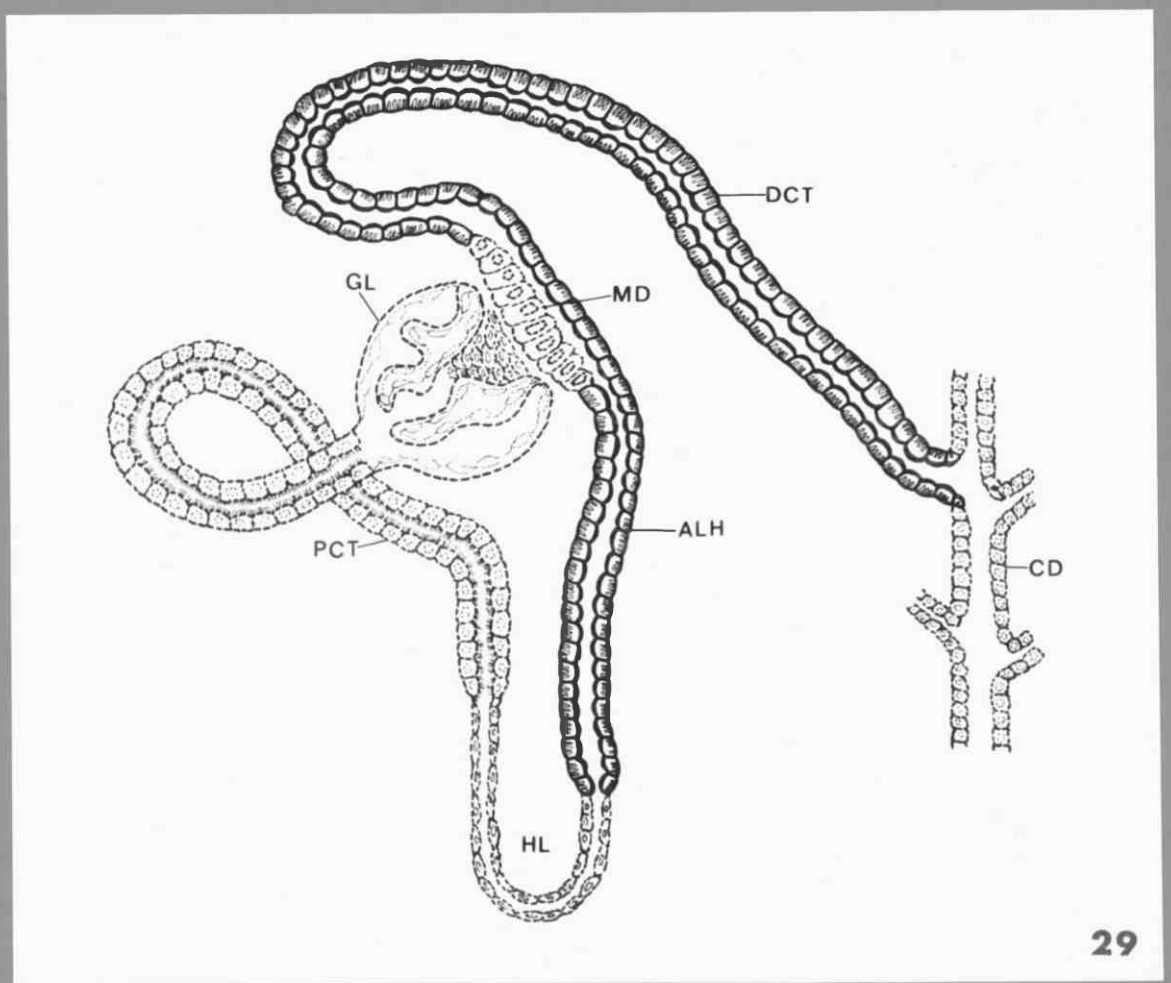

lb
lpm
g
27

Fig 28. Immunoelectron micrograph of a MD of the hamster kidney. No reaction is visible either on the luminal border or in the intracellular membranes of its cells. On the other hand, the plasma membrane system of the cells of DCT opposite to the MD are positive for the T-H specific reaction. Fixation was in PLP (containing 1% paraformaldehyde). Thus, because of the slightly less concentrated fixative used, the overall fixation is somewhat poor. Magnification x 10,000.

Fig 29. Diagram of a single nephron of the hamster kidney showing the distribution of T-H in the cells ALH and DCT and its absence in those of the PCT, thin descending and ascending limb of loop of Henle, glomerulus (GL) and CD. The presence of a T-H specific reaction in the ALH and DCT is indicated by dark bold lines.



28



29

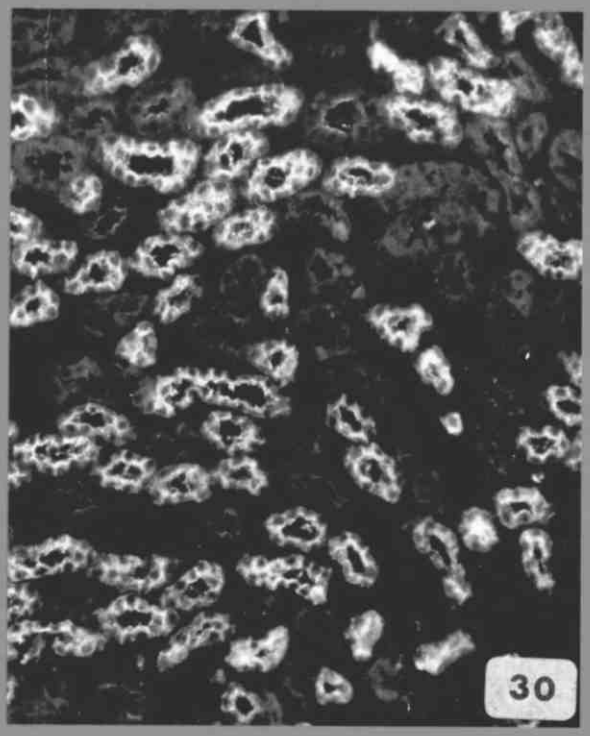
N.B. Figs. 30-36 are from a surgically removed human kidney. The material was fixed by immersion and Figs. 30-33 were taken on an epifluorescence microscope.

Fig 30. Localization of T-H glycoprotein in the adult human kidney. Specific fluorescent staining in the cells of ALH and DCT of the inner cortex. Fixation with formal calcium chloride. Magnification X 240.

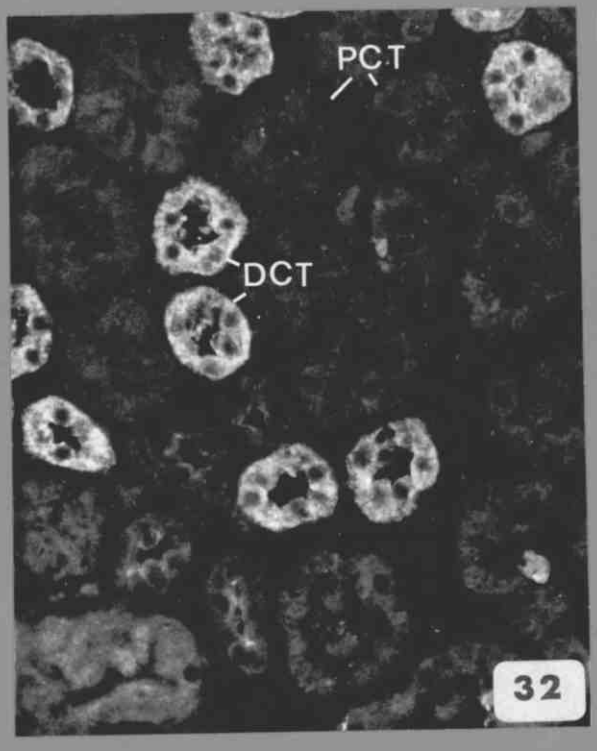
Fig 31. Adult human kidney, outer medullary zone. Specific fluorescent staining indicating the presence of T-H, is seen in the cells of ALH which lie among the CD which are unstained. Fixation as in Fig. 30. Magnification X 350.

Fig 32. Outer cortical zone of the adult human kidney showing the uniform distribution of T-H specific fluorescence in the cells of DCT. Cells of PCT are unstained. Magnification x 600.

Fig 33. Human kidney. In the cortex, specific fluorescent staining is present in the cells of DCT. Cells of the MD along with those of PCT and the glomerulus (GL) are negative. Magnification x 750


30


31


PCT
DCT
32

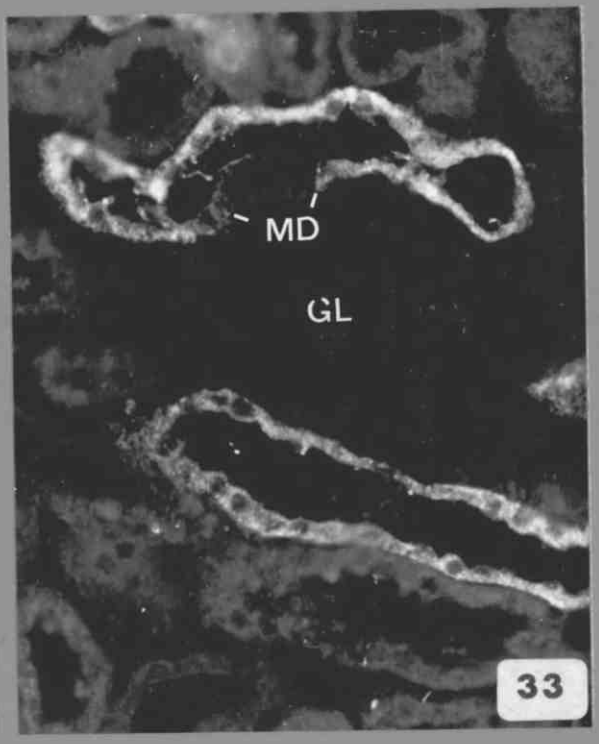
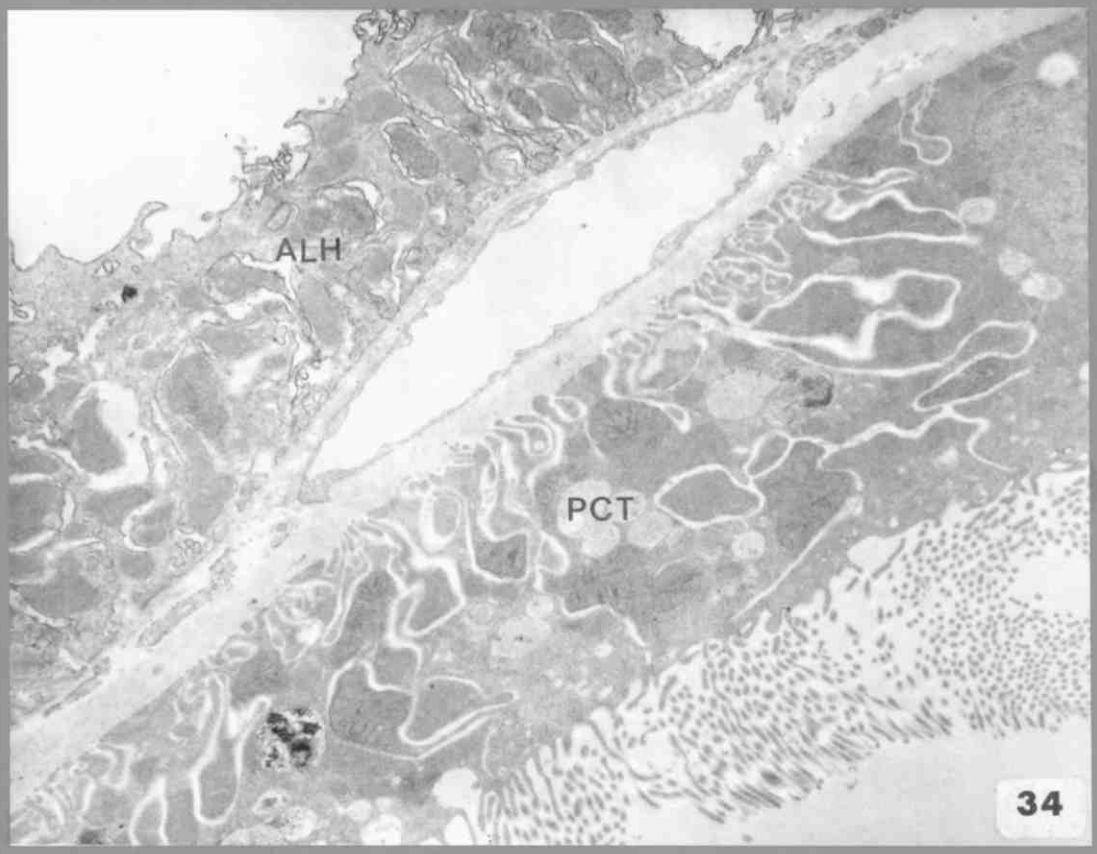

MD
GL
33

Fig 34. Electron micrograph of adult human kidney fixed by immersion in PLP and stained immunologically for T-H glycoprotein by the method of Nakane and Kawaoi. Deposits of the reaction product are present in the plasma membrane system of the cells of the ALH, while it is totally lacking in those of the PCT. Magnification x 15,000.

Fig 35. Electron micrograph of a DCT of the adult human kidney fixed and stained as in Fig. 34. Once again the immunoperoxidase reaction is seen in the plasma membrane system. The apparent positive reaction in some of the cristae mitochondrion (m) is unusual. Magnification x 17,000.


ALH
PCT
34

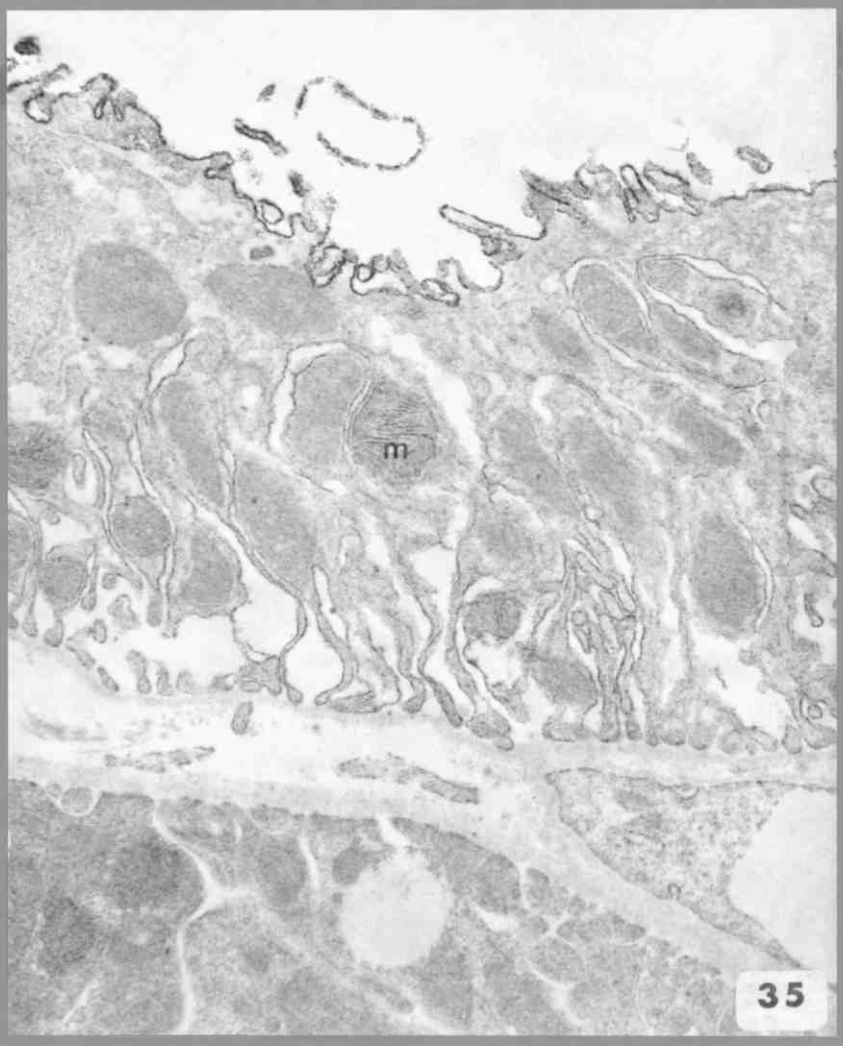
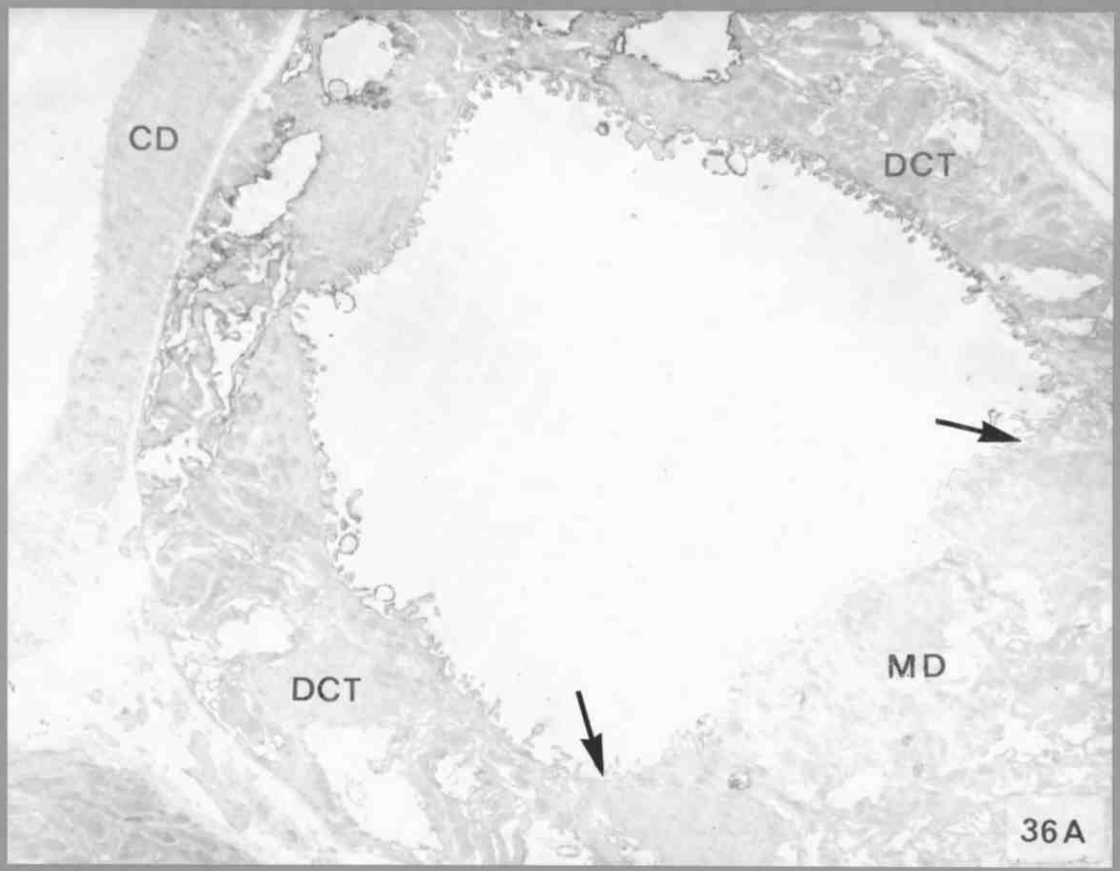

m
35

Fig 36A. Adult human kidney. Cells of the MD and CD can be seen to be devoid of the glycoprotein, while it is present in patches in the membrane system of the DCT cells. This patchyness is probably a consequence of the immersion fixation. Fixation and staining procedures were similar to those used for Fig. 34. Magnification x 10,000.

Fig 36B. A part of the MD of the adult human kidney at higher magnification. Note, the junction of a T-H containing DCT cell with that of the adjacent MD cells which almost completely lack the glycoprotein.
Magnification X 22,000.


CD
DCT
DCT
MD
36A

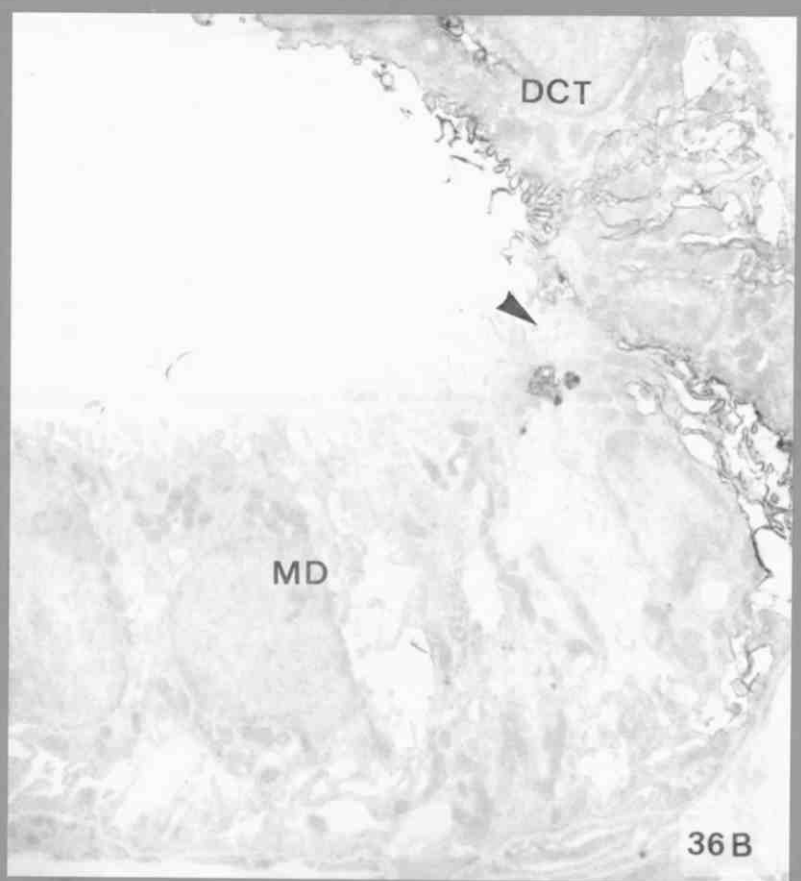

DCT
MD
36B

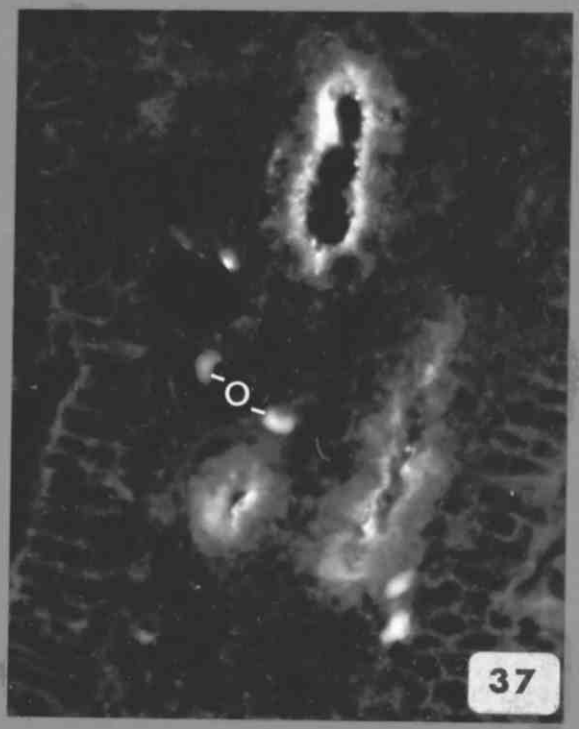
Fig 37. Foetal hamster kidney, 12 days post coitum. Positive fluorescent staining is present predominantly on the luminal border of distal tubules (undifferentiated ALH) of the medulla. (Also see Fig. 45). Fixation by immersion in formal calcium chloride. Magnification x 500.

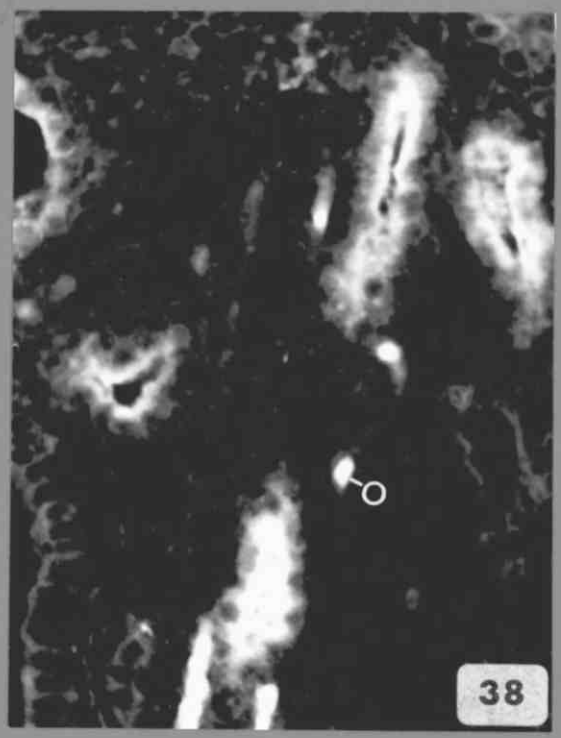
Fig 38. Foetal hamster kidney, 14 days post coitum. Distal tubules with predominantly luminal T-H positive staining are once again seen in the medulla. Note that the intensity of fluorescence is greater than seen on the 12th day (Fig.37). Also see Fig. 46. Magnification x 500.

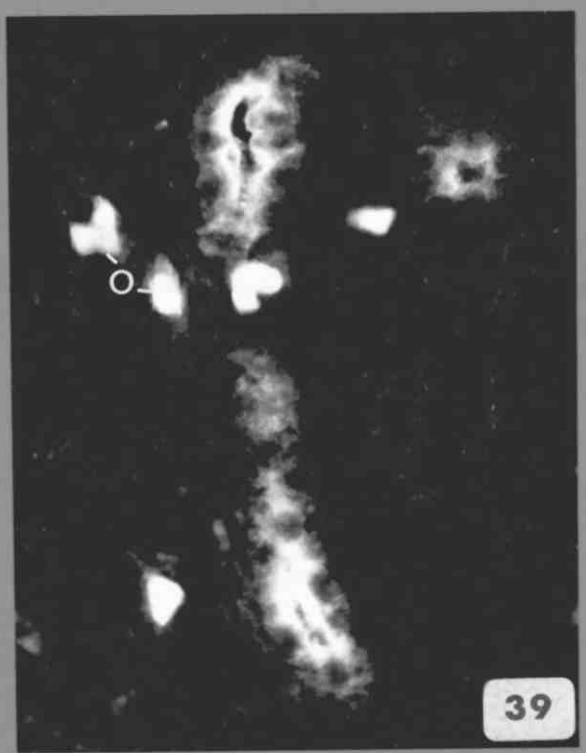
Fig 39. T-H positive staining of foetal hamster kidney obtained after 14 days post coitum. Distal tubules in the inner cortical region showing positive fluorescent staining mainly on the luminal border. Magnification x 550.

Fig 40. Foetal hamster kidney obtained on 15th day post coitum. Rays of positively stained tubules can be seen extending from deep in the medulla (M) towards the presumed cortical region (C). Magnification x 400.

(N.B. In Figs. 37-39, the objects labelled as '0' which did not fluoresce green are presumably artifacts). Also, Figs. 37-44 were photographed on an epifluorescence microscope).


O
37


O
38


O
39

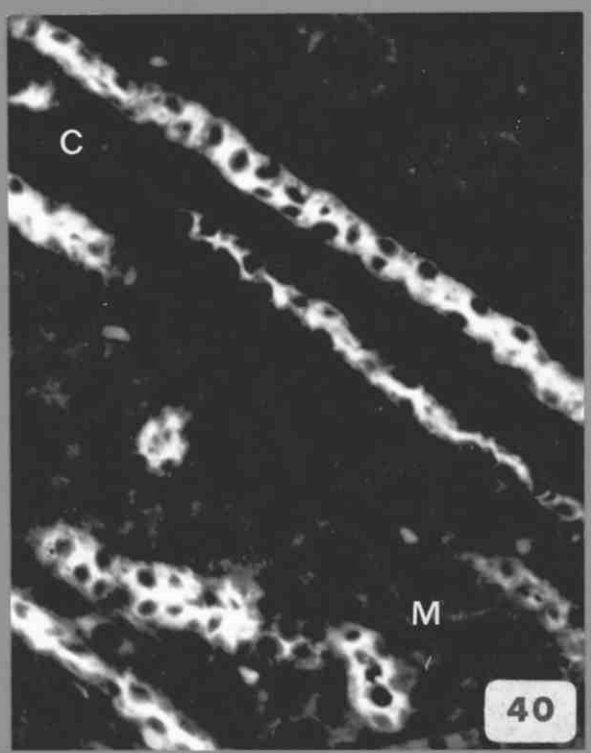
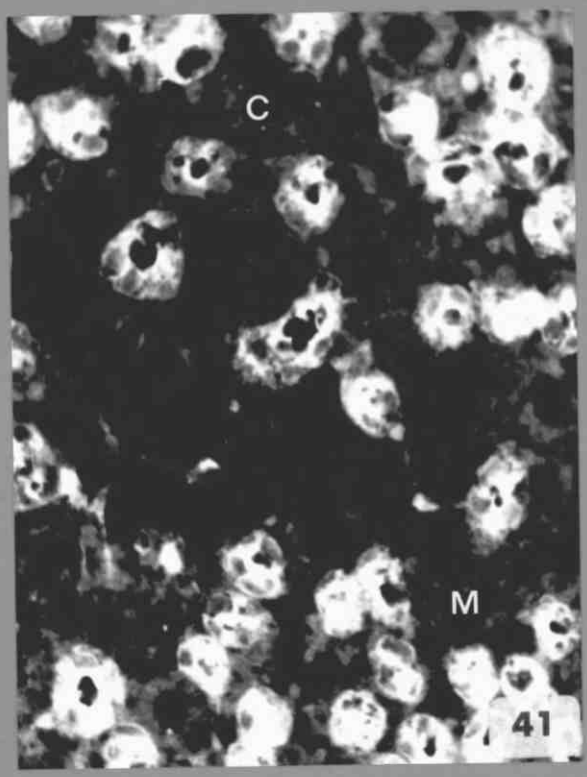

C
M
40

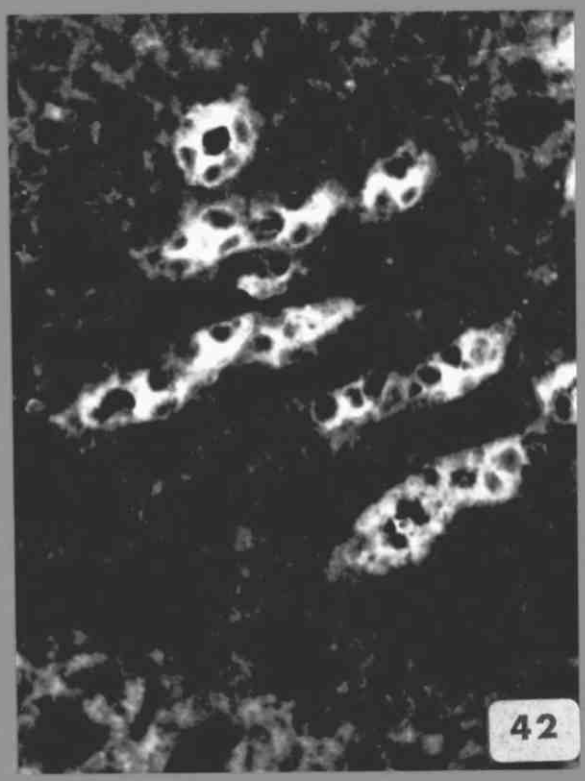
Fig 41. Hamster kidney obtained 1 day after birth, demonstrating positive T-H staining of distal tubules in the medulla (M) and in the cortex (C). Magnification x 400.

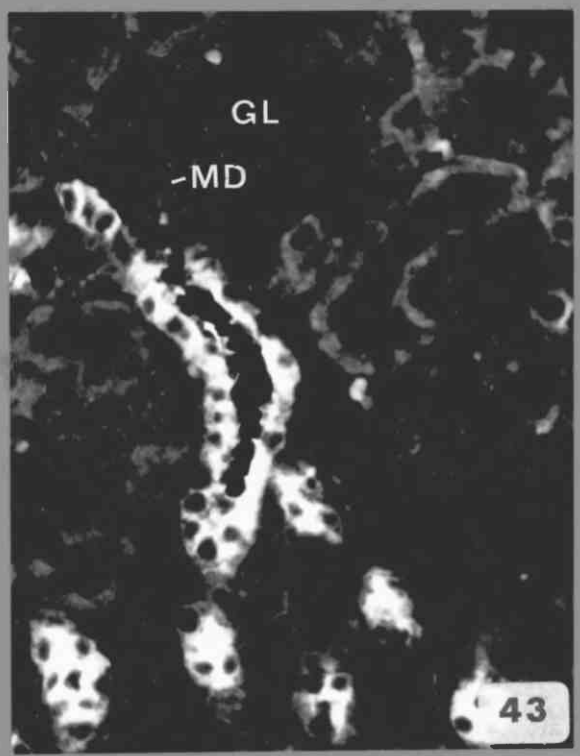
Fig 42. T-H staining of the hamster kidney obtained 3 days after birth. Positive fluorescent staining can be seen in the cells of medullary ALH. Magnification X 400.

Fig 43. 3 days old hamster kidney. Cells of the MD can be seen to be devoid of T-H specific fluorescence. (GL), Glomerulus. Magnification x 400.

Fig 44. T-H staining of 23 days old hamster kidney. Fluorescence is seen in presumably both, ALH and DCT. Nuclei (n) of the cells of these tubules can be seen to lack the glycoprotein. Magnification x 400.


C
M
41


42


GL
MD
43

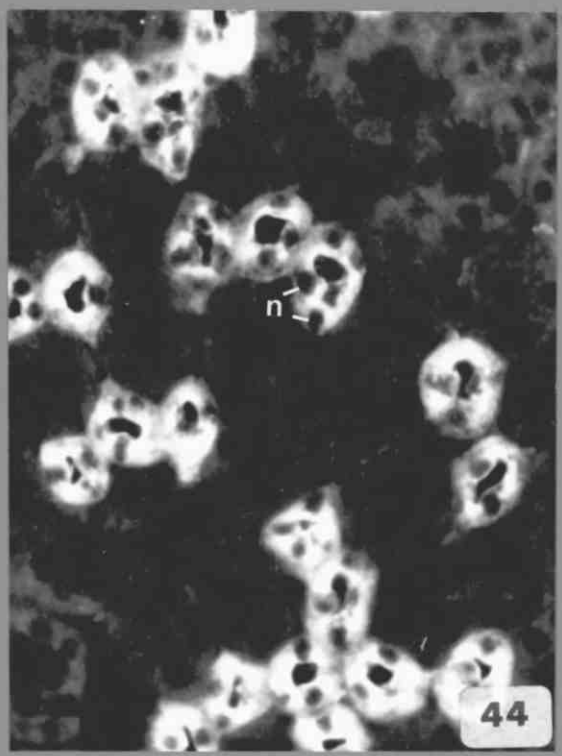
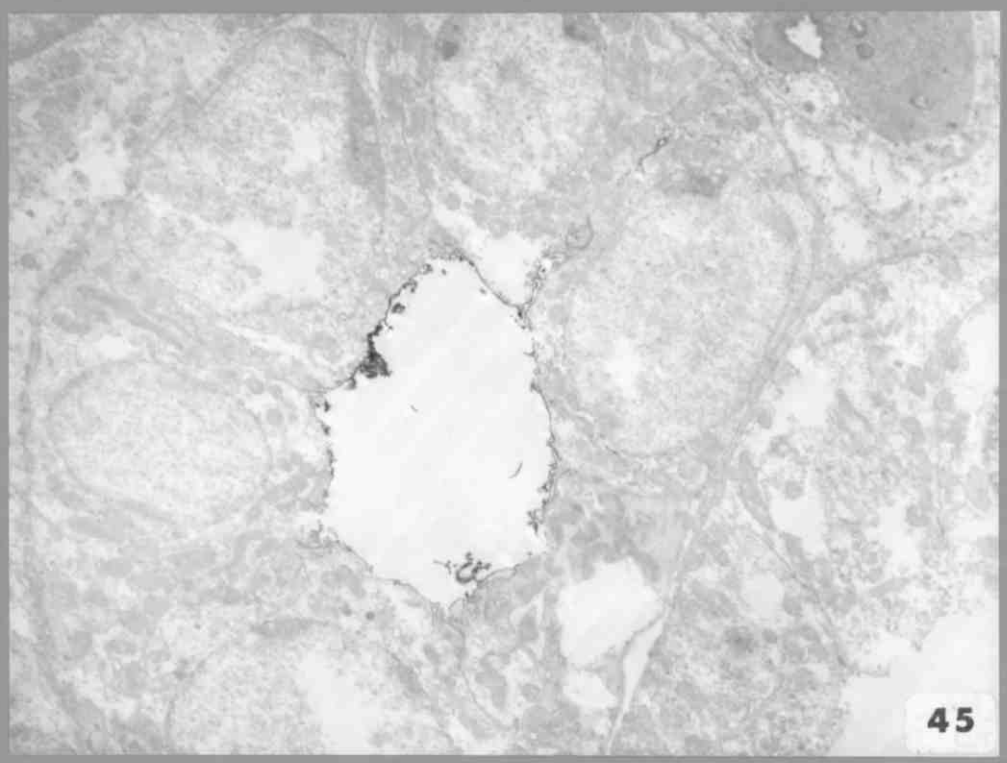
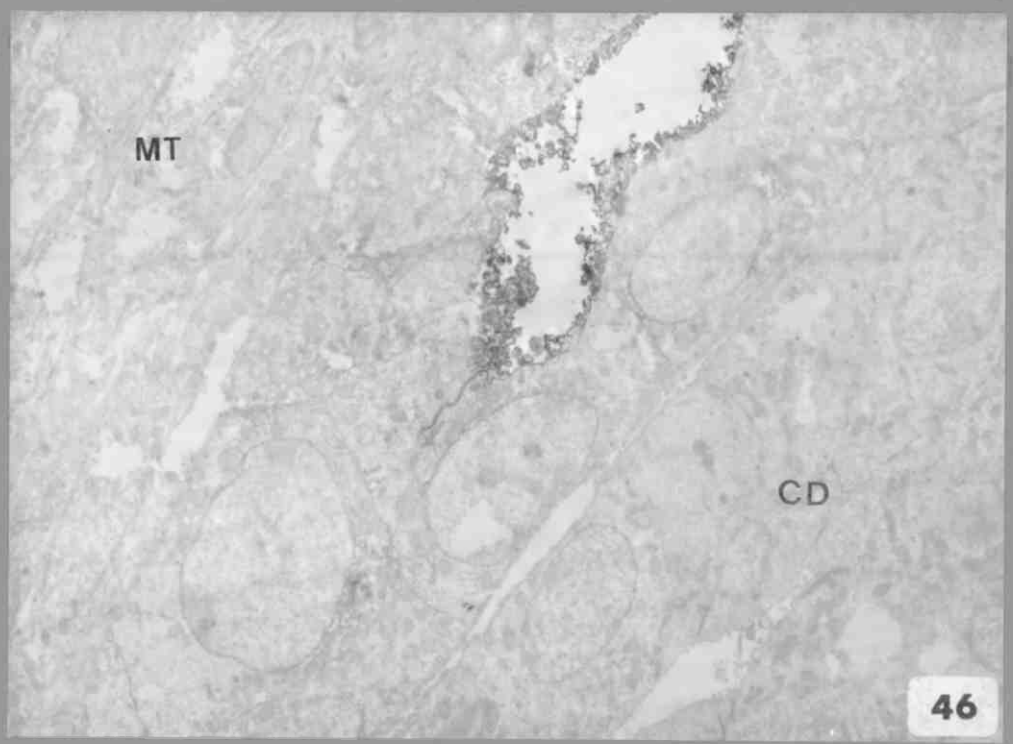

n
44

Fig 45. Localization of T-H glycoprotein in the 12 days foetal hamster kidney by immunoelectron microscopy. The reaction is almost exclusively confined to the luminal border (lb) of the medullary distal tubules (Also see Fig. 37). Fixation by immersion with PLP and staining by the method of Nakane and Kawaoi. Magnification x 15,000.

Fig 46. 13 days foetal hamster kidney. The intensity of T-H positive peroxidase reaction on the luminal border (lb) of the distal tubule is slightly more than seen on 12th day (also see Fig. 38). Cells of the CD and mesenchymal tissue (MT) do not show any reaction. Magnification x 10,000.



45

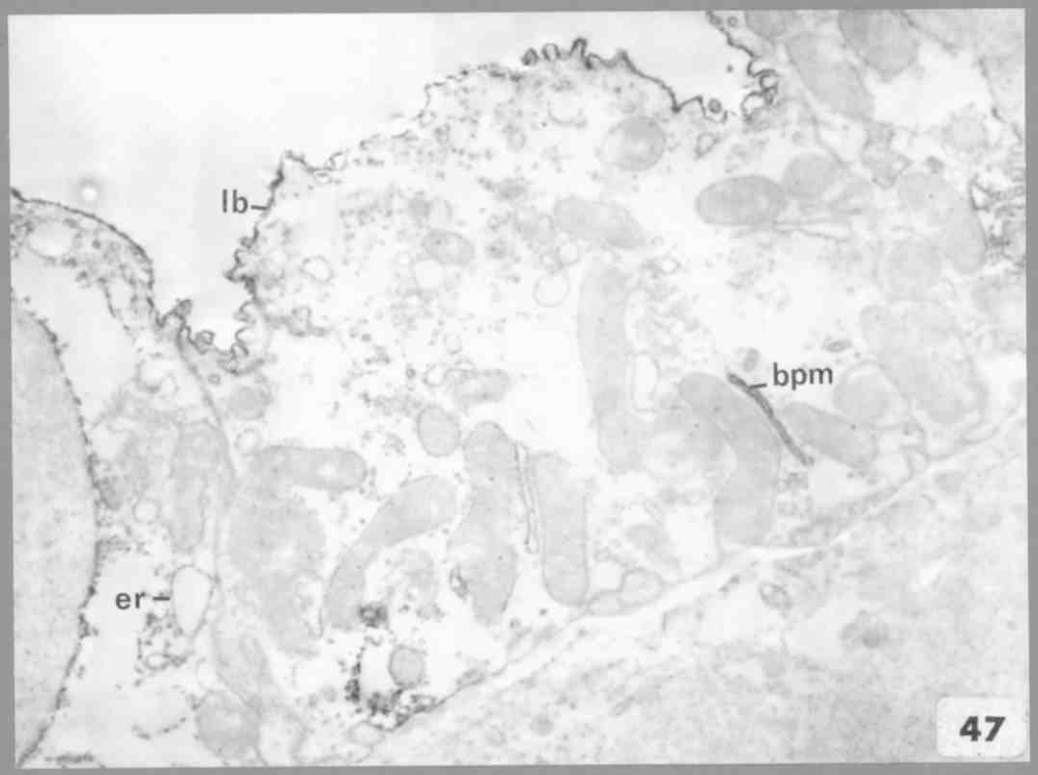


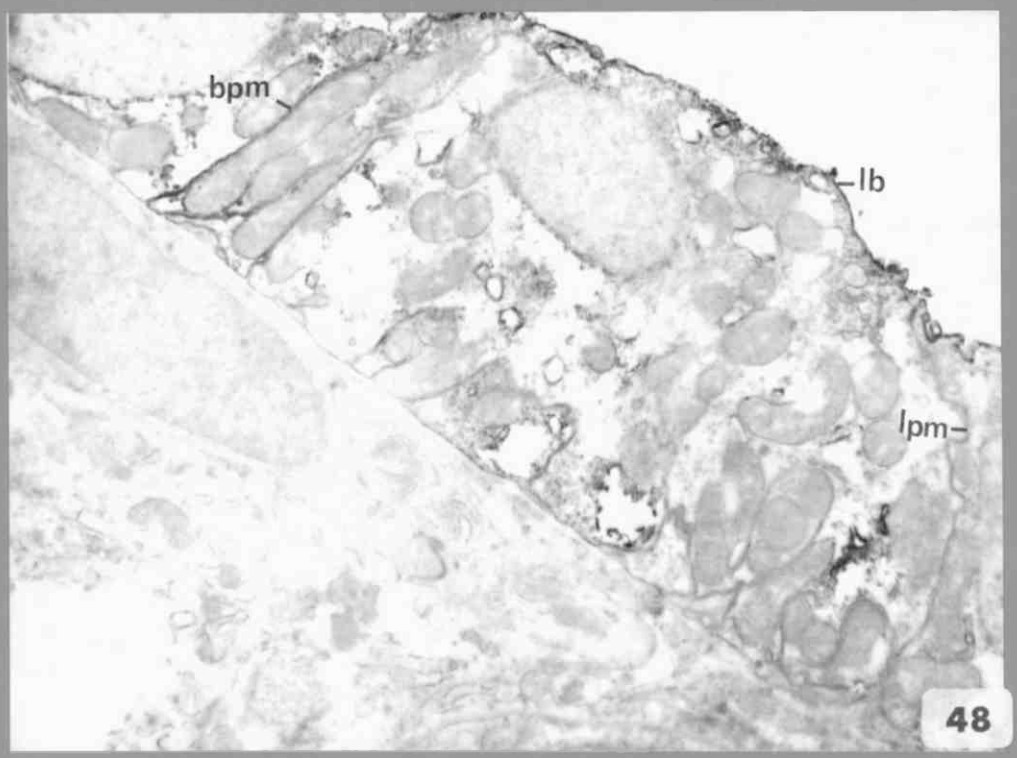
46

Fig 47. Immunoperoxidase staining for T-H in the 14 days foetal hamster kidney. Along with the prominently stained luminal border (lb), a slight amount of scattered staining is also seen in the invaginations of the basal plasma membrane (bpm) and also perhaps in the endoplasmic reticulum (er). Method of fixation and staining procedures were similar to those used for Fig 45. Magnification x 20,000.

Fig 48. 4 days old hamster kidney fixed by immersion with PLP and stained by the method of Nakane and Kawaoi. The reaction product is seen to be associated not only with the luminal border (lb) but also with the lateral membranes (lpm), invaginations of the basal plasma membrane (bpm) and also perhaps with the endoplasmic reticulum (er) of a cell of the DCT. Magnification x 20,000.

(N.B. On account of the immersion fixation used in Figs. 45-48, the cell preservation is poor and the reaction product has a somewhat patchy distribution).


lb
bpm
er
47


bpm
lb
lpm
48

(N.B. Figs 49-55 were taken on an epifluorescence microscope).

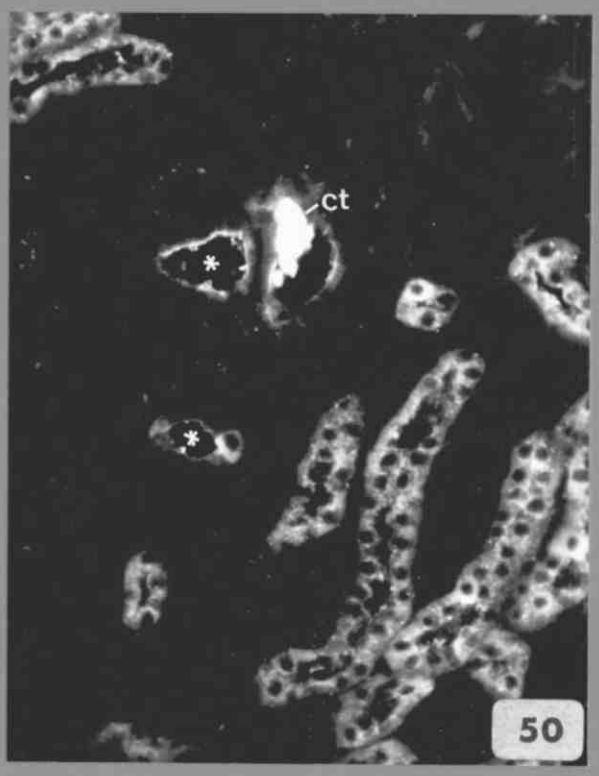
Fig 49. 4 days adrenalectomized hamster kidney showing a marked reduction in the amount of T-H specific fluorescence in the cells of some of the DCT of the outer cortex (*). In the affected tubules, such a reduction is seen mainly in the basal parts of the cells. Fixation by perfusion with formal calcium chloride. Magnification x 500.

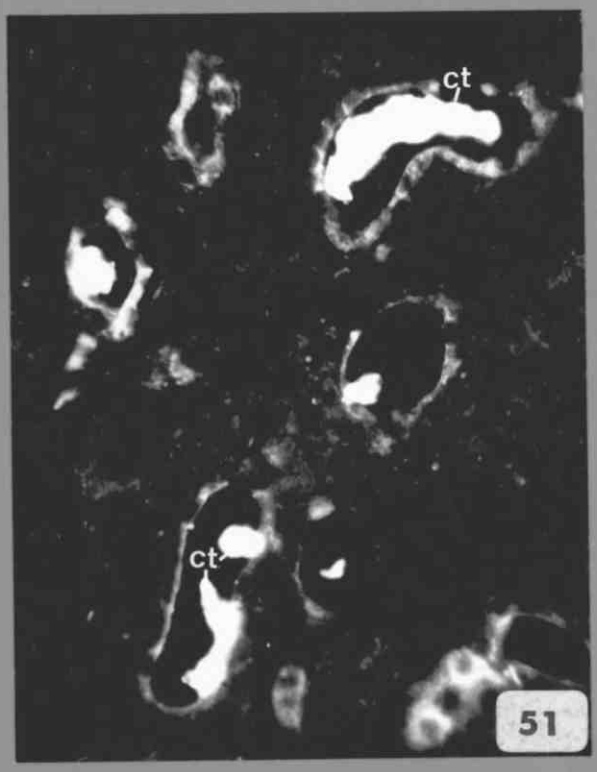
Fig 50. 4 days adrenalectomized hamster kidney. As in Fig 49, cells of some of the DCT (*) clearly shows disappearance of T-H glycoprotein. Also the lumen of one of the affected DCT is seen to contain brilliantly fluorescing cast (ct). Fixation as in Fig 49. Magnification x 500.

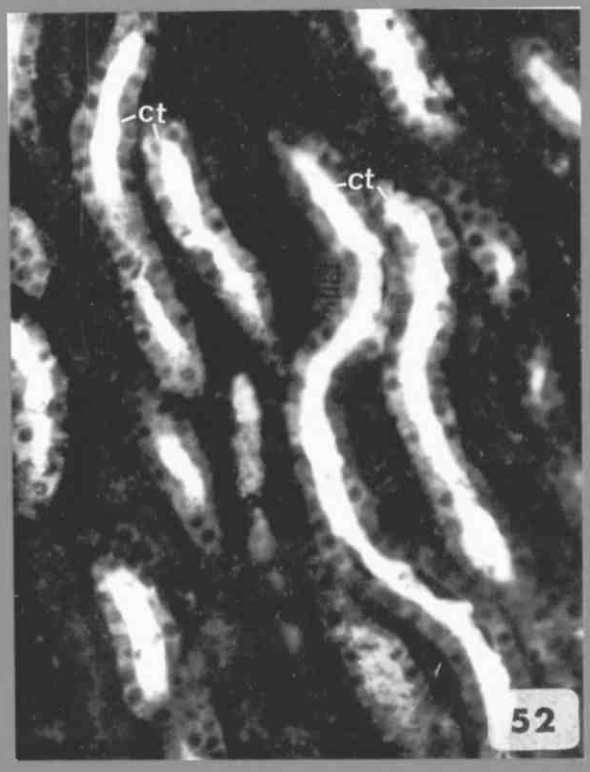
Fig 51. Section from the cortex of the 6 days adrenalectomized hamster kidney. Note that the cells of almost all the DCT have been affected and thus show a varying degree of reduction of T-H. Furthermore, the lumina of these tubules are seen to be filled with the brilliantly fluorescing casts. Fixation as in Fig. 49. Magnification x 500.

Fig 52. Section from the outer medulla of a 6 days adrenalectomized hamster kidney. The loss of T-H is also seen in the cells of ALH. As in the DCT (Fig 51), the lumina of ALH is also filled with the fluorescing casts (ct). Fixation as in Fig 49. Magnification x 450.


*
*
49

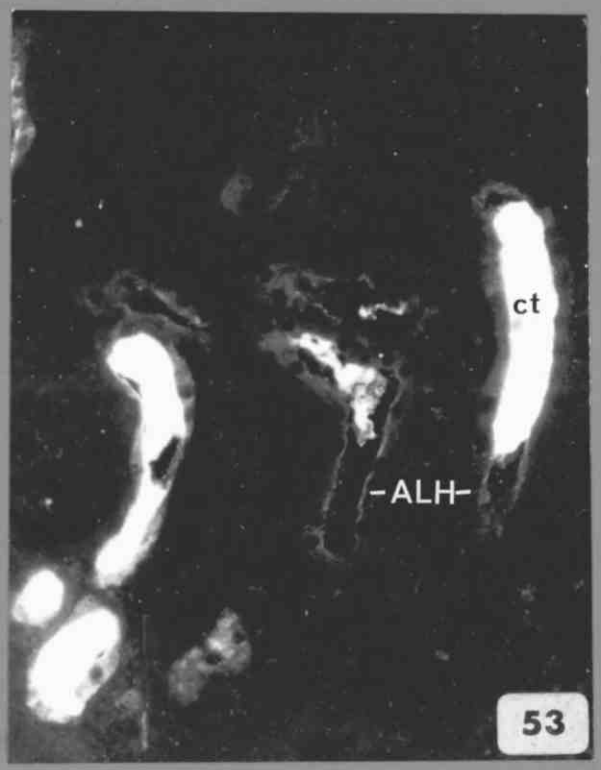

ct
*
*
50

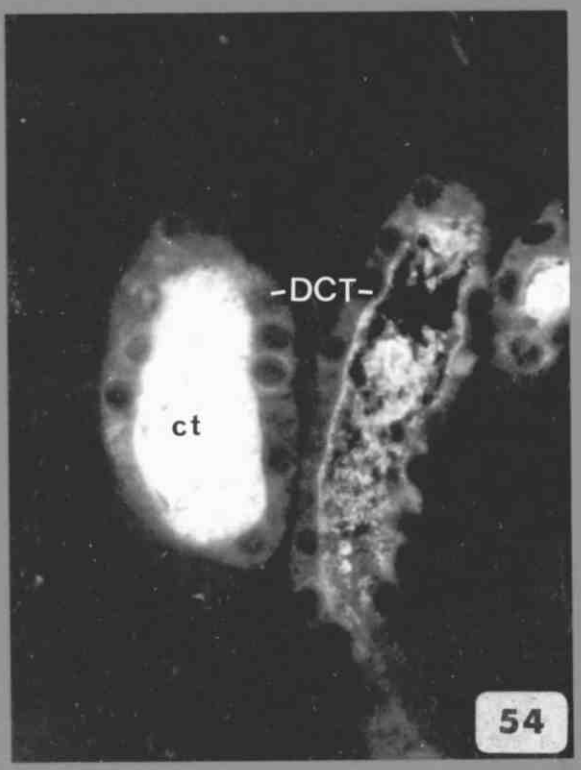

ct
ct
51


ct
ct
52

Figs 53 & 54. The loss of T-H is even more apparent in the cells of ALH (Fig 53) and DCT (Fig 54)of the 8 days adrenalectomized hamster. Furthermore, almost all the tubules are seen to be blocked with brilliantly fluorescing casts. Fixation as in Fig 49. Magnification x 640.

Fig 55. Kidney section from the inner cortex of a control hamster killed 8 days after the sham operation. Note that no casts are present in the lumina of ALH and DCT and their cells are fluorescing brilliantly. Fixation as in Fig 49. Magnification x 320.


ct
-ALH-
53


-DCT-
ct
54

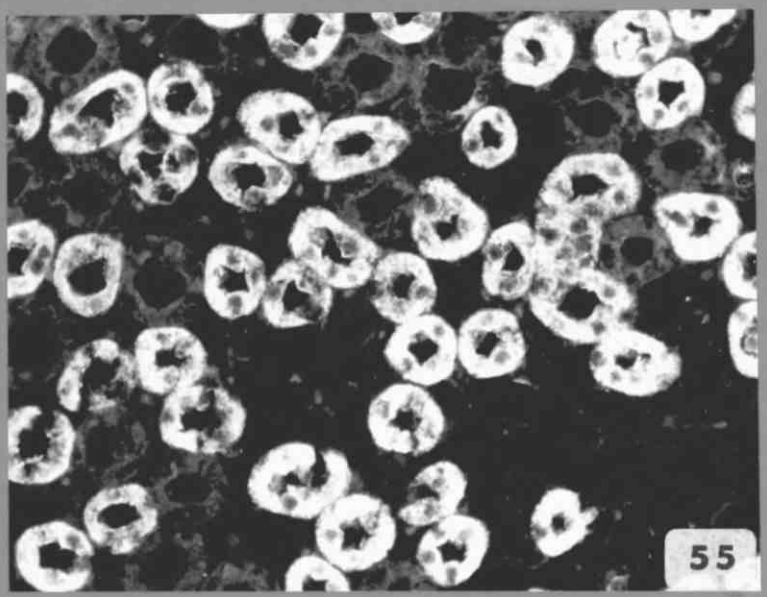
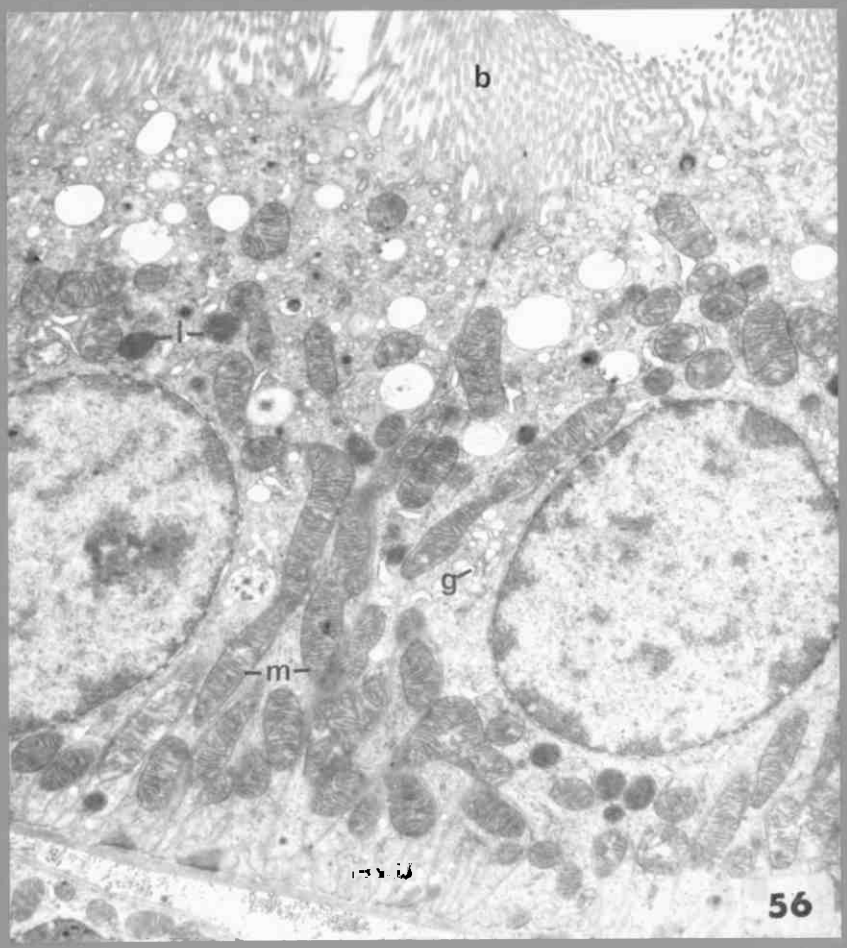
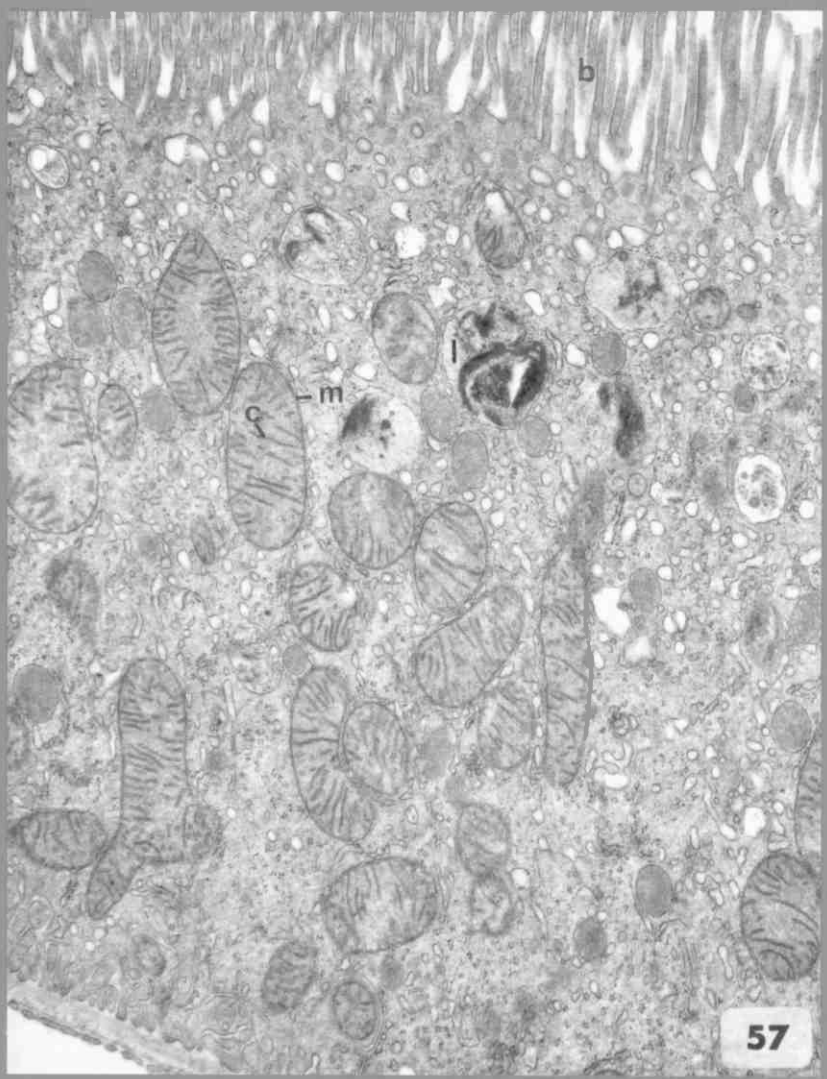
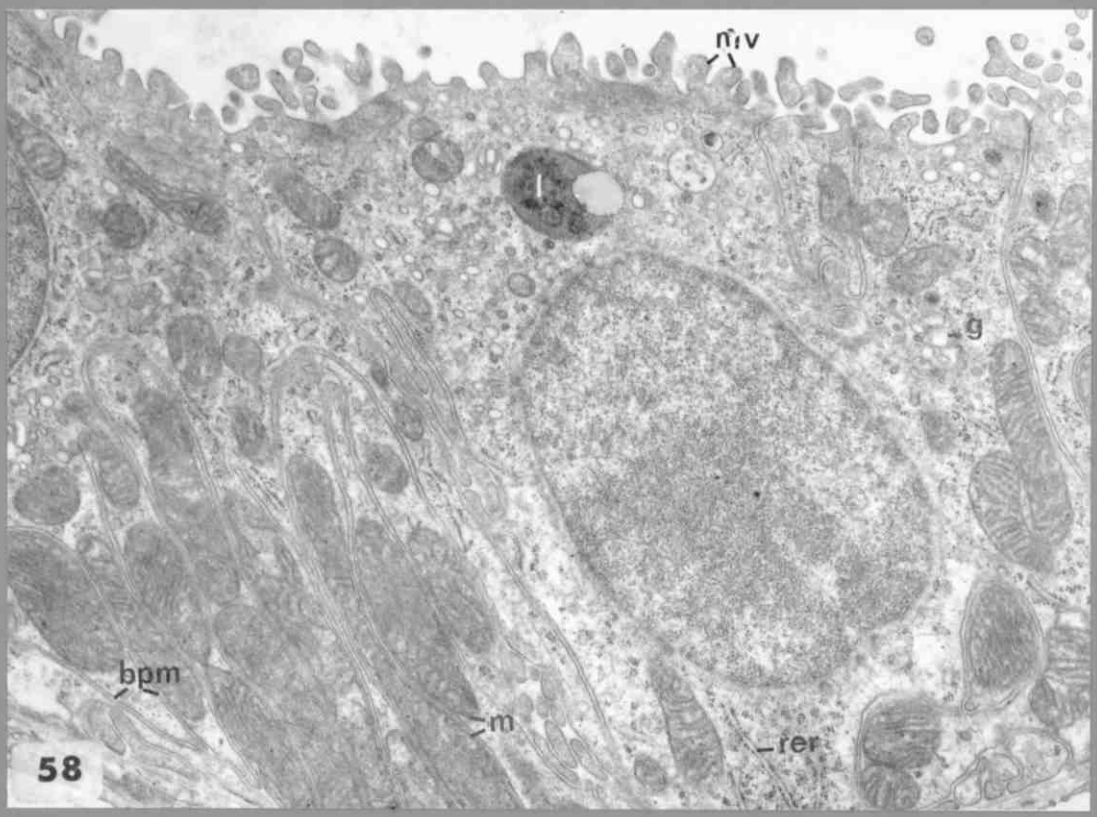

55

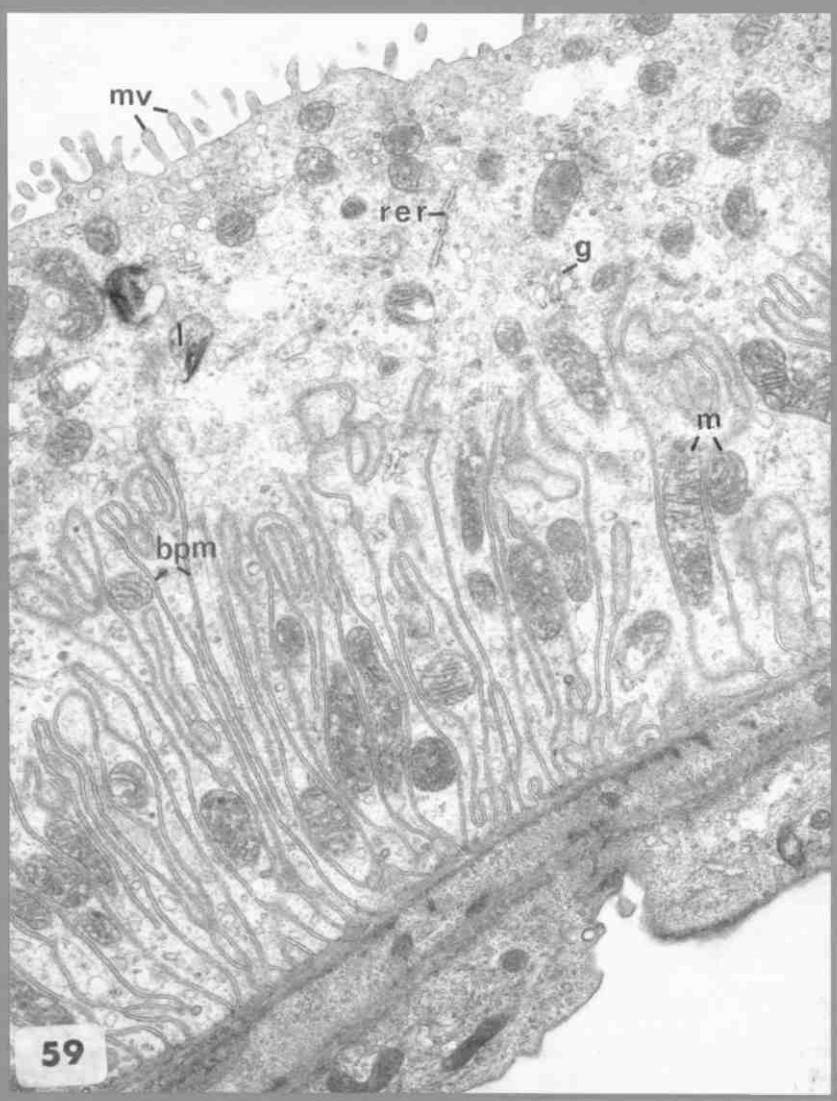
Fig 56 & 57. In the 8 days adrenalectomized hamster kidney fixed in ½ strengthened Karnovsky's fluid (Fig 56), there seem to be no significant alterations in the ultrastructure of any of the important cell organelles (e.g. mitochondria, 'm'; Golgi body, 'g' and lysosomes, 'l' etc.) of the cells of the PCT, when it is compared with those of the normal animal (Fig 57). A well developed brush border (b) is apparent in both cases. Similarly, the size and shape of the mitochondria (m) and the arrangement of their cristae (c) of the adrenalectomized animal also, compare favourable with those of the normal animal. After post fixation in osmium tetroxide, the section was stained with lead citrate and uranyl acetate. Magnifications x 15,000 and x 20,000 respectively.


b
l
g
m
56

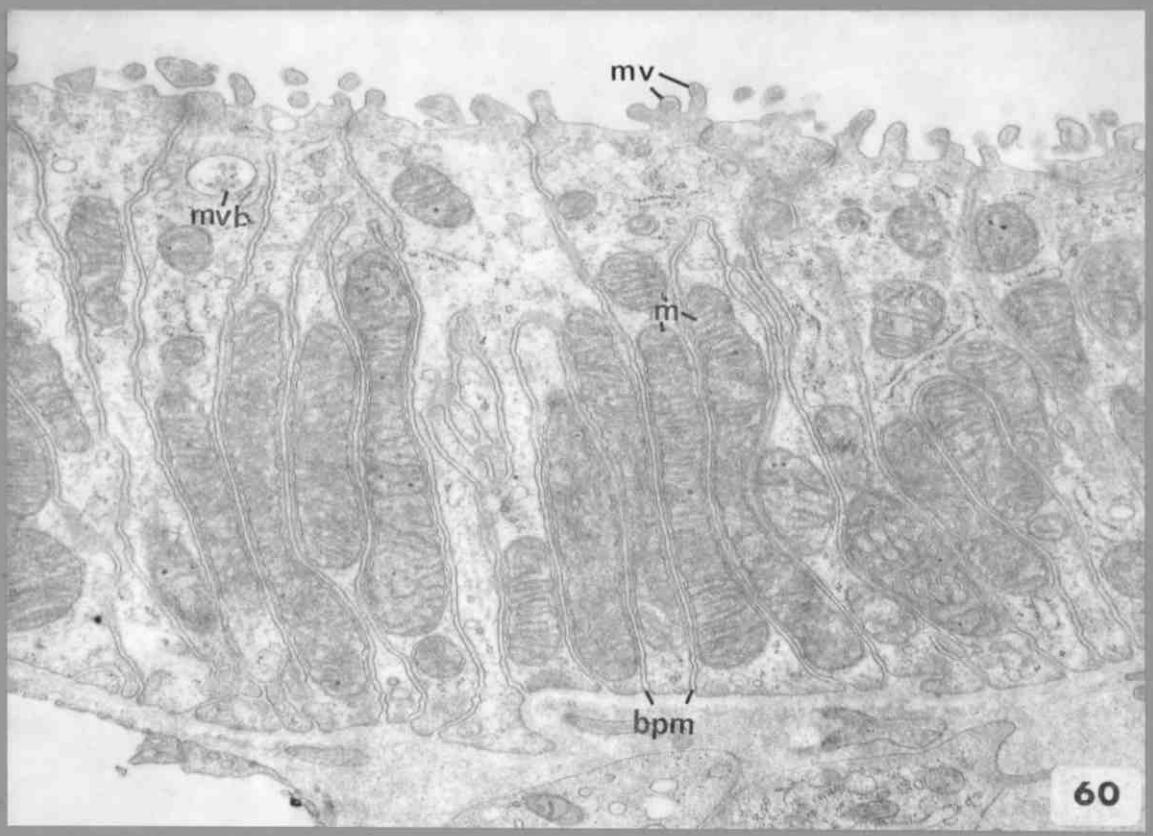

b
l
m
c
57

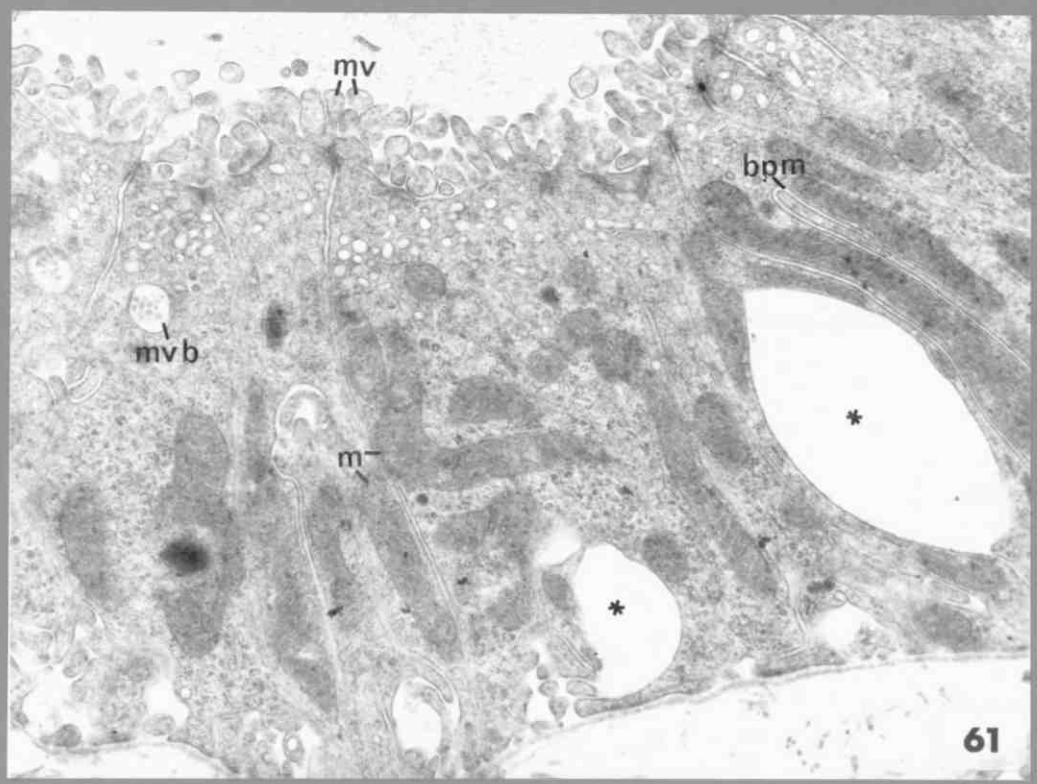
Figs 58 and 59. As in the normal control hamster (Fig 59), the cell organelles of the ALH of the 8 days adrenelactomized animal (Fig. 58) appears to be normal. The mitochondria (m) are regularly arranged within the interdigitations of the basal plasma membrane (bpm) and the luminal cell membrane with its few short microvilli (mv) is also in no way different from that of the normal control kidney. 'g' Golgi body; 'l' lysosomes; 'rer', rough endoplasmic reticulum; 'mvb', multivesicular bodies. Methods of fixation and post staining were as in Figs. 56 and 57. Magnifications x 20,000 and x 17,000, respectively.


mv
l
g
bpm
m
rer
58

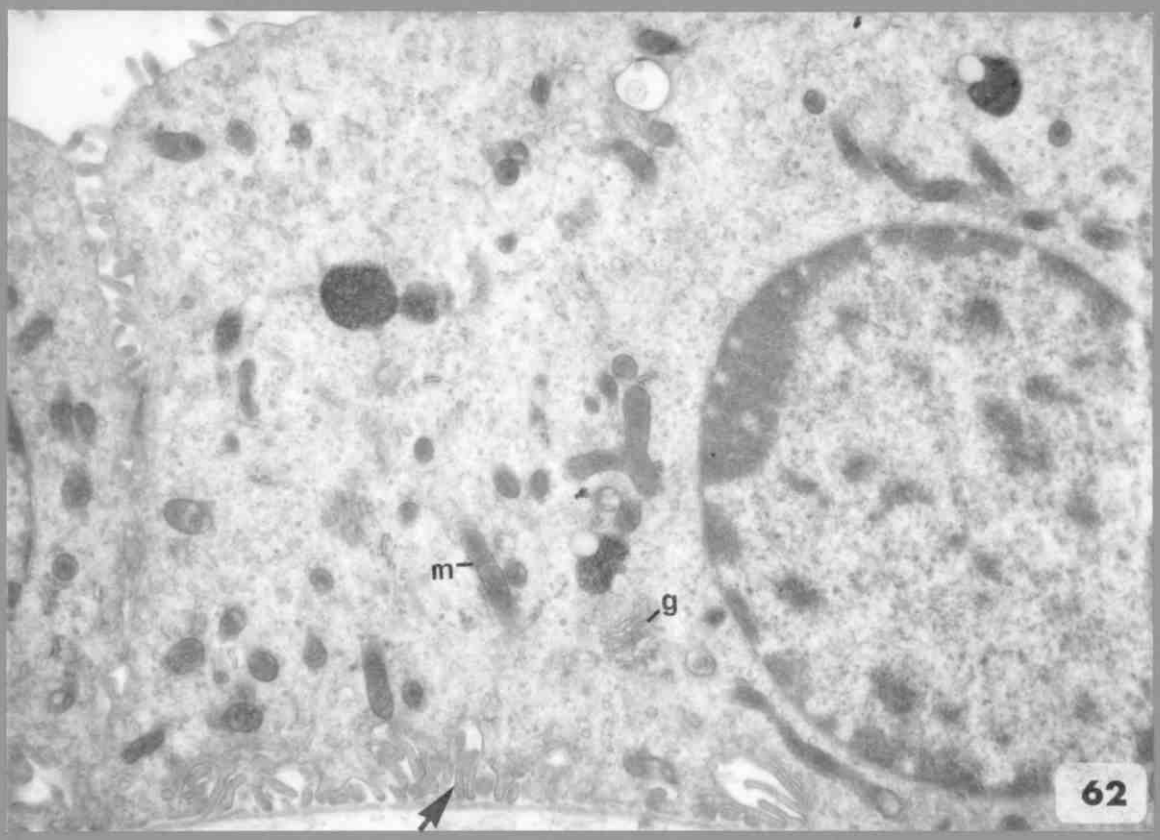

mv
rer
g
l
m
bpm
59

Figs 60 and 61. Once again, as in the normal control (Fig 60), the cells of the DCT of the 8 days adrenalectomized hamster kidney (Fig 61) are seen to be regularly interdigitated with deep, parallel and vertical infoldings of the basal plasma membrane (bpm). Amongst these infoldings are packed long and slender mitochondria (m). Some of the infoldings of the adrenalectomized animal however, are extremely dilated (*). 'mvb', multivesicular body; 'mv' microvilli. Methods of fixation and post staining were similar to those used for Figs. 56 and 57. Magnifications x 20,000 and x 17,000 respectively.


mv
mvb
m
bpm
60


mv
bpm
mvb
m
*
*
61

Figs 62 and 63. Cells of the CD of the 8 days adrenalectomized hamster kidney (Fig. 62) are quite closely similar to those of the normal hamster kidney (Fig 63). Small and short interdigitations of the basal plasma membrane (arrows) and the distribution of few scattered organelles (like mitochondria, 'm'; Golgi body, 'g' etc.) is also in no way different from those of the normal kidney. Fixation and post staining procedures were as in Fig 56 and 57. Magnifications x 20,000 and x 18,000 respectively.


m
g
62

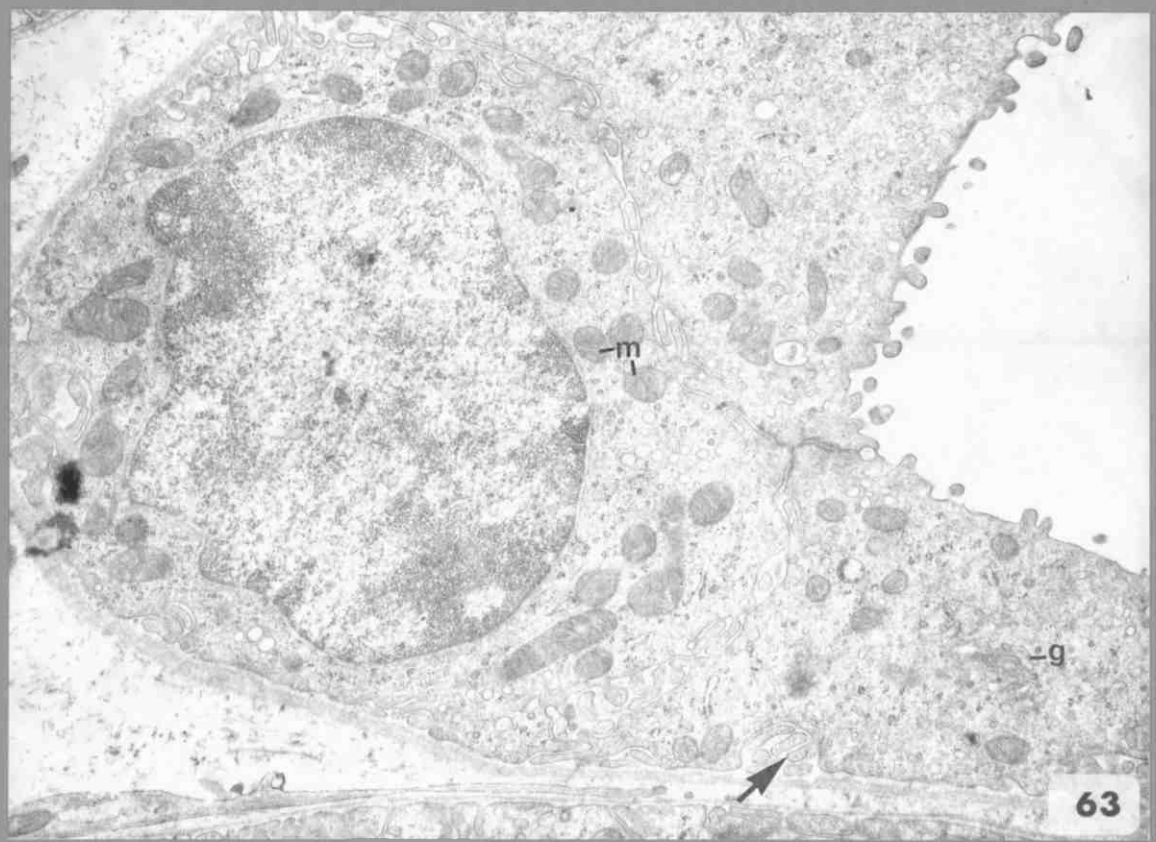
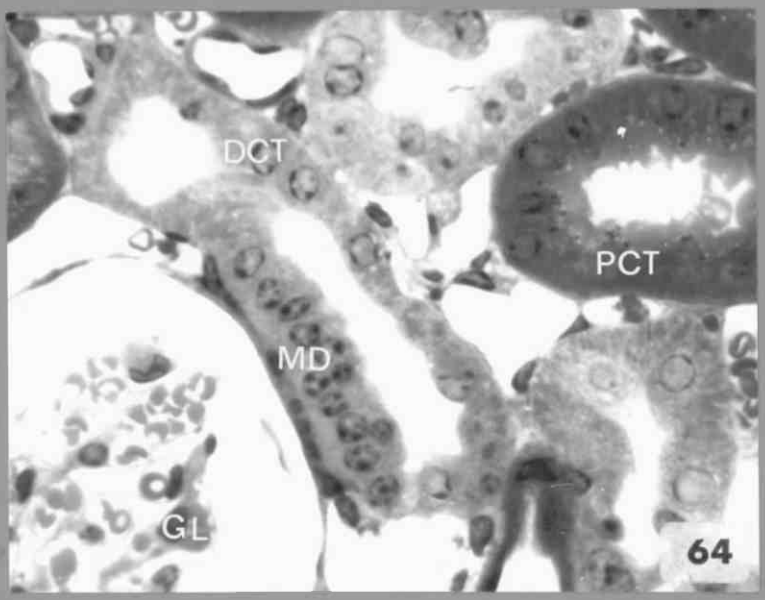

m
g
63

Fig 64. 1 μm resin embedded section of the normal hamster kidney fixed in ½ Karnovsky's glutaraldehyde showing a MD proximal to a glomerulus (GL). Note that the columnar cells of the MD form a distinct cushion in contrast to the cells of the DCT. Post fixation was in Palade's osmium tetroxide and the section was stained with Azure II. Magnification x 15,000.

Fig 65. Low power electron micrograph of a DCT of the hamster kidney showing the MD with its specialized columnar cells. Apparently, one transitional cell (arrows) with its slightly less dense cytoplasm can be seen on either side of the MD. A portion of the glomerulus (GL) and the extra-glomerular mesangial cells (EGM) can be seen near the bottom. After initial fixation in ½ strength Karnovsky's glutaraldehyde, the material was post fixed in Palade's osmium tetroxide and the ultrathin section stained with lead citrate and uranyl acetate. Magnification x 4,000.


DCT
PCT
MD
GL
64

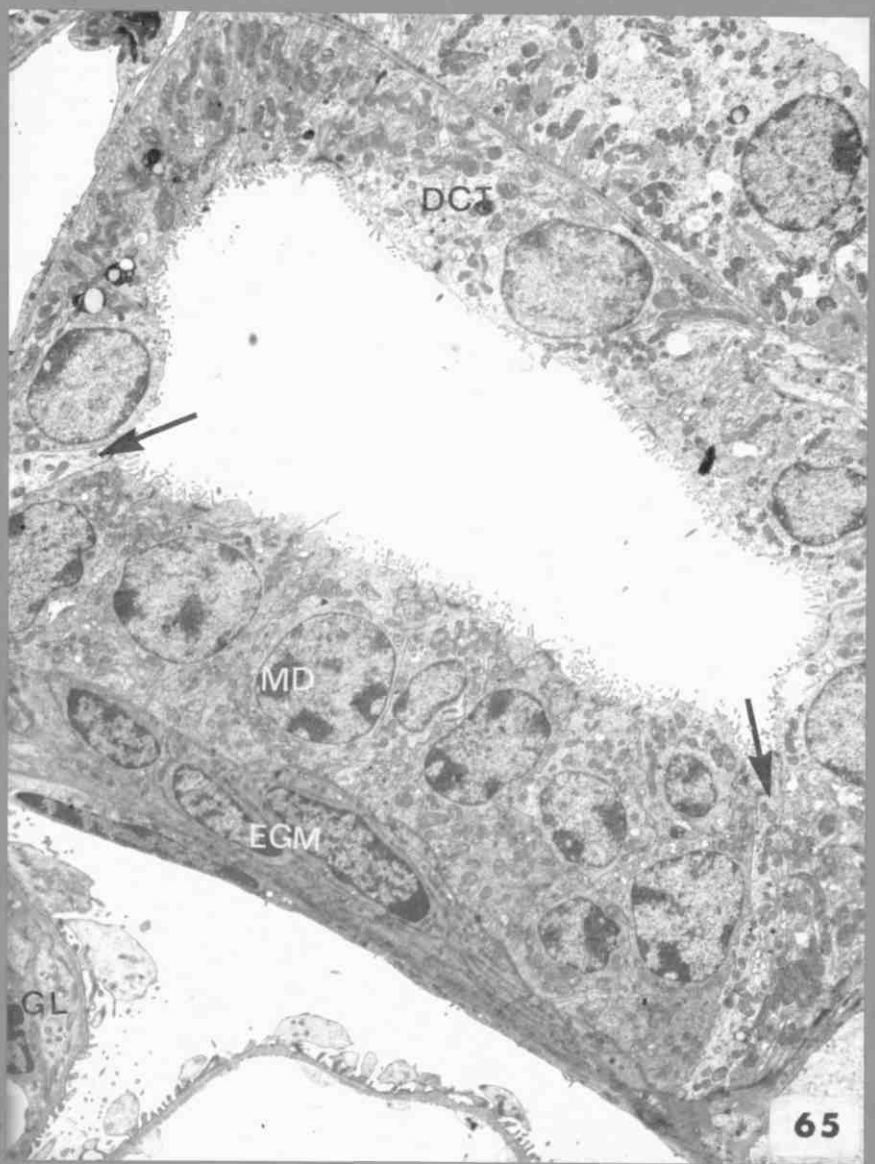
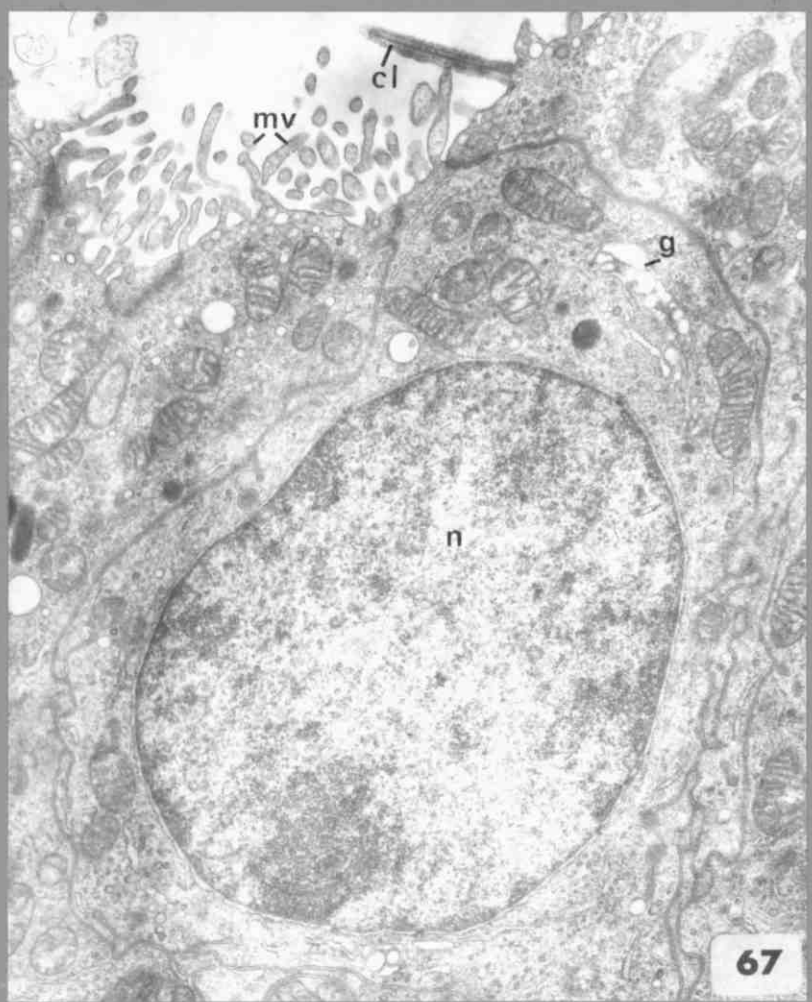

DCT
MD
EGM
GL
65

Fig 66. Electron micrograph of that part of the hamster MD where the epithelium appears to be more than one cell layer in thickness (this is probably due to an oblique cut). One transitional cell (arrow) with its slightly less dense cytoplasm can be seen on the right hand corner of the photograph. Fixation and staining as in Fig. 65. Magnification x 15,000.

Fig 67. Electron micrograph of a single cell of the hamster MD to show regular, long, finger like microvilli (mv) on the luminal side of the cell. Also seen is a cilium (cl) projecting into the lumen and a Golgi body (g) to the top left hand of the nucleus (n). Magnification x 22,000.



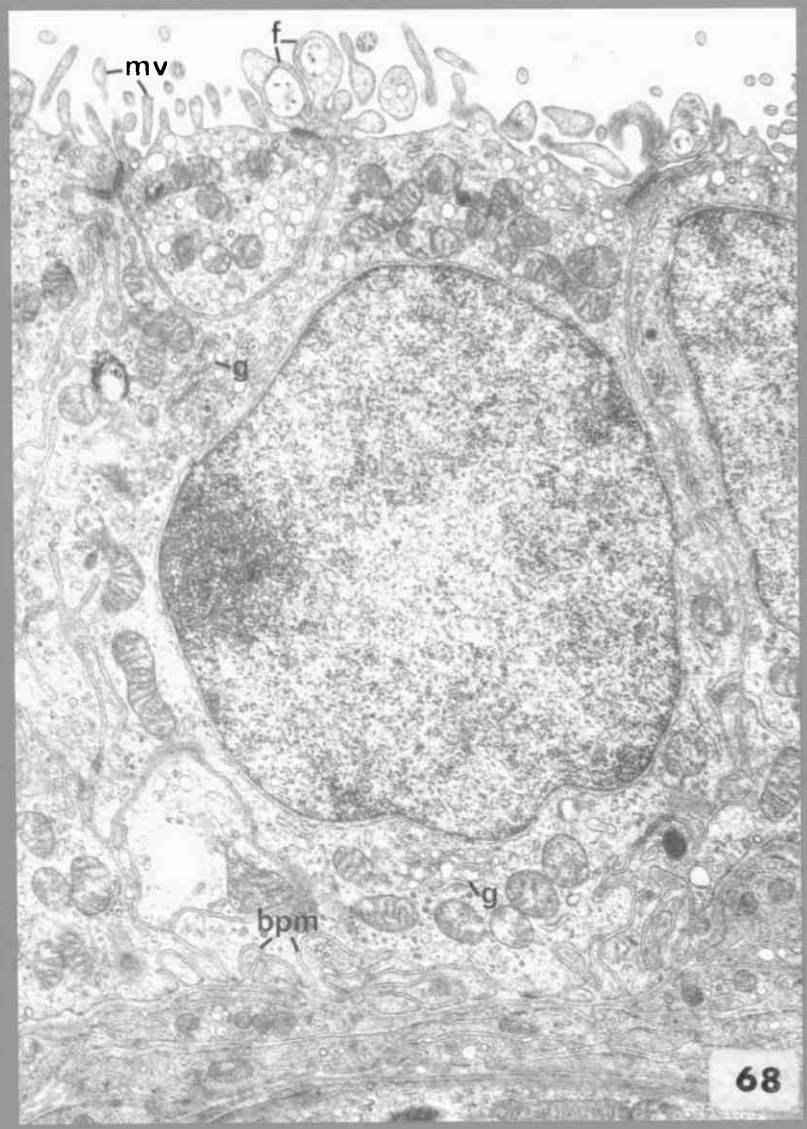
66



67

Fig 68. Electron micrograph of a MD cell of the hamster kidney showing profiles of the Golgi apparatus (g) in the para- as well as infranuclear positions. Also seen are short, blunt and irregular folds (f) of the luminal plasma membrane together with regular, long and finger like microvilli (mv). Note the complex infoldings of the basal plasma membrane (bpm) which are restricted to the basal half of the cell and lack any distinct orientation. Magnification x 15,000.

Fig 69. An MD cell at a higher magnification showing one vesicle (arrow) which appears to be derived by the invagination of the luminal plasma membrane. Note that the subsurface cytoplasm is filled with numerous membrane bounded vesicles (v) which also are possibly derived from the invaginations of the luminal plasma membrane. At the luminal margin, the cell surface plasma membranes of adjacent cells form the so called tight junctions (tj). Magnification x 40,000.


f
mv
g
g
bpm
68

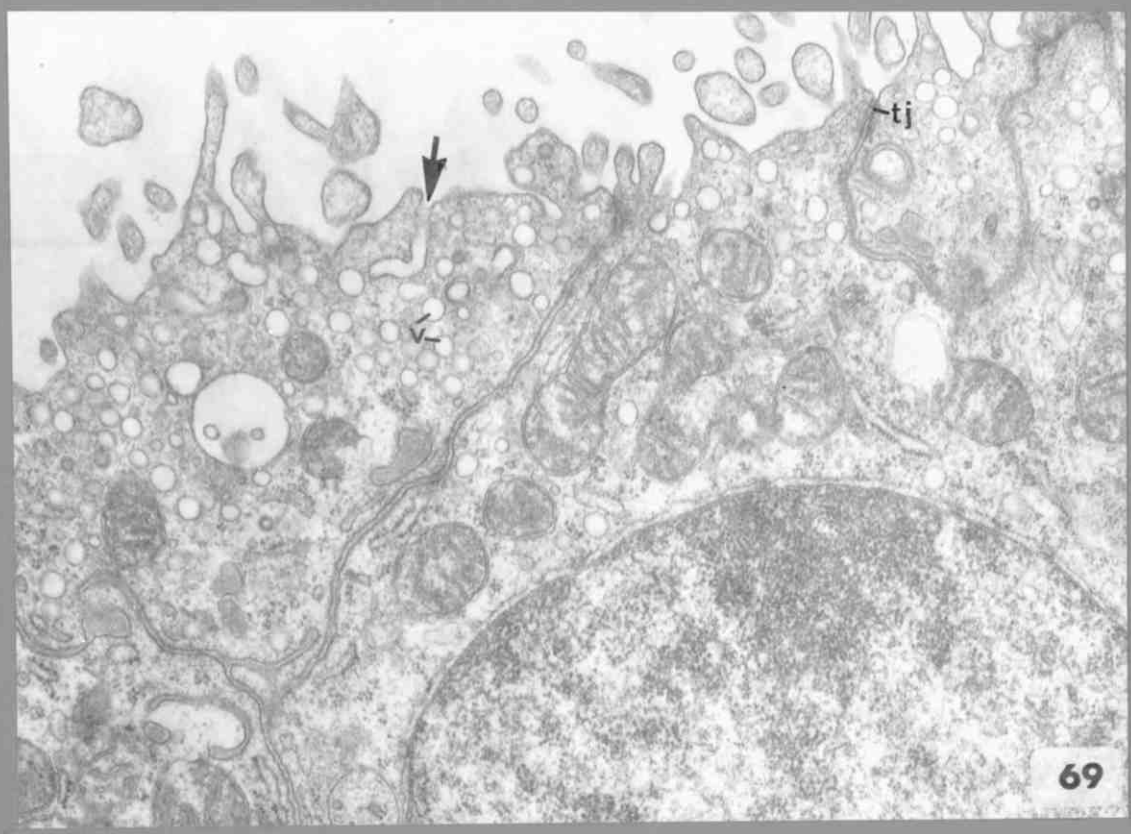

tj
v
69

Fig 70. MD cell of the hamster kidney at a higher magnification showing the basal region. Dark membrane bounded granules (mg) are present within this region. Large vesicles (lv) and rough endoplasmic reticulum (rer) are also seen. Magnification x 40,000.

Fig 71. MD cell of the hamster kidney, showing in detail, the complex infoldings of the basal plasma membrane (bpm) which are restricted to the basal half of the cell and lack any distinct orientation. The basal lamina (bl) appears to be continuous. Microtubules (mt) can be seen on one side of the nucleus (n). Also seen are polyribosomes (r) and an infranuclear Golgi body (g). Note that two small vesicles (arrows) are seen in contact with the basal plasma membrane. Magnification x 30,000.


lv
mg
rer
70

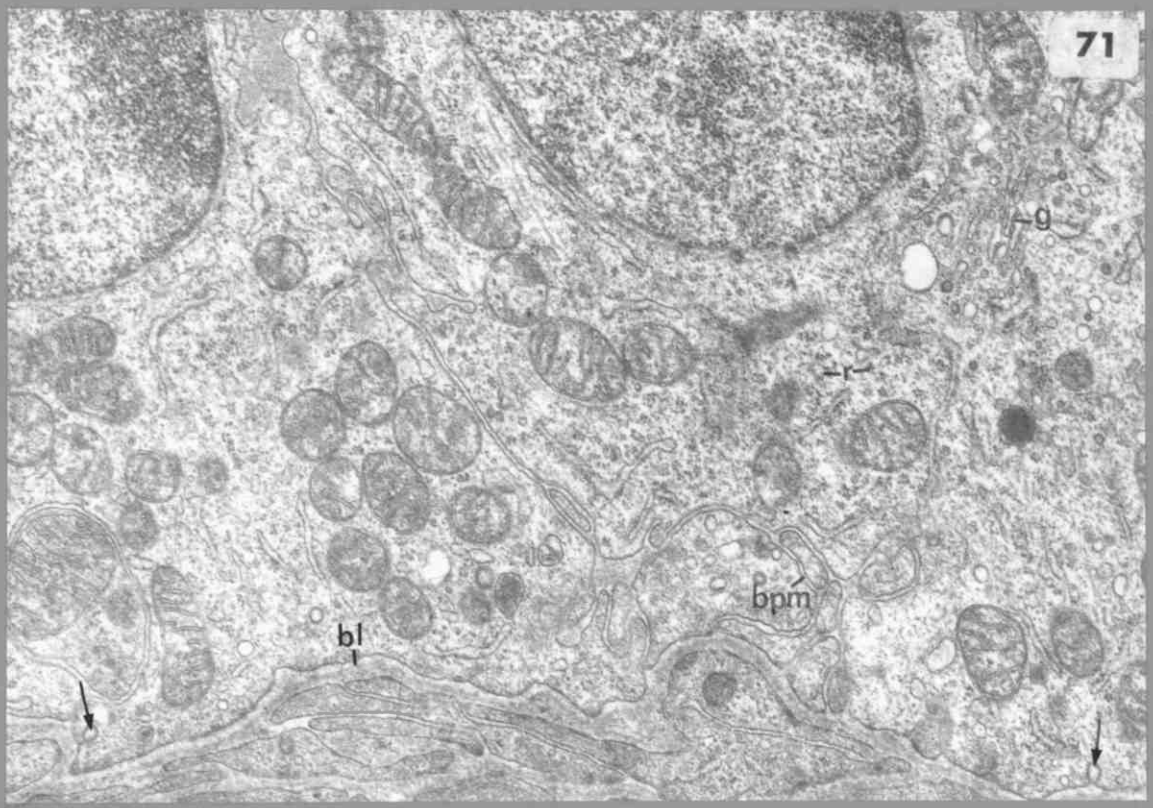
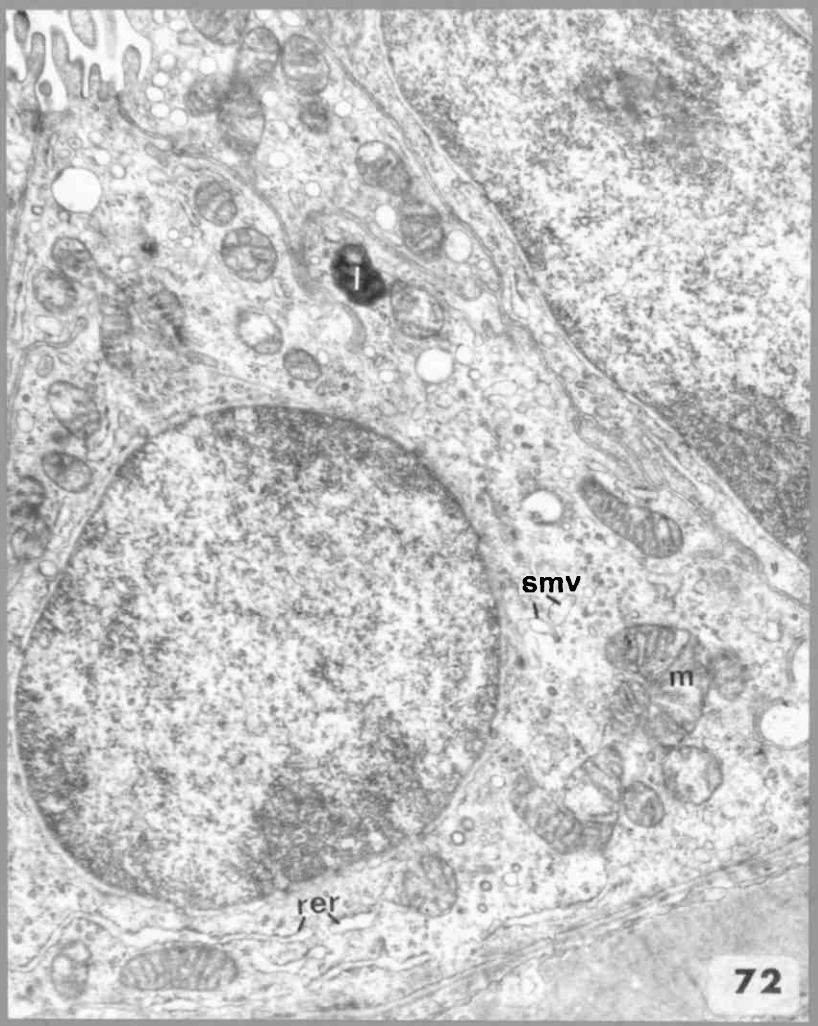

71
g
r
bpm
bl

Fig 72. Electron micrograph of a MD cell of the hamster kidney showing a lysosome (l), rough endophasmic reticulum (rer) and single membrane bounded vacuoles (smv) which are devoid of ribosomes. Note that the mitochondria (m) with circular or oval profiles are scattered randomly throughout the cell. Magnification x 25,000.

Fig 73. A cell of the ALH of the hamster kidney showing two profiles of the Golgi complex (g) in the classical paranuclear position, slightly above the equator of the nucleus. Magnification x 25,000.


i
smv
m
rer
72

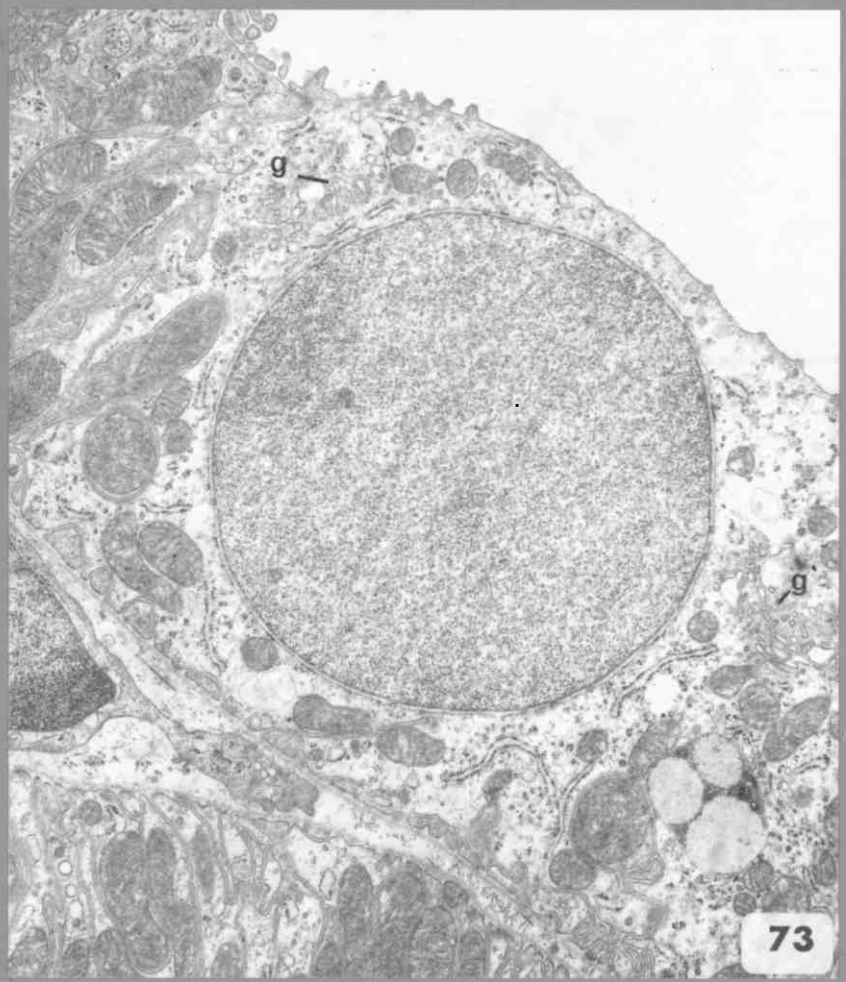
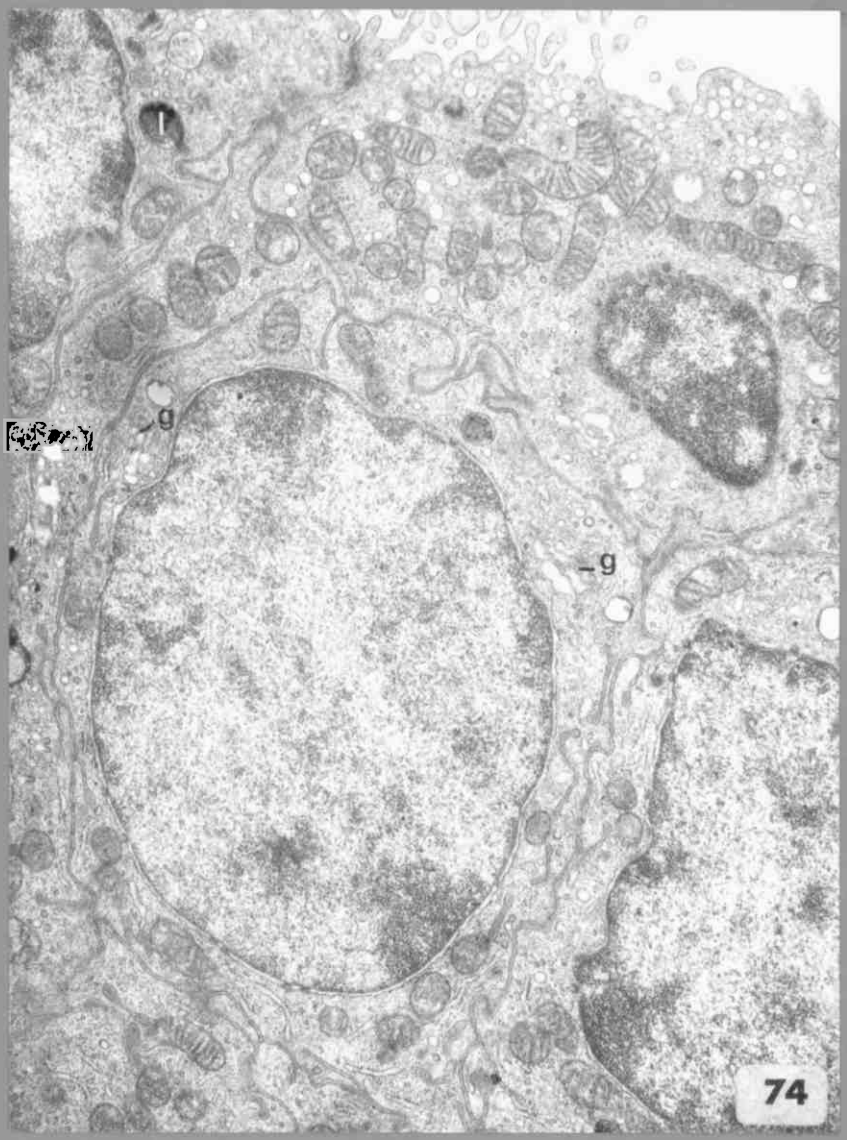

g
g
73

Fig 74. Electron micrograph of a part of a MD of the hamster kidney. Note the comparable position of the Golgi complex (g) to that seen in the cell of ALH in Fig. 73. Circular and elliptical profiles of mitochondria (m) and a lysosome (l) are also seen. Magnification x 20,000.

Fig 75. Typical appearance of two MD cells with numerous finger like microvilli (mv). The cell on left shows only one profile of a Golgi body (g) in the infranuclear position while the cell on the right shows three profiles in a similar position. Also seen are multivesicular bodies (mvb) and a lysosome (l). Magnification x 20,000.


l
g
g
74

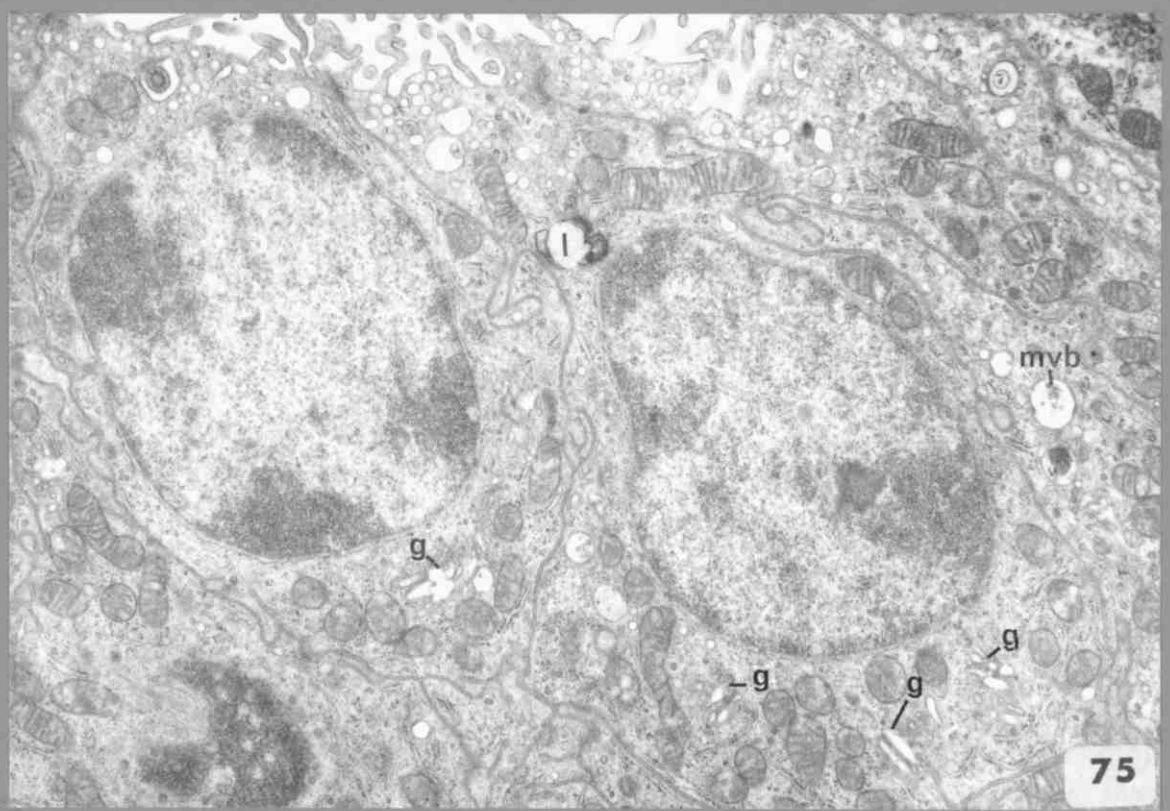
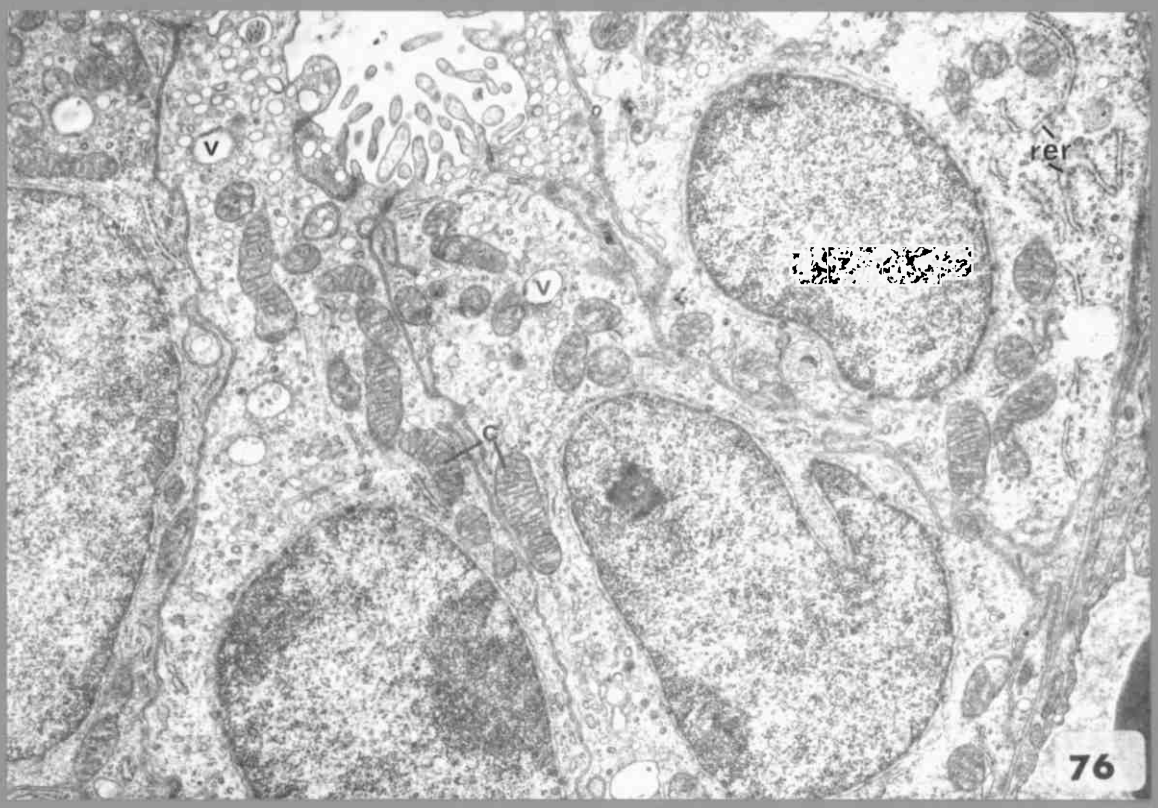

l
mvb
g
g
g
g
75

Fig 76. A part of the hamster kidney MD showing randomly distributed circular and oval profiles of mitochondria. The cristae mitochondriales (c) appears to be lamellate in form. (v), vacuoles; (mvb), multivesicular body, (rer), rough endoplasmic reticulum. Magnification x 17,500.

Fig 77. Electron micrograph of a part of CD from the hamster kidney. The material was fixed by perfusion with 2% paraformaldehyde and 30-40 µm thick cryostat sections stained for acid phosphatase by the method of Barka and Anderson modification of Gomori's medium (Barka and Anderson, 1962). Large and numerous acid phosphatase containing bodies or lysosomes (l) are seen in almost all the cells. Magnification x 10,000.


v
v
rer
c
76

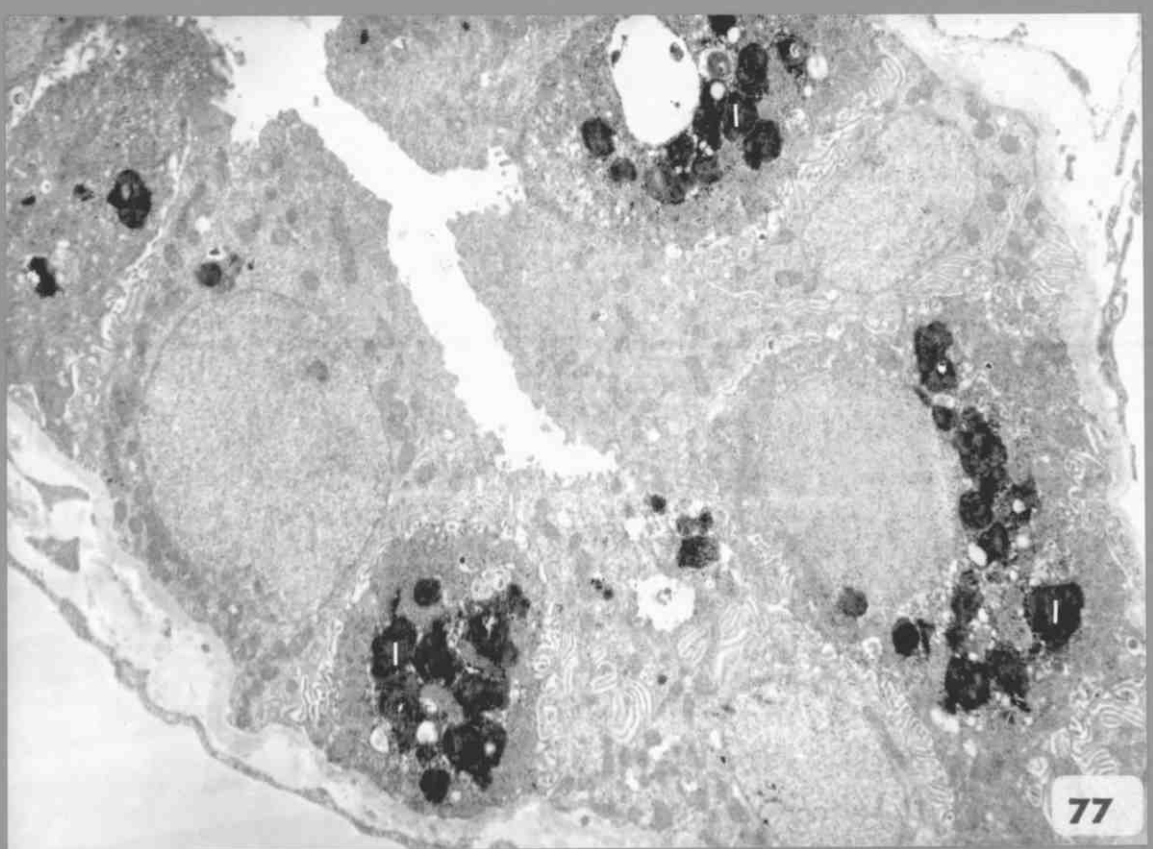
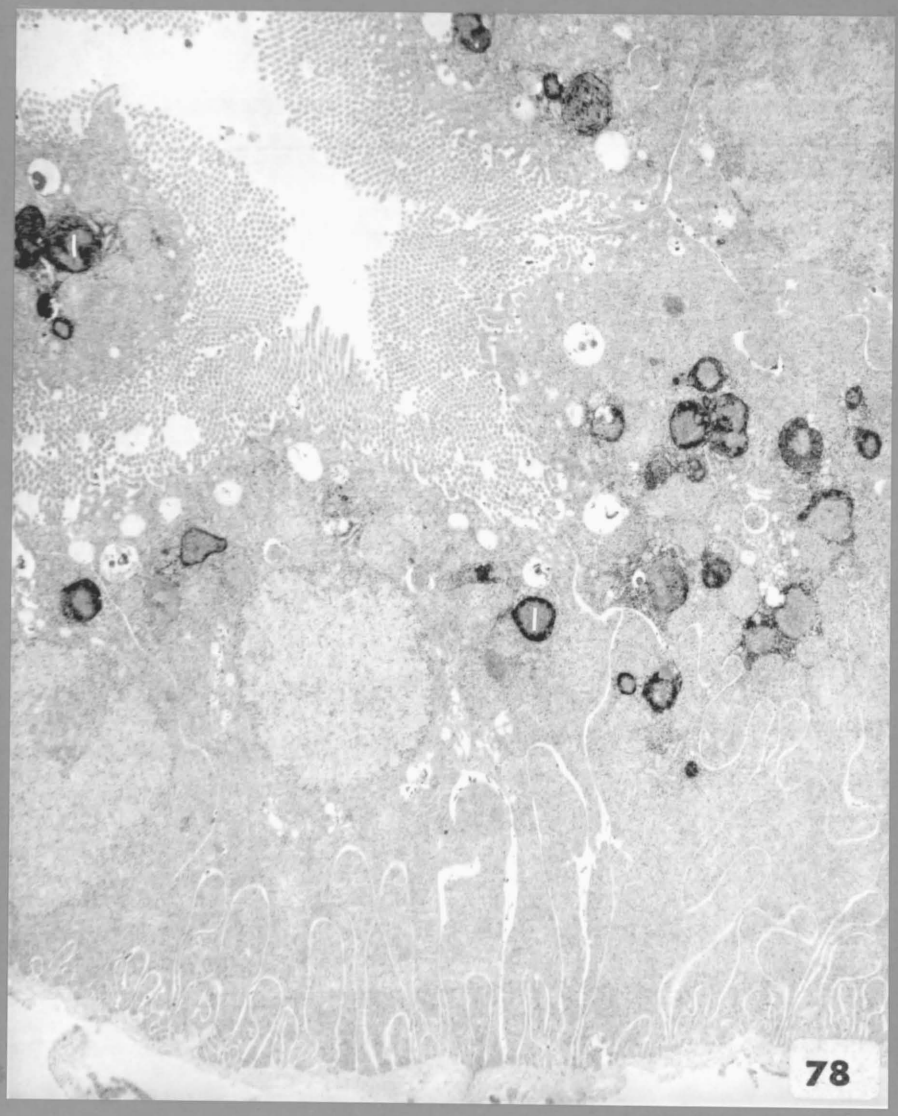
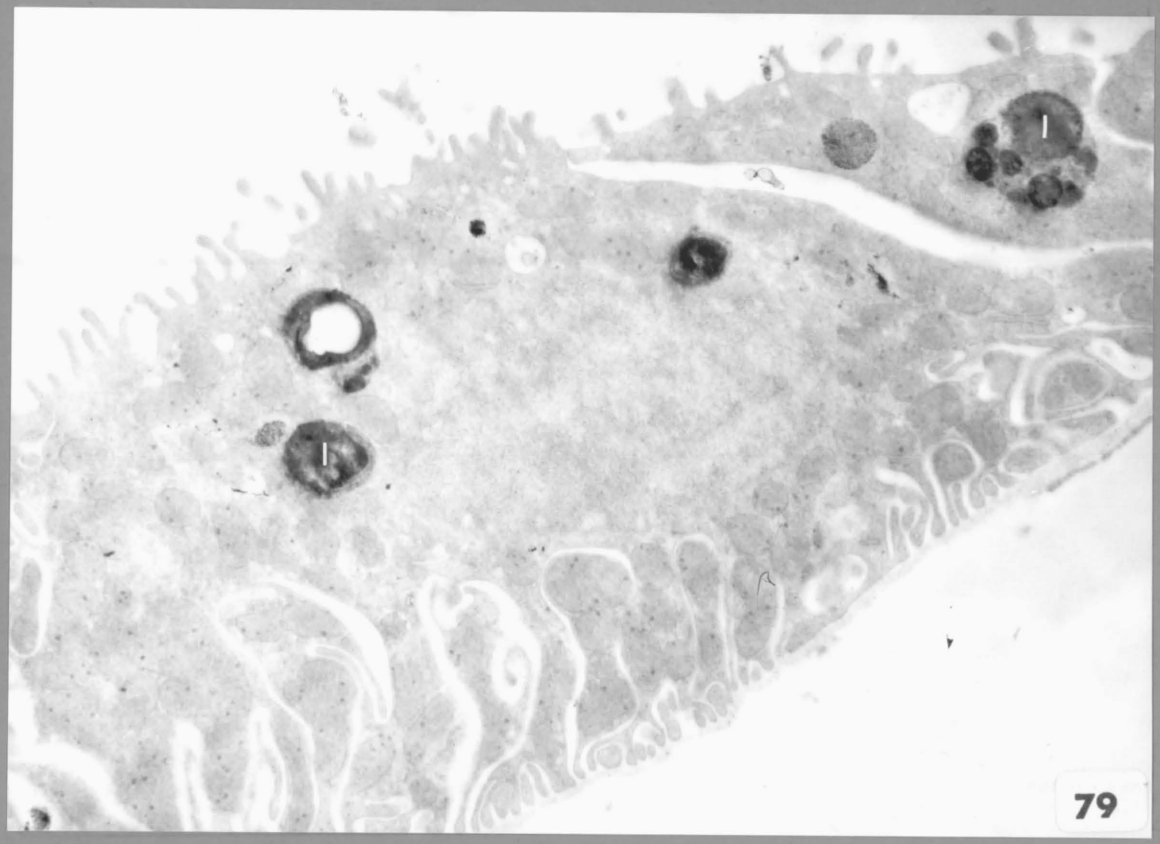

l
l
l
77

Fig 78. A part of the PCT of the hamster kidney to show the distribution of acid phosphatase containing lysosomes (l). Fixation and the staining procedures were as in Fig 77. Magnification x 17,000.

Fig 79. A part of the DCT of the hamster kidney to show the distribution of acid phosphatase containing lysosomes (l). Note that the number of these bodies is comparatively much less than seen in the CD (Fig 77) and PCT (Fig. 78). Fixation and the staining procedures were similar to those used for Fig 77. Magnification x 25,000.



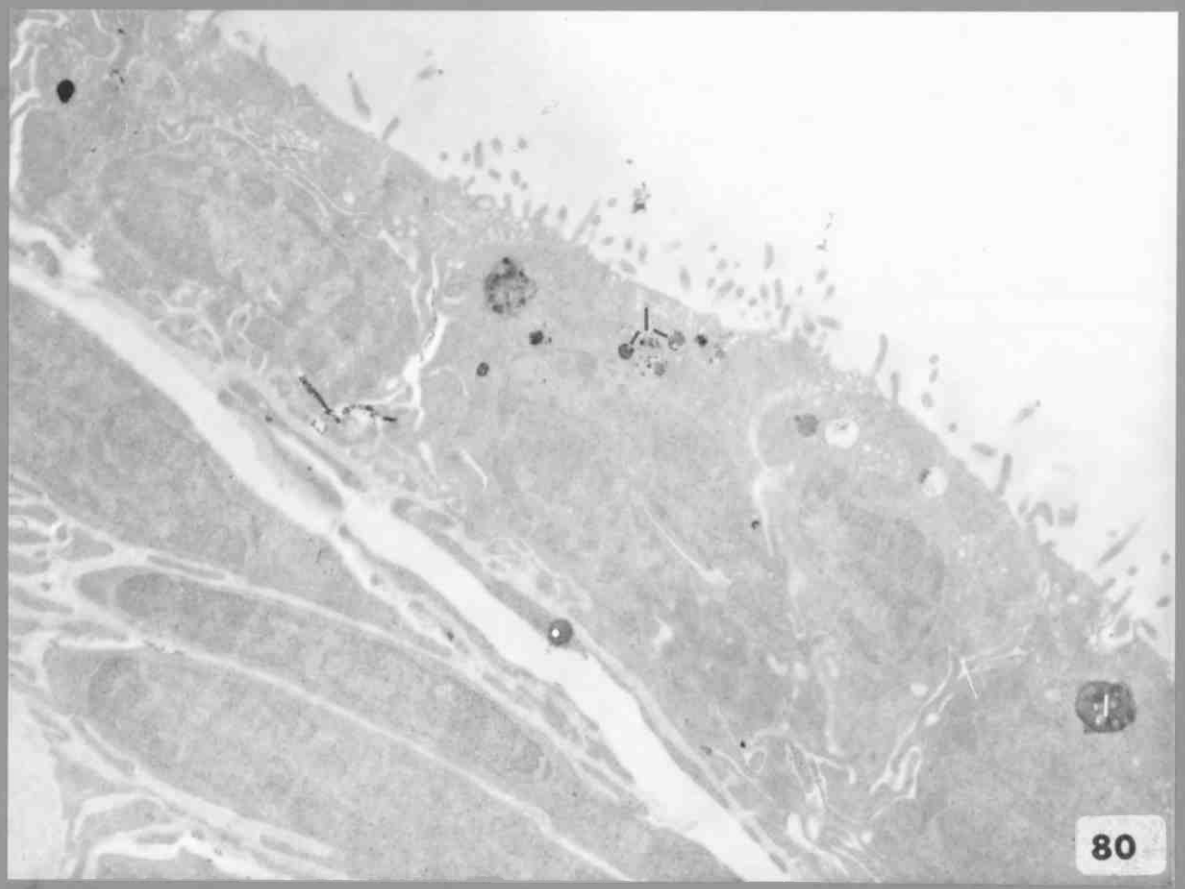
78

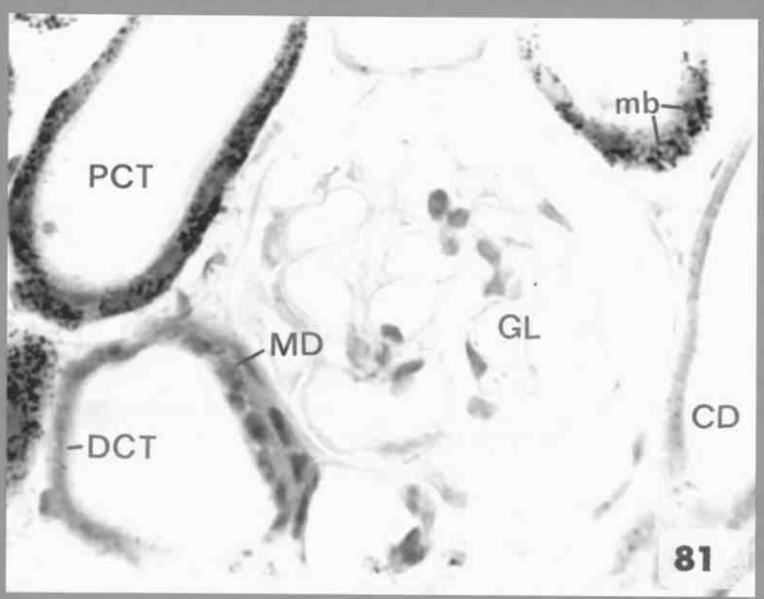


79

Fig 80. A part of the MD of the hamster kidney showing the distribution of lysosomes (l) which have been stained for acid phosphatase by the same technique as used for Fig. 77. Note that the lysosomes in MD cells are of variable sizes (most ofthem are much smaller than those in the CD, PCT and DCT cells) and sporadic in distribution. Magnification x 20,000.

Fig 81. Hamster kidney cortex. After fixation with paraformaldehyde -glutaraldehyde, 30-40 µm thick cryostat sections were stained for catalase by treating with a saturated solution of diaminobenzidine (7 mg/10 ml) in Tris HCl buffer, pH 7.6. The catalase containing peroxisomes or the so called microbodies (mb) are quite abundant in PCT cells and appear to be totally absent in the DCT, MD, CD and glomerulus (GL). Magnification x 650.


80


mb
PCT
GL
MD
CD
DCT
81

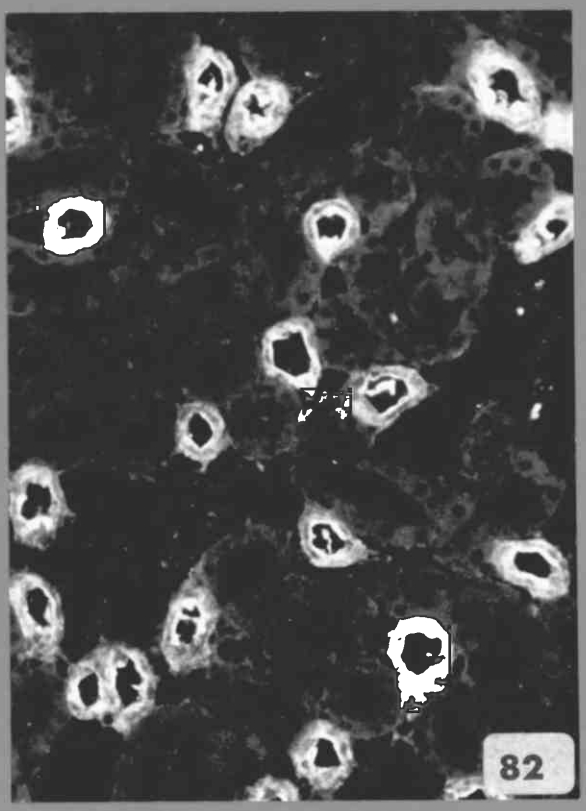
(N.B. Figs. 82-85 were taken on an epifluorescence) microscope.

Fig 82. Adult Wistar rat kidney, inner medullary zone. T-H specific fluorescence is seen in the cells of ALH which lie among the non-stained thin descending and ascending limbs of loops of Henle and CD. Note that the luminal border as well the cell interior (except their nuclei) fluoresces brilliantly. 5 μm thick paraffin section obtained from the material fixed by perfusion with formal calcium chloride. Magnification x 550.

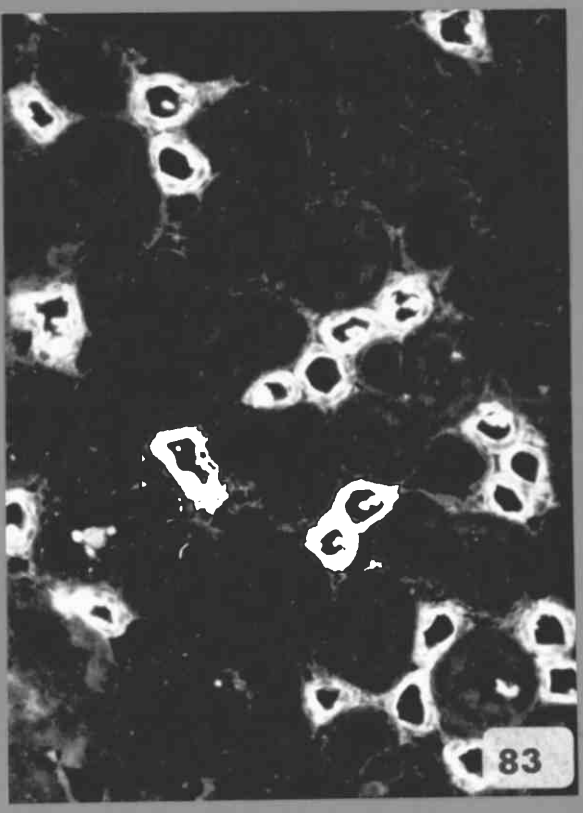
Fig 83. Adult Wistar rat kidney, outer cortex. T-H specific fluorescence is seen in the cells of DCT. As in ALH (Fig. 82), the cells are stained heavily for T-H. Fixation as in Fig 82. Magnification x 550.

Fig 84. Adult Wistar rat kidney, outer cortex. The cells of DCT are seen to be stained for T-H glycoprotein. Cells of the MD, on the other hand, are completely devoid of the glycoprotein and thus lack fluorescein staining. (GL), Glomerulus. Fixation as in Fig 82. Magnification x 800.

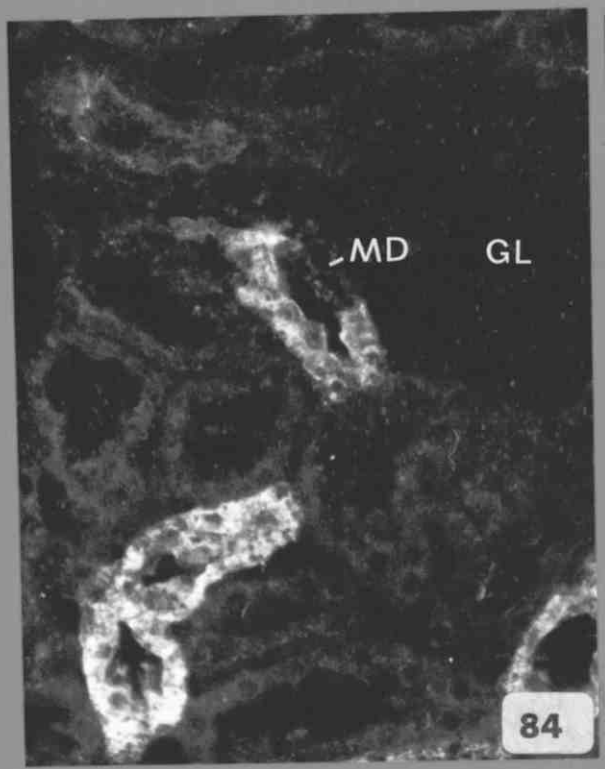
Fig 85. Adult Wistar rat kidney, outer cortex. As in Fig 84, the cells of DCT are once again seen to be fluorescing brilliantly. The cells of the MD, on the other hand, appear to possess some staining only on the luminal surface (see also Fig 88). Fixation as in Fig. 82. Magnification x 800.



82



83



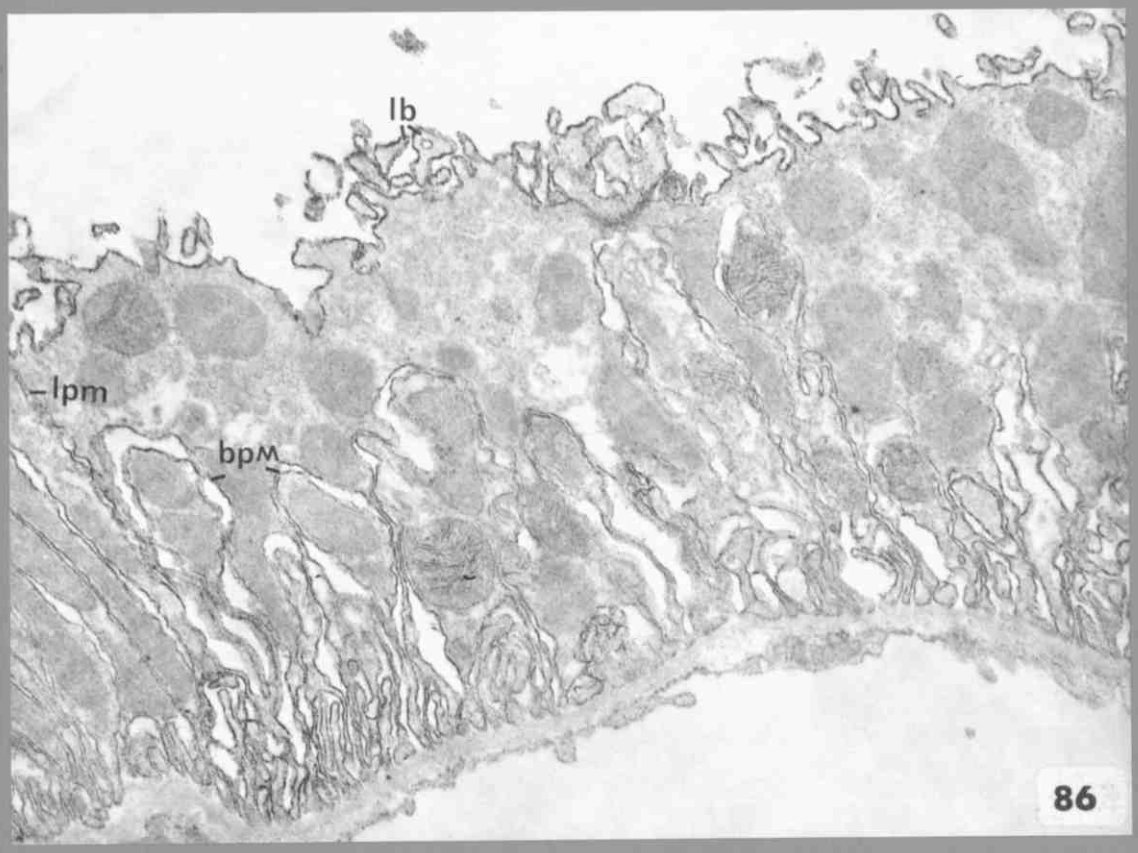
84



85

Fig 86. Immunoelectron microscopic localization of T-H glycoprotein in the cells of the ALH of the Wistar rat kidney. Material was fixed by perfusion with PLP and stained for T-H by the method of Nakane and Kawaoi (1974). Intense staining is seen on the luminal border (lb), lateral plasma membranes (lpm) and the basal plasma membrane (bpm), including its infoldings. A slight amount of reaction seen in some of the mitochrondria is unusual. Magnification x 18,000.

Fig 87. Immunoelectron microscopic localization of T-H glycoprotein in the cells of the DCT of the Wistar rat kidney. Once again deposits of the reaction product are seen on the luminal border (lb), lateral plasma membranes (lpm) and in the basal plasma membrane, including its infoldings. Note that the basal lamina (bl) is clearly negative. Magnification x 18,000.


lb
lpm
bpm
86

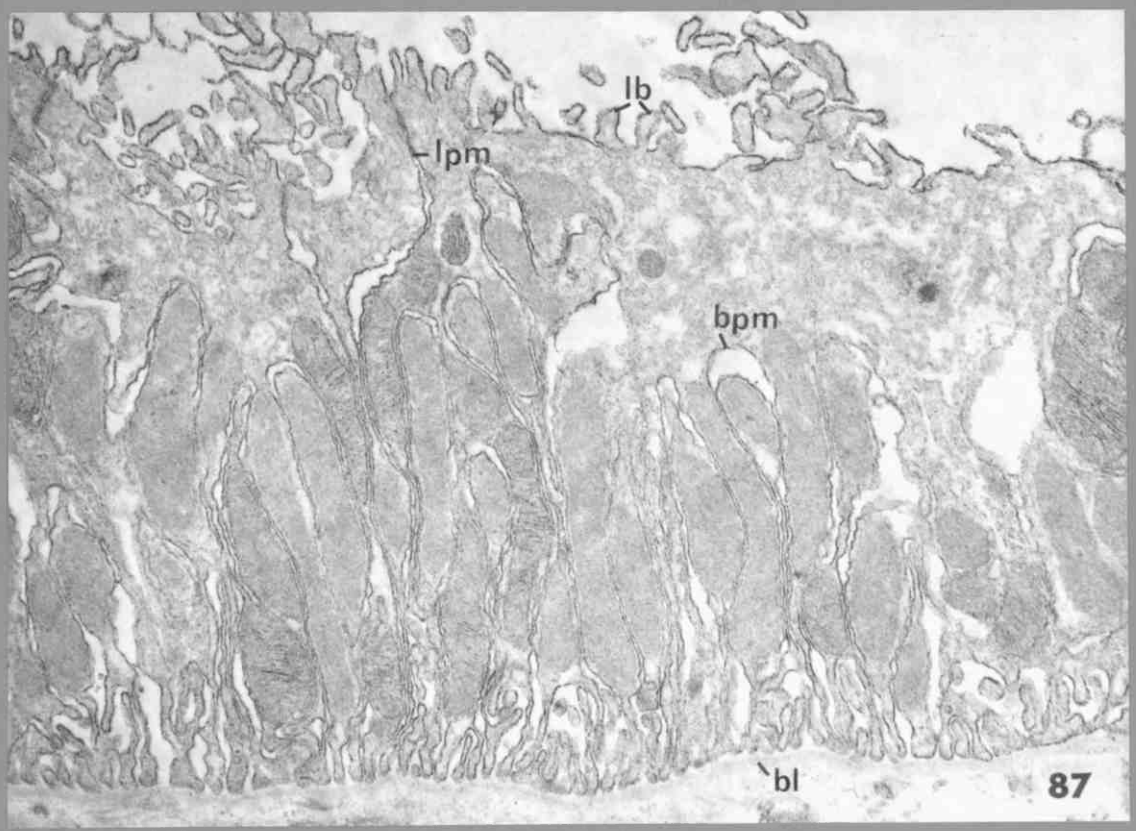
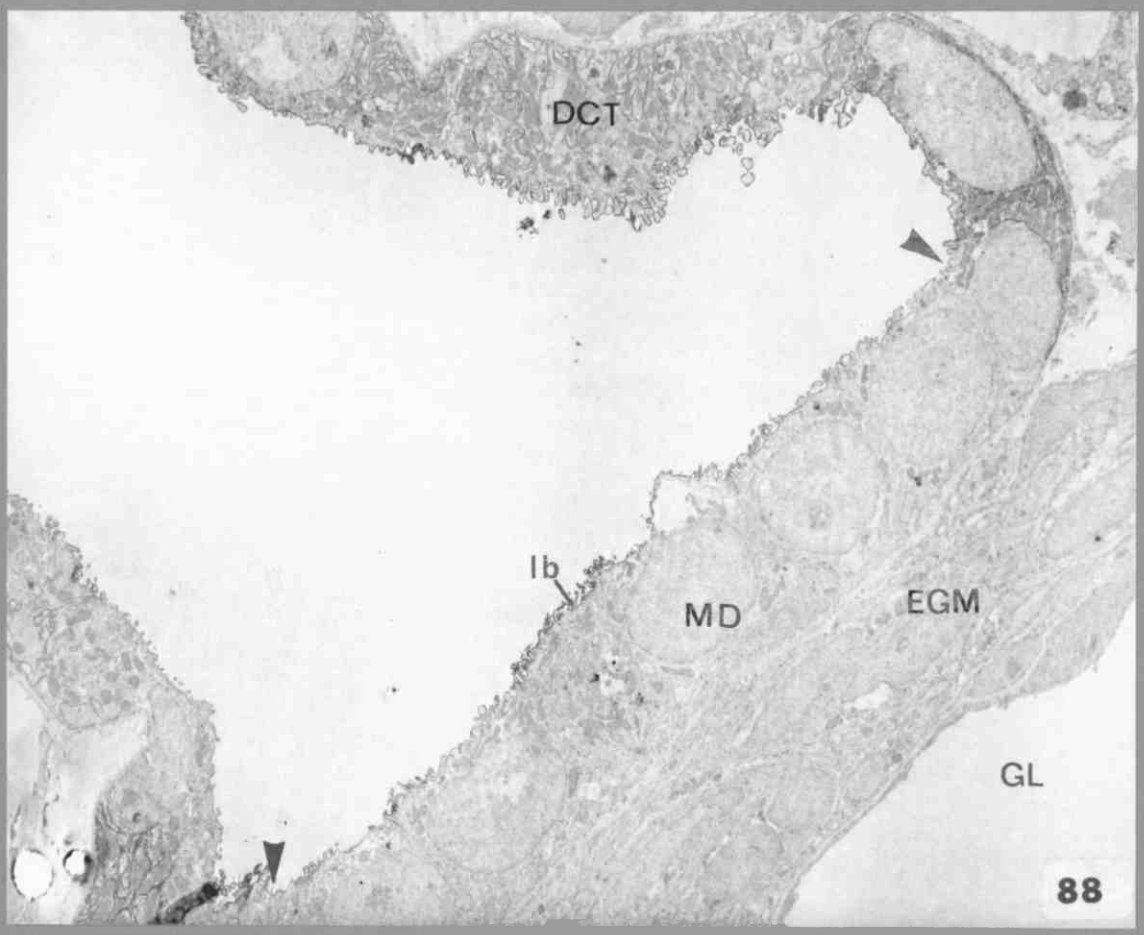

lb
lpm
bpm
bl
87

Fig 88. Adult Wistar rat kidney. Fixation and staining procedures were as in Fig 86. As by immunofluorescence microscopy, T-H by immunoelectron microscopy is once again seen to be present on the luminal border (lb) of some of the MD. No reaction is seen in other parts of the plasma membrane. In the rest of the cells of the DCT, on the other hand, T-H is present in the total membrane system. (EGM), extra-glomerular mezangium; (GL), Glomerulus. Magnification x 7,000.

Fig 89. High power immunoelectron micrograph to show the junction (arrow) of MD with the DCT. Note that in the DCT cells, the reaction is present in the total membrane system. In the MD cells, on the other hand, such reaction is seen only on the luminal border (lb). Magnification x 15,000.


DCT
Ib
MD
EGM
GL
88

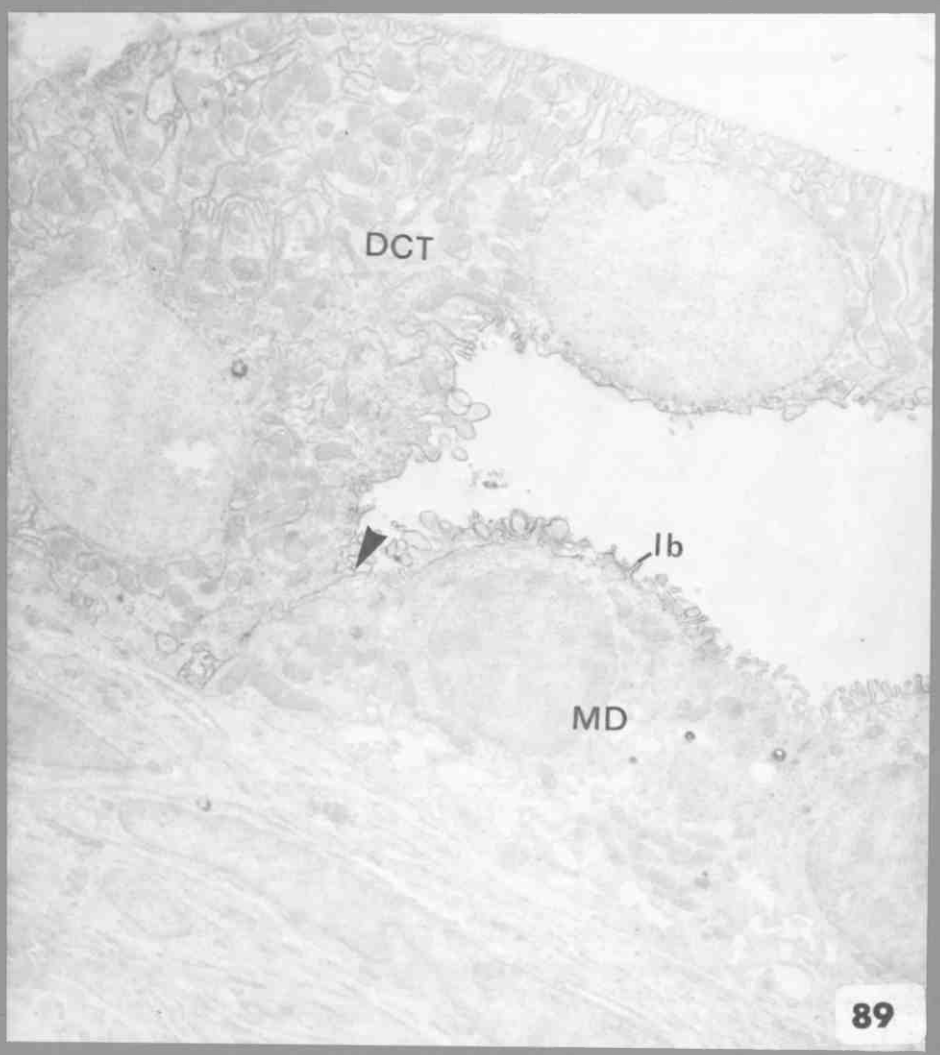
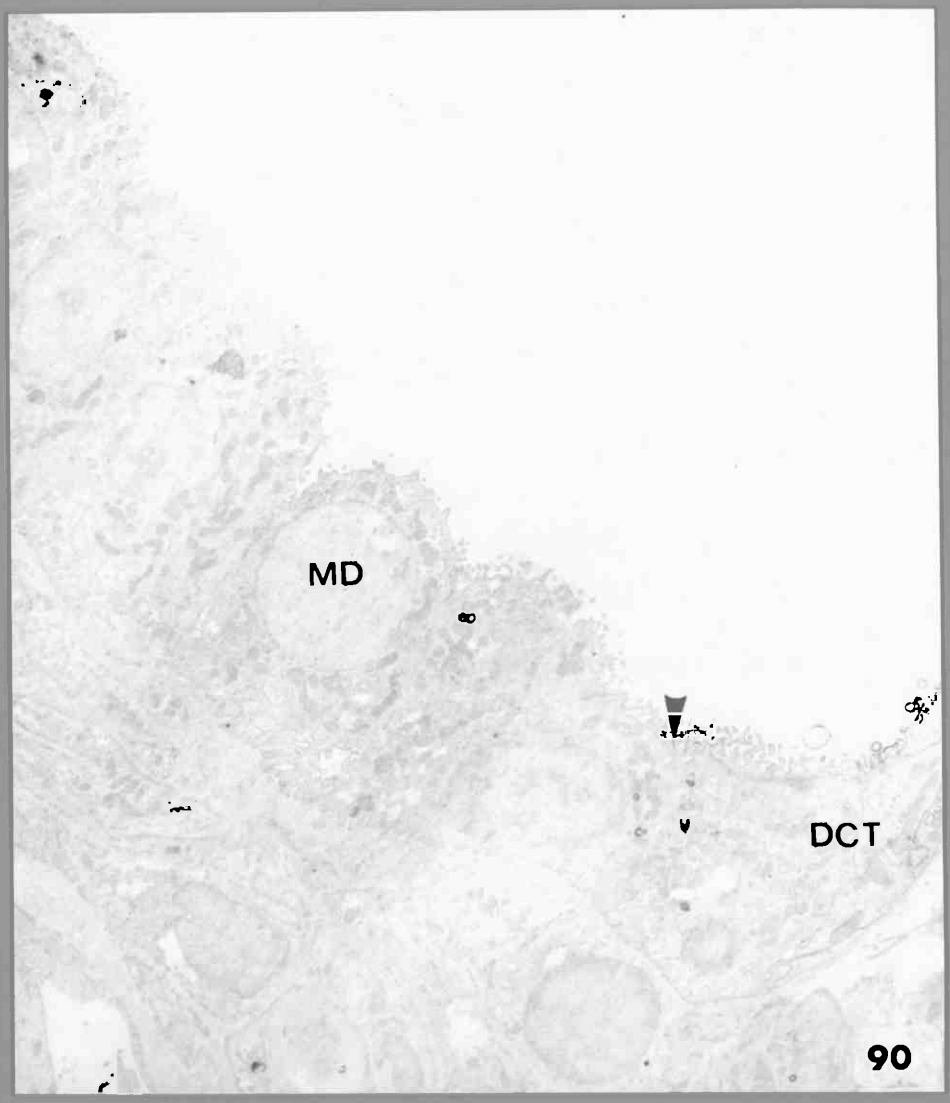

DCT
Ib
MD
89

Fig 90. Adult Wistar rat kidney. Contrary to the presence of T-H glycoprotein in the first type of MD cells (Fig 88 and 89), the T-H in the second type of MD is totally absent. The plasma membranes of both, the luminal surface as well as the interior of the cells are negative for the glycoprotein. In a cell of the DCT (right hand corner), the glycoprotein is however, still present. Magnification x 15,000.


MD
DCT
90

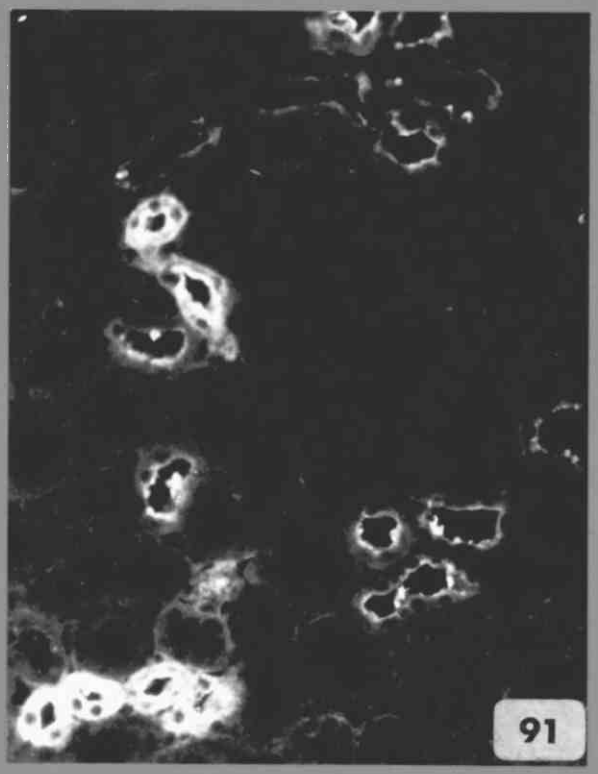
(N.B. Figs 91-94 were taken on an epifluorescence microscope)

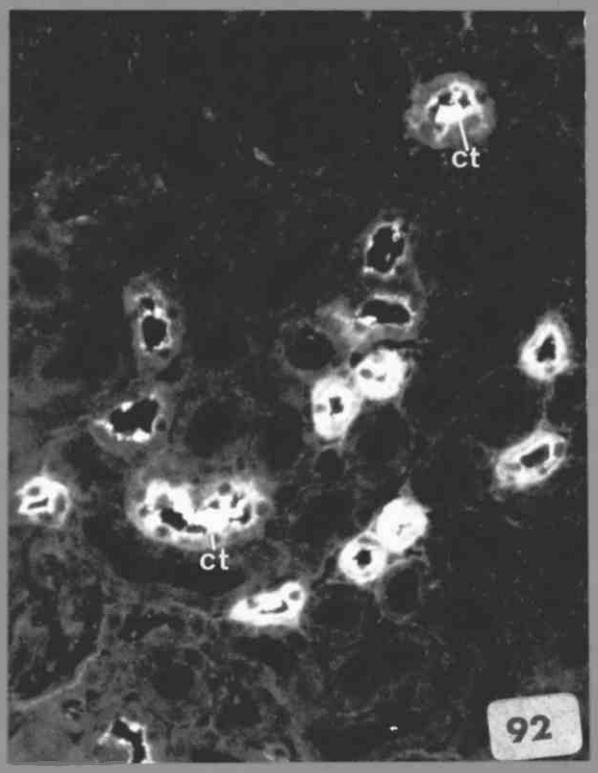
Fig 91. Kidney of adult Wistar rat killed 3 days post-adrenalectomy. Fluorescence microscopy shows a substantial reduction of T-H in the cells of a high proportion of DCT present in the outer cortex. The cell interior of the affected tubules appear to have lost their T-H positive fluorescent staining while their luminal border is still fluorescing. Fixation by perfusion with formal calcium chloride. Magnification x 600.

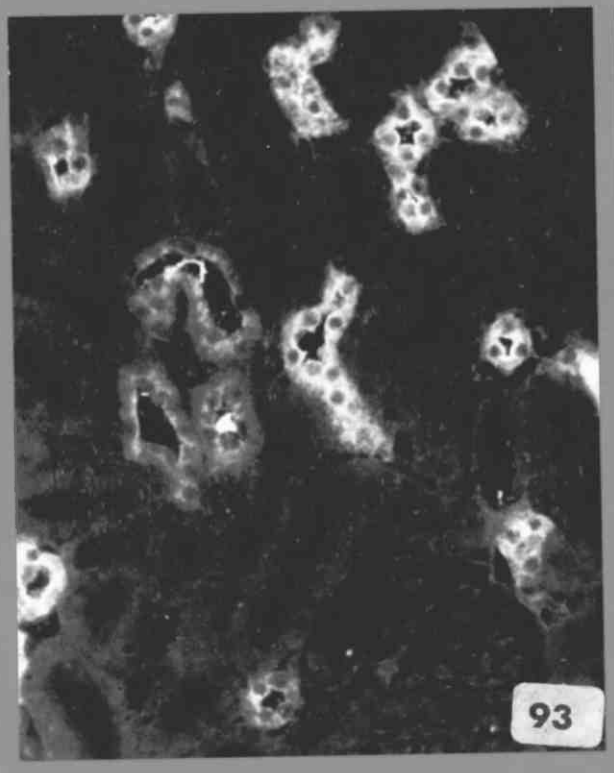
Fig 92. Adult Wistar rat, kidney obtained 3 days after adrenalectomy. The lumina of some of the affected DCT is shown to be filled with brilliantly fluorescing casts (ct). Magnification x 600.

Fig 93. Adult Wistar rat kidney, obtained 15 days after adrenalectomy. Note that the number of DCT showing the effect of adrenalectomy (and the extent of reduction of T-H specific fluorescence) is much less than that seen in the 3 days adrenalectomized animal (Fig 91). In some areas, the fluorescence is virtually indistinguishable from those of the normal animals. Magnification x 600.

Fig 94. Kidney of adult Wistar rat killed 7 days post-adrenalectomy. While some of the DCT present in the outer cortex clearly shows the effect of adrenalectomy (i.e. reduced T-H specific fluorescence), the MD cells, on the other hand, seems to be unaffected i.e. as is to be seen in the normal animals, the majority of MD still retain the glycoprotein on their luminal surface. Magnification x 600.


91


ct
ct
92


93

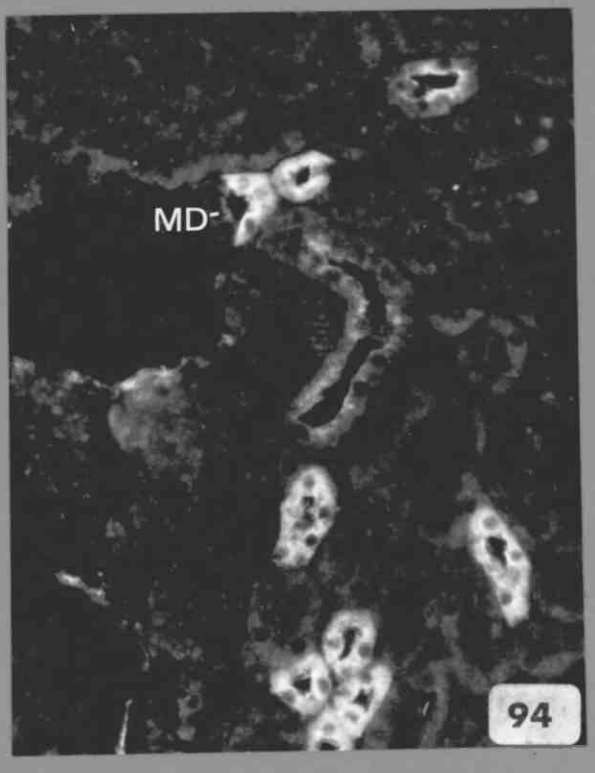
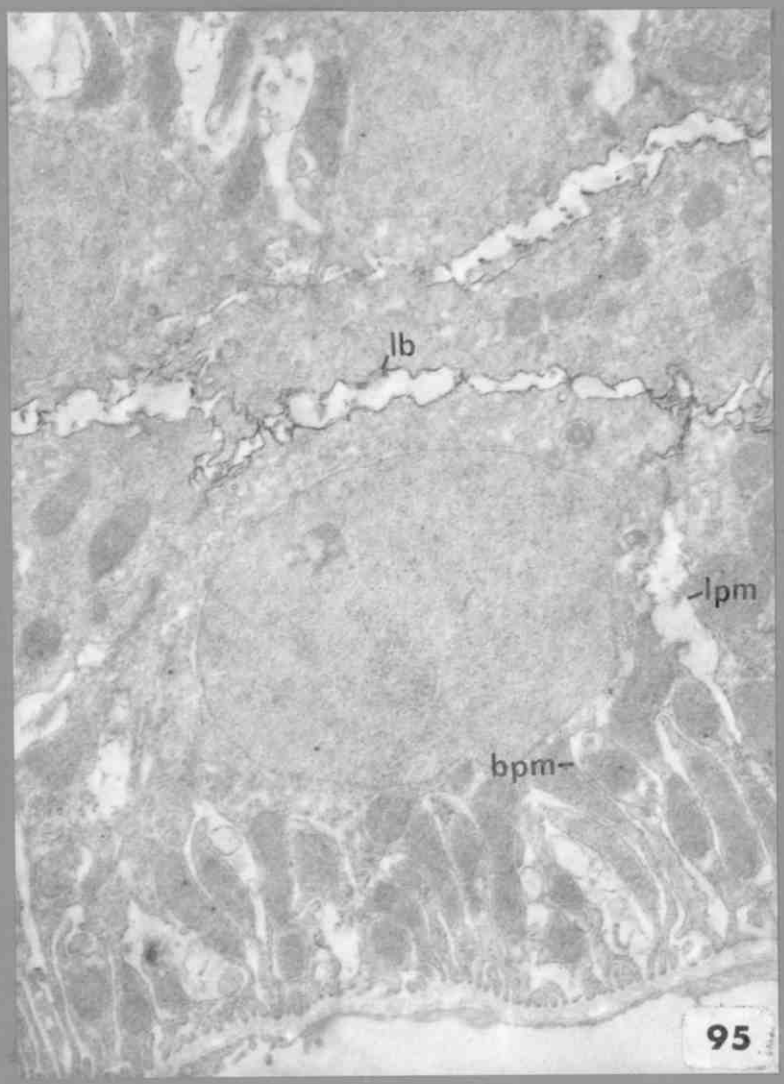

MD-
94

Fig 95. 3 days adrenalectomized Wistar rat kidney. By immuno-electron microscopy it is shown that in a cell of the DCT of the outer cortex, T-H has completely disappeared from the lateral (lpm) and basal plasma membrane (bpm), including the infoldings of the latter. The glycoprotein is however, still seen to be present on the luminal border (lb). Fixation was by perfusion with PLP and the staining by the method of Nakane and Kawaoi. Magnification x 17,500.

Fig 96. 20 days adrenalectomized Wistar rat kidney.. By immuno-electron microscopy it is shown that on this day, the cells of most of the DCT possess the full complement of the glycoprotein i.e. T-H is present on the luminal border (lb), lateral (lpm) as well as basal plasma membrane (bpm) including the infoldings of the latter. Magnification x 17,000.


lb
lpm
bpm
95

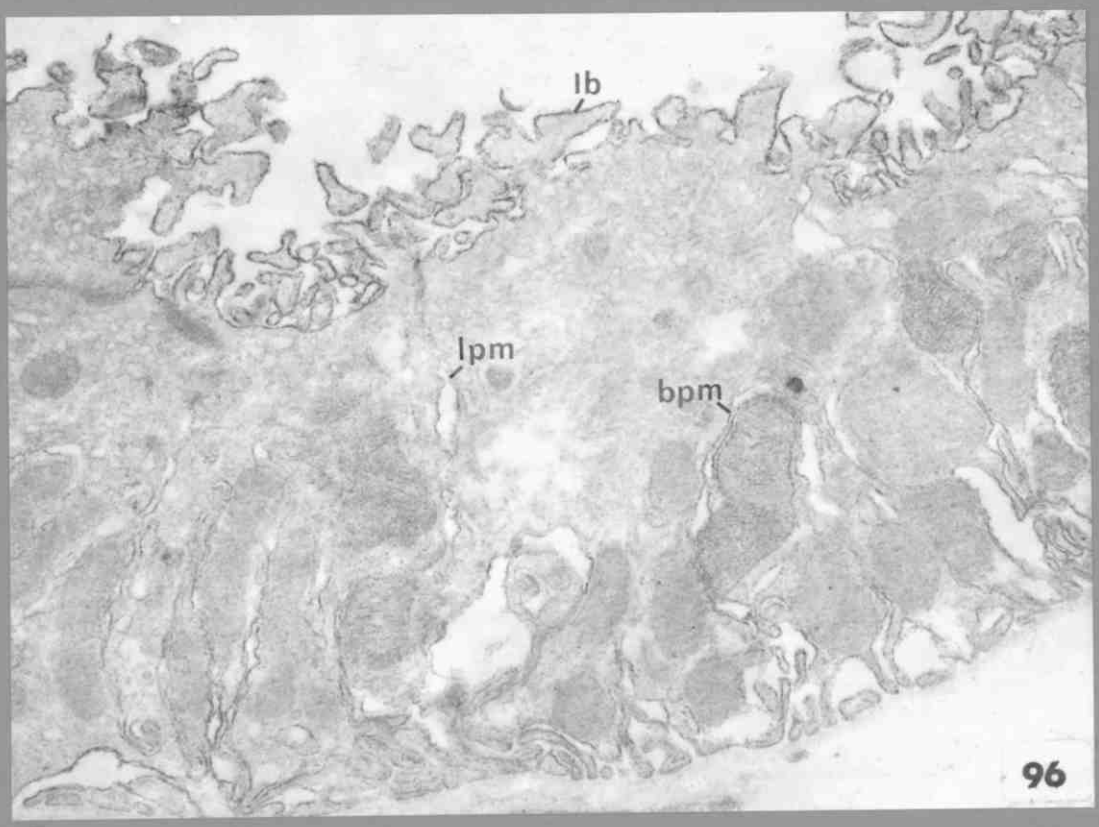
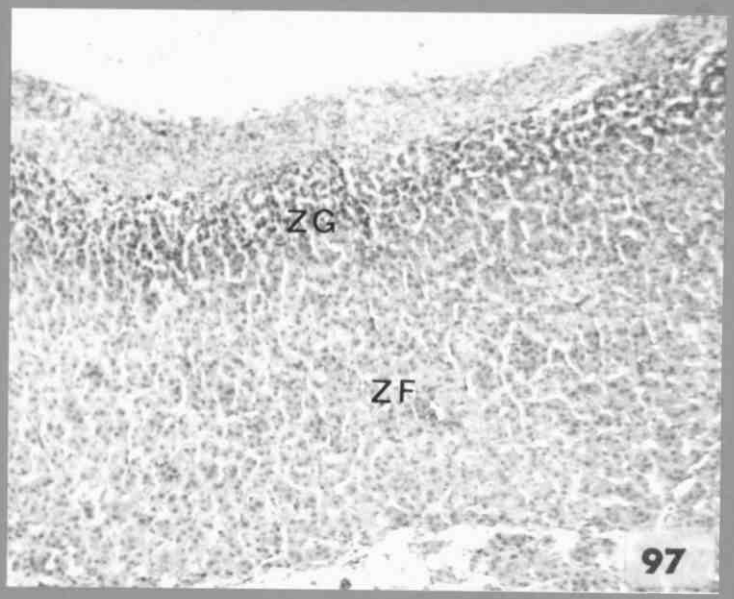
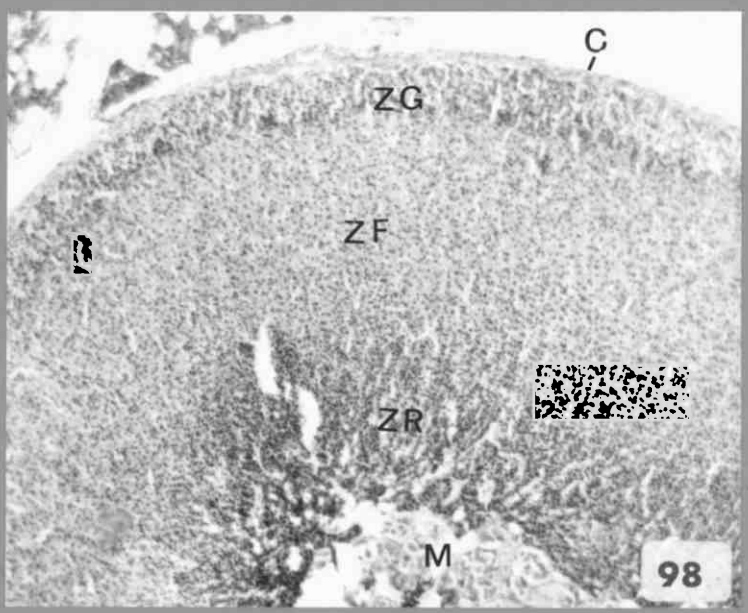

lb
lpm
bpm
96

Fig 97. Photomicrograph of accessory adrenal cortical tissue removed from a 15 days bilaterally adrenalectomized sprague-Dawley rat. 8 μm thick paraffin embedded section stained with haematoxylin and eosin. It shows a thin outer layer of zona glomerulosa (ZG) and a thick inner layer of zona fasciculata (ZF). Note that the zona reticularis and the medulla are completely missing. Magnification x 400.

Fig 98. Photomicrograph of the normal adrenal gland obtained from the same rat referred to in Fig. 97. In the cortex are seen three typical zones - the zona glomerulosa (ZG) adjacent to the capsule (C), the zona fasciculata (ZF) and the zona reticularis (ZR). Cells of the Medulla (M) are also visible. Magnification x 320.


ZG
ZF
97


C
ZG
ZF
ZR
M
98